Thermal Buckling and Postbuckling of Symmetrically Laminated Composite Plates

by

Carol Ann Meyers

Thesis submitted to the Faculty of the

Virginia Polytechnic Institute and State University

in partial fulfillment of the requirements for the degree of

Master of Science

in

Engineering Mechanics

APPROVED:

M. W. Hyer, Chairman

O. H. Griffin, Jr.

E. R. Johnson

December, 1990

Blacksburg, Virginia

Thermal Buckling and Postbuckling of Symmetrically Laminated Composite Plates

by

Carol Ann Meyers

M. W. Hyer, Chairman

Engineering Mechanics

(ABSTRACT)

This paper discusses an investigation into thermal buckling and post-buckling of symmetrically laminated composite plates. In this study thermal buckling is investigated for laminates under two different simple support conditions, fixed and sliding. These laminates are subjected to the conditions of a uniform temperature change and a linearly varying temperature change along the length of the plate. Postbuckling in the presence of a uniform temperature change and nonlinear response to imperfections in the form of a thermal gradient through the thickness of the plate and a lack of initial flatness are also studied. The buckling response is studied using variational methods, specifically the Trefftz criterion. Postbuckling and responses to imperfections are studied using nonlinear equilibrium conditions. A Rayleigh-Ritz formulation is used to obtain numerical results from the formulations for the prebuckling response, the buckling response, and the postbuckling and imperfection responses. The analyses are applied to graphite-reinforced materials with $(\pm 45/0_2)_s$ and $(\pm 45/0/90)_s$ lamination sequences. Numerical results are obtained for these laminates and also for the case of these laminates being rotated 30° inplane. For the first laminate, for example, such a rotation results in a $(+75/-15/30_2)_s$ stacking sequence. Such skewing of the principal material directions may be encountered when using fiber-reinforced materials in a structurally tailored design. In addition, the influence on thermal buckling of a lack of ideal boundary conditions in the form of boundary compliance and thermal expansion, which would occur in any real set-up, are investigated.

Acknowledgements

The author would like to acknowledge the financial support of the Aircraft Structures Branch of the NASA Langley Research Center through Grant NAG-1-343, The NASA-Virginia Tech Composites Program. Dr. Mark J. Shuart is the grant monitor for this particular area of research. The author would also like to thank her family, especially her husband, Larry, her chairman, M. W. Hyer, her thesis committee, O. H. Griffin and E. R. Johnson, and her friends for their help, support and patience. Special thanks are also due to Paula Davis and Mara Knott for their invaluable help in dealing with the oddities of Script.

Table of Contents

List of Illustrations

List of Tables

1.0 Introduction and Background

While fiber-reinforced polymer matrix composite materials have been used successfully on a number of military and commercial aircraft structures, their use on structures that operate at elevated temperatures for sustained periods of time has been limited. This situation may change with the envisioned high-speed civil transport. On the basis of potential structural efficiency and projected fabrication costs of composite materials, some proponents of the high-speed civil transport contend that an affordable aircraft will not be possible without extensive use of polymer matrix materials in primary structures. The use of these materials in a sustained elevated temperature environment, however, poses a wide variety of challenges. Among these challenges are: the large scale synthesis of polymers capable of retaining their properties at an elevated temperature; the processing of these polymers to make affordable composites; the measurement and subsequent modelling of structural and material response; the design of efficient structures that can operate at elevated temperature, and the verification of these designs through actual tests. The ability to design structures with the complexity of a high-speed transport will be based on having the appropriate analytical tools for combined thermal and structural analysis. Much of this will be new and will require time to develop the tools and to interpret the results. Thus, a logical approach is to understand the issues associated with simpler structural elements before approaching more complex structures. This thesis describes a study directed at the latter point, namely, understanding the response of a simple structural element in an elevated temperature environment. Specifically, this thesis addresses the issue of thermally induced buckling and postbuckling of symmetrically laminated fiber-reinforced plates. As buckling and postbuckling are responses that occur in an ideal situation, i.e., perfectly flat plates, no temperature gradients through the thickness, etc., the response of plates in the presence of imperfections is also addressed. Because in any real set-up the presence of compliance and thermal expansion in the frame or fixture supporting the plate may also affect thermal buckling, these issues are also addressed. The study described is analytical in nature and is based on using Rayleigh-Ritz formulations in conjunction with variational methods.

Though plates are a very limited structural form, thermally induced buckling and postbuckling involve many issues. Among these are: the inclusion of temperature-dependent material properties; the inclusion of time-dependent material properties due to the elevated temperature effects in polymers; thermal gradients, both in the plane of the plate and through the thickness; plate aspect ratio; plate boundary conditions; and the degree of material property orthotropy. In this study, neither temperature-dependent nor time-dependent material property effects will be addressed. However, the influence of temperature gradients and material property orthotropy will be studied. Though only simple supports will be studied, two different simple support conditions will be considered. The first set, which will be referred to as the fixed edge case, will assume that all three components of the displacements at all four edges are zero. The second set, which will be referred to as the sliding edge case, will assume that the out-of-plane displacements and the inplane displacements normal to the edges are zero at all four edges. The inplane displacements parallel to the edges, however, are not restricted to zero. That is, the edges of the plate may slide tangentially. Clearly, these two sets of boundary conditions result in different prebuckling stress states. The question to be addressed is the degree to which the two different simple support boundary conditions influence buckling and postbuckling response. The influence of plate aspect ratio on buckling is studied. In this study, one more effect will be considered. To take full advantage of the directionally dependent properties of composites, many applications of composite materials involve structural tailoring. Hence the plate's principal material directions may not be aligned with any of the edges of the plate. This is referred to here as material axis skewing. More specifically, to serve as an example, a quasi-isotropic stacking sequence of $(\pm 45/0/90)_s$ may be rotated in its plane by 30° to form a $(+75/-15/30/-60)_s$ stacking arrangement. This study will explore the influence of this material axis skewing on buckling, postbuckling, and the response in the presence of imperfections.

This thesis begins in the next chapter with a review of some of the relevant past work in the area of thermally induced buckling and postbuckling. In ch. 3 a description is given of the specific class of problems studied in this thesis. The geometry, definitions, and nomenclature are introduced. The variational principles used to study buckling, postbuckling, and imperfection response are also introduced, and the use of the Rayleigh-Ritz method as it is applied here is described in general terms.

Chapter 4 focuses on buckling response. Inherent in the study of buckling is the issue of prebuckling. The prebuckling response of the plate is determined by using the first variation in the total potential energy under the condition that the out-of-plane deflections are zero. It is shown that for certain cases the prebuckling solution is trivial, while for other cases it is as involved, or even more so, than the buckling solution. Buckling is studied, using the prebuckling response, by examining the first variation of the second variation and allowing for out-of-plane deflections. Numerical examples are given to illustrate the specific issues discussed with regard to buckling. Buckling due to a spatially uniform change in temperature, and buckling due to a temperature gradient along the length of the plate are considered. The influence on the buckling response of varying the material properties, as well as the influences of square and rectangular plate aspect ratios, quasi-isotropic and orthotropic stacking arrangements, and fixed and sliding boundary conditions, are also considered. In all of these cases, the influence of material axis skewing is studied. Convergence of the buckling calculations is also discussed, as is the sensitivity of the buckling calculations to variations in the material properties.

Postbuckling response is discussed in ch. 5. This problem is computationally more involved than the buckling problem. The coupling of the inplane and out-of-plane displacements, in conjunction with the Rayleigh-Ritz formulation, results in a coupled set of nonlinear algebraic equations that must be solved. Hence, to keep the computational work within bounds, the specific issues discussed in conjunction with postbuckling response are somewhat more limited than the issues considered in the buckling chapter. Only a spatially uniform change in temperature and square laminates are considered. However, the influence of material axes skewing, fixed and sliding boundary conditions, and quasi-isotropic and orthotropic stacking sequences are discussed. Convergence of the postbuckling solution is also evaluated.

Chapter 6 concerns the response of plates in the presence of imperfections. All laminates deviate in some form and to some degree from the ideal situation. Spatially varying properties due to nonuniform cure, variable ply thickness, and lack of initial flatness represent but some of the the deviations from the ideal situation. Also, testing laminates, whatever the form of loading, will introduce other deviations from the ideal. When testing laminates, thermal gradients, friction, perhaps even the air currents in convective ovens, contribute to the lack of ideal test conditions. Here two forms of imperfections will be considered, one due to the laminate itself, and one due to testing. In particular, imperfections in the form of initial out-of-plane deflections of the plate and in the form of a through-the-thickness temperature gradient are modelled. With either imperfection present the problem is not one of buckling or of postbuckling, rather it is a forced response problem. In general, such problems in the presence of imperfections lead to a response that asymptotically approaches the postbuckling response, as is the case here. Again, the influence of material axis skewing, boundary conditions, and degree of orthotropy are studied, but now in the context of a slight out-of-plane initial shape, and a slight temperature gradient through-the-thickness of the plate. These calculations for the case of imperfections describe the response that is likely to be observed in any experimental set-up. The calculations provide insight as to why observations might deviate from the ideal.

In designing an experimental fixture, or in analyzing a composite plate attached to a frame made of some other material, the effects of a fixture with a finite stiffness and a nonzero coefficient of thermal expansion on the thermal buckling response need to be considered. Chapter 7 discusses the sensitivity studies conducted to determine the influence of the lack of infinite fixturing stiffness and the presence of fixturing thermal expansion in any real set-up.

Lastly, a discussion of the study, conclusions, and recommendations for future research are presented in ch. 8.

2.0 Literature Review

One of the earliest studies to examine thermal buckling of fiber-reinforced plates is that conducted by Whitney and Ashton [1] in 1971. The stability, vibration, and bending behavior of composite plates subjected to a uniform increase in temperature, or to a swelling due to moisture absorption, is studied using an energy formulation in conjunction with the Rayleigh-Ritz method. For the thermal buckling problem, the prebuckling solution is obtained using displacement equations derived from the equilibrium equations of laminated plate theory. Only symmetric laminates for which all the prebuckling solutions are trivial are considered. Two cases are examined for thermal buckling. In the first case, the effect of ply angle on the buckling temperature is studied for angle-ply $(\pm\theta)_s$ plates with two edges free and two edges clamped so as to constrain movement normal to the clamped edge. Due to the negative thermal expansion coefficient of graphite fibers, there can exist a range of values for θ such that the coefficient of thermal expansion for an angle-ply, graphite/epoxy laminate is negative. In [1], it is found that for this range of θ, the temperature must be decreased to cause buckling in plates with two free edges. Moreover, there is, theoretically, a value of θ for which such a plate cannot be buckled either by raising, or lowering the temperature. In the second case, the effect of varying θ for $(\pm\theta/0)_s$ laminates subjected on all four sides to sliding simple support conditions is examined. For plates supported on all four edges, it is shown that buckling can only occur for positive changes in temperature. This case is investigated for graphite/epoxy, boron/epoxy, S glass/epoxy, and aluminum plates. Because of the low (or negative) coefficient of expansion for all the fibers considered, the fiber-reinforced plates show greater resistance to thermal buckling than aluminum. A similar treatment of the subject is given by Whitney [2].

Flaggs and Vinson [3] consider hygrothermal effects in the buckling of moderately thick composite plates. Using a formulation similar to Whitney and Ashton, but one which also accounts for transverse shear and normal deformation, a study is made of the effects of temperature change and moisture content upon the uniaxial prebuckling stress resultants for $(0/\pm 45/90)_s$ graphite/epoxy plates subject to sliding simple support and clamped boundary conditions. In all cases studied the hygrothermal loads reduce the prebuckling stress resultants necessary to cause buckling.

In [4], Stavsky develops a thermoelastic theory for thin anisotropic plates which were heterogeneous through the thickness. This theory is formulated from differential equations of equilibrium in terms of the transverse deflection, and Airy's stress function. Nonlinear terms are included to obtain the thermal postbuckling equations. A similar formulation is used by Stavsky [5] to study the thermal buckling of circular plates composed of cylindrically orthotropic layers. Biswas [6] also develops thermal buckling equations from the equations of equilibrium for orthotropic plates of irregular shape. Critical buckling temperatures are found in [6] for a square plate, a circular plate, and a square plate with rounded edges, under fixed simple support conditions. This is done by using a conformal mapping technique and Galerkin's method to solve the system of equations. Chen and Chen [7] use Galerkin's method with displacement equations of equilibrium to study thermal buckling due to a uniform change in temperature for antisymmetric angle-ply plates under clamped and fixed simple support boundary conditions. For all cases considered, the prebuckling solutions are trivial. Results are given showing the effects of ply angle, aspect ratio, a/b, modulus ratio, E_1/E_2, and thermal expansion coefficient ratio, α_1/α_2, on the buckling temperature.

Thangaratnam, et al. [8] employ the finite-element method to study the thermal buckling of symmetric and antisymmetric cross-ply and angle-ply laminates. Prebuckling solutions are obtained by minimizing the potential energy with respect to the generalized displacement vector of the element used. For plates with clamped edges and both fixed and sliding simple support boundary conditions, the effect on the buckling temperature of varying aspect ratio, modulus ratio, thermal expansion coefficient ratio, and number of layers is examined. They find that the buckling temperature for the clamped plate is always higher than for a simply supported plate. The buckling temperature is determined to decrease with increasing modulus ratio, and with increasing expansion coefficient ratio (for $\alpha_1 > 0$). The variation of the buckling temperature with fiber orientation θ is found to be significantly influenced by the plate aspect ratio.

Many other studies in thermal buckling of fiber-reinforced plates have been conducted by Tauchert, together with Huang [9,10], or alone [11]. In [9] the thermal buckling of symmetric angle-ply laminates is investigated for plates with both fixed and sliding simple support boundary conditions. Buckling and prebuckling equations are formulated using variational methods and solved using the Rayleigh-Ritz technique. For plates with fixed simple supports, the prebuckling solution is found to be trivial. However, for plates with sliding simple supports and an odd number of layers, the prebuckling stress resultants are found to vary throughout the laminate. This is due to the presence of A_{16}, A_{26}, and N_{xy} terms for the case of an odd number of layers. Numerical results are given showing the effects of aspect ratio, number of layers, and ply angle on the buckling temperature and associated mode shape. Using displacement equations of equilibrium, thermal buckling and prebuckling equations are developed in [10] for thin anti-symmetric angle-ply laminates. These are solved using an assumed double series solution for plates subject to sliding simple support boundary conditions. For this case, the prebuckling solutions are trivial. The effects of ply angle, aspect ratio, and number of layers on the critical buckling temperature are investigated. The work done in [10] is extended in [11] for thick anti-symmetric angle-ply plates by including transverse normal and shear deformations in the original formulation. As in [10], all prebuckling solutions are again found to be trivial. The effects of ply angle, aspect ratio, and span-to-thickness ratio on buckling temperature are considered and the results are compared to those in obtained [10]. An optimization procedure is also proposed in [11] which used Powell's method to maximize resistance to thermal buckling using ply angle as the design parameter.

Few papers are available addressing the issue of thermal postbuckling of composite plates. As mentioned previously, Stavsky [4] develops thermal postbuckling equations for thin anisotropic plates that are heterogeneous through the thickness. Biswas [12] derives governing equations in terms of displacements and Airy's stress function for the nonlinear analysis of heated orthotropic plates. Using Galerkin's method, a one-term solution is obtained in [12] for plates with fixed simple supports subjected to a temperature gradient that is linear through the thickness. Results for deflections and membrane stress are given for plates with various aspect ratios. Chen and Chen [13] also study the postbuckling of antisymmetric angle-ply plates with sliding simple supports under a 'tent shaped' thermal field using the finite-element method. Results are given for plates with various ply angles, numbers of layers, and aspect ratios.

Huang and Tauchert examine thermal postbuckling of anti-symmetric angle-ply laminates due to an uniform increase in temperature in [10] and [14]. In both studies, the plates have sliding simple support boundary conditions. Double series expressions are assumed for the displacements and the total potential energy of the laminate is minimized at each temperature increment with respect to the coefficients of these series using Powell's method. Results are given showing the effects of ply angle and number of layers on the plate's response. Huang and Tauchert [15] have also studied the large deformation of antisymmetric angle-ply laminates with sliding simple supports due to nonuniform temperature loadings. Both an inplane parabolic temperature field and a temperature gradient that is linear through the thickness of the plate are considered. Using the same method as in [10] and [14], the response of plates to these thermal fields is studied for laminates with various aspect ratios, ply angles, and numbers of layers. These results are compared with the results obtained from the small-deformation formulation developed by Wu and Tauchert [16,17].

All of the papers cited above are purely analytical. No experimental results appear to be available for the thermal buckling or postbuckling of fiber-reinforced composite plates. In addition, no attention has been given to material axis skewing, nor to the influence of initial out-of-plane deflections.

3.0 Description of Problem and Solution Approach

In this chapter a description of the problem studied and a general discussion of the approaches to the various solutions are given. The nomenclature to be used in the following chapters is also introduced.

3.1 Description of Problem

Consider a rectangular plate of length a in the x direction, width b in y direction, and thickness H. The temperature change, ΔT, is, in general, a function of the spatial location x, y, and z. As shown in Fig. 1, the reference coordinate system has its origin at one corner of the plate. The x-y plane is coincident with the geometric midplane of the plate, and the z axis is perpendicular to this plane. As usual, the geometric midplane will be the reference surface of the plate. The plates under consideration are symmetrically laminated. Only thin plates are studied. In the laminate nomenclature the orientation of the layers is defined relative to the +x axis. Two sets of boundary conditions, fixed and sliding simple supports, are considered. For fixed simple support conditions, all four edges are fixed against inplane normal and

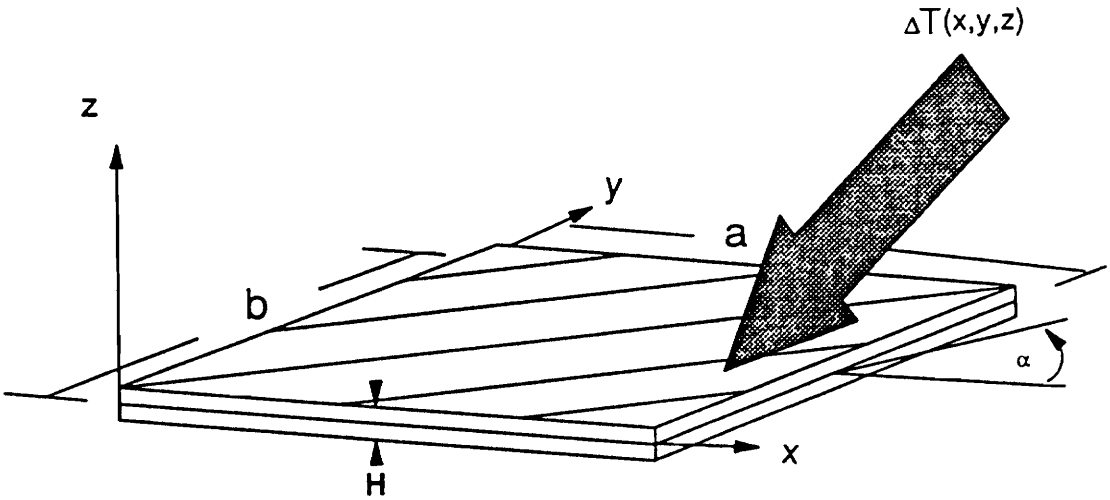

Fig. 1. Description of Problem.

tangential displacements, and out-of-plane displacements. For sliding simple supports, all four edges are fixed against inplane normal displacements and out-of-plane displacements, but are free to move, or 'slide', tangentially. The sliding is assumed to be frictionless. For both support conditions there are zero moments along the edges. Explicitly stated, the boundary conditions for the fixed simple support conditions are,

$$\text{at } x = 0,\ a: \quad \begin{aligned} &\text{i) } u^o = 0 \\ &\text{ii) } v^o = 0 \\ &\text{iii) } w^o = 0 \\ &\text{iv) } M_x = 0. \end{aligned} \tag{3.1a}$$

$$\text{at } y = 0,\ b: \quad \begin{aligned} &\text{i) } u^o = 0 \\ &\text{ii) } v^o = 0 \\ &\text{iii) } w^o = 0 \\ &\text{iv) } M_y = 0. \end{aligned} \tag{3.1b}$$

For the sliding simple supports,

$$\text{at } x = 0,\ a: \quad \begin{aligned} &\text{i) } u^o = 0 \\ &\text{ii) } N_{xy} = 0 \\ &\text{iii) } w^o = 0 \\ &\text{iv) } M_x = 0. \end{aligned} \tag{3.2a}$$

$$\text{at } y = 0,\ b: \quad \begin{aligned} &\text{i) } N_{xy} = 0 \\ &\text{ii) } v^o = 0 \\ &\text{iii) } w^o = 0 \\ &\text{iv) } M_y = 0. \end{aligned} \tag{3.2b}$$

The topics of specific interest are:

1. Buckling due to a uniform temperature change;

2. Buckling due to a temperature change that varies linearly with x;

3. Postbuckling due to a uniform temperature change;

4. Geometrically nonlinear response due to a temperature field that is uniform in x and y, but which varies slightly through the thickness of the plate.

5. Geometrically nonlinear response due to a uniform temperature change and lack of initial flatness;

Also of interest in this study are the effects on thermal buckling, postbuckling, and imperfection response of the laminate material axes being rotated inplane by some angle α relative to the +x axis. Specifically, if a $(\pm 45/0/90)_s$ laminate is rotated by $\alpha = 30°$, the resulting laminate can be thought of as a $(+75/-15/+30/-60)_s$ laminate. Such skewing of material axes relative to the support boundaries could well be the situation for a tailored structure. The angle α is measured with respect to the +x axis and is shown in Fig. 1.

3.2 Solution Approach

Energy and variational methods are well suited to this study. Equilibrium conditions are obtained by setting the first variation of the total potential energy to zero. Stability of the equilibrium conditions can then be determined by examining the second variation of the total potential energy. The Trefftz stability criterion [18] states that the transition from stable to unstable equilibrium occurs when the first variation of the second variation goes to zero. If the second variation is identically zero for some nonzero variations in the displacements at equilibrium, then the third variation must be examined, and so on. In the framework of these variational approaches, approximate solutions are sought using the Rayleigh-Ritz method.

With this approach in mind, the total potential energy of the plate is given by:

$$\pi = \frac{1}{2}\int\int\int\left\{\left(\sigma_x - \sigma_x^P\right)\varepsilon_x + \left(\sigma_y - \sigma_y^P\right)\varepsilon_y + \left(\tau_{xy} - \tau_{xy}^P\right)\gamma_{xy}\right\}dxdydz. \qquad (3.3).$$

Note that no external work terms are given in eqn. 1 because there are no loads applied to the plate and the boundaries are stationary or considered frictionless. The stress components superscribed with a "P" denote preloading effects. In this study they will always be due, at least, to thermally-induced deformation, but may also be due, for example, to imperfections in the plate. They will be defined shortly. The strains in the energy expression are given by

$$\begin{aligned} \varepsilon_x &= \varepsilon_x^o + z\kappa_x^o \\ \varepsilon_y &= \varepsilon_y^o + z\kappa_y^o \\ \gamma_{xy} &= \gamma_{xy}^o + z\kappa_{xy}^o, \end{aligned} \qquad (3.4).$$

where the quantities superscribed with a zero are reference surface strains and curvatures. These quantities are, of course, functions of x and y. Including the effects of moderate rotations, the reference surface strains are

$$\begin{aligned} \varepsilon_x^o &= \frac{\partial u^o}{\partial x} + \frac{1}{2}\beta_x^{o2} \;;\quad \varepsilon_y^o = \frac{\partial v^o}{\partial y} + \beta_y^{o2} \\ \gamma_{xy}^o &= \frac{\partial u^o}{\partial y} + \frac{\partial v^o}{\partial x} + \beta_x^o\beta_y^o, \end{aligned} \qquad (3.5)$$

where

$$\beta_x^o = -\frac{\partial w^o}{\partial x} \quad \text{and} \quad \beta_y^o = -\frac{\partial w^o}{\partial y} \qquad (3.6)$$

are identified with cross-sectional rotations. The reference surface curvatures are given by

$$\kappa_x^o = \frac{\partial \beta_x^o}{\partial x} \;;\quad \kappa_y^o = \frac{\partial \beta_y^o}{\partial y} \;;\quad \kappa_{xy}^o = \frac{\partial \beta_x^o}{\partial y} + \frac{\partial \beta_y^o}{\partial x}. \qquad (3.7)$$

The stresses in the energy expression are given by the relations

$$
\begin{aligned}
\sigma_x &= \overline{Q}_{11}\left(\varepsilon_x - \varepsilon_x^P\right) + \overline{Q}_{12}\left(\varepsilon_y - \varepsilon_y^P\right) + \overline{Q}_{16}\left(\gamma_{xy} - \gamma_{xy}^P\right) \\
\sigma_y &= \overline{Q}_{12}\left(\varepsilon_x - \varepsilon_x^P\right) + \overline{Q}_{22}\left(\varepsilon_y - \varepsilon_y^P\right) + \overline{Q}_{26}\left(\gamma_{xy} - \gamma_{xy}^P\right) \\
\tau_{xy} &= \overline{Q}_{16}\left(\varepsilon_x - \varepsilon_x^P\right) + \overline{Q}_{26}\left(\varepsilon_y - \varepsilon_y^P\right) + \overline{Q}_{66}\left(\gamma_{xy} - \gamma_{xy}^P\right).
\end{aligned}
\tag{3.8}
$$

These may be rewritten as

$$
\begin{aligned}
\sigma_x &= \overline{Q}_{11}\varepsilon_x + \overline{Q}_{12}\varepsilon_y + \overline{Q}_{16}\gamma_{xy} - \sigma_x^P \\
\sigma_y &= \overline{Q}_{12}\varepsilon_x + \overline{Q}_{22}\varepsilon_y + \overline{Q}_{26}\gamma_{xy} - \sigma_y^P \\
\tau_{xy} &= \overline{Q}_{16}\varepsilon_x + \overline{Q}_{26}\varepsilon_y + \overline{Q}_{66}\gamma_{xy} - \tau_{xy}^P.
\end{aligned}
\tag{3.9}
$$

In eqn. 3.9, the stress components denoting preloading effects are

$$
\begin{aligned}
\sigma_x^P &= \overline{Q}_{11}\varepsilon_x^P + \overline{Q}_{12}\varepsilon_y^P + \overline{Q}_{16}\gamma_{xy}^P \\
\sigma_y^P &= \overline{Q}_{12}\varepsilon_x^P + \overline{Q}_{22}\varepsilon_y^P + \overline{Q}_{26}\gamma_{xy}^P \\
\tau_{xy}^P &= \overline{Q}_{16}\varepsilon_x^P + \overline{Q}_{26}\varepsilon_y^P + \overline{Q}_{66}\gamma_{xy}^P,
\end{aligned}
\tag{3.10}
$$

where ε_x^P, ε_y^P, and γ_{xy}^P are the strains due to preloading effects.

Substituting the strains into the energy expression, eqn. 3.3, yields

$$
\begin{aligned}
\pi\left(u^o, v^o, w^o\right) = \frac{1}{2}\int_0^a \int_0^b \int_{\frac{-H}{2}}^{\frac{+H}{2}} \Big\{ &\left(\sigma_x - \sigma_x^P\right)\left(\varepsilon_x^o + z\kappa_x^o\right) + \left(\sigma_y - \sigma_y^P\right)\left(\varepsilon_y^o + z\kappa_y^o\right) \\
&+ \left(\tau_{xy} - \tau_{xy}^P\right)\left(\gamma_{xy}^o + z\kappa_{xy}^o\right)\Big\} dxdydz.
\end{aligned}
\tag{3.11}
$$

Then, integrating with respect to z, through the thickness of the laminate, results in

$$
\begin{aligned}
\pi\left(u^o, v^o, w^o\right) = \frac{1}{2}\int\int \Big\{ &\left(N_x - N_x^P\right)\varepsilon_x^o + \left(N_y - N_y^P\right)\varepsilon_y^o + \left(N_{xy} - N_{xy}^P\right)\gamma_{xy}^o \\
&+ \left(M_x - M_x^P\right)\kappa_x^o + \left(M_y - M_y^P\right)\kappa_y^o + \left(M_{xy} - M_{xy}^P\right)\kappa_{xy}^o\Big\} dxdy,
\end{aligned}
\tag{3.12}
$$

where the stress resultants have the usual definitions for symmetric laminates, namely

$$
\begin{aligned}
N_x &= \int_{\frac{-H}{2}}^{\frac{+H}{2}} \sigma_x dz = A_{11}\varepsilon_x^o + A_{12}\varepsilon_y^o + A_{16}\gamma_{xy}^o - N_x^P \\
N_y &= \int_{\frac{-H}{2}}^{\frac{+H}{2}} \sigma_y dz = A_{12}\varepsilon_x^o + A_{22}\varepsilon_y^o + A_{26}\gamma_{xy}^o - N_y^P \\
N_{xy} &= \int_{\frac{-H}{2}}^{\frac{+H}{2}} \tau_{xy} dz = A_{16}\varepsilon_x^o + A_{26}\varepsilon_y^o + A_{66}\gamma_{xy}^o - N_{xy}^P \\
M_x &= \int_{\frac{-H}{2}}^{\frac{+H}{2}} z\sigma_x dz = D_{11}\kappa_x^o + D_{12}\kappa_y^o + D_{16}\kappa_{xy}^o - M_x^P \\
M_y &= \int_{\frac{-H}{2}}^{\frac{+H}{2}} z\sigma_y dz = D_{12}\kappa_x^o + D_{22}\kappa_y^o + D_{26}\kappa_{xy}^o - M_y^P \\
M_{xy} &= \int_{\frac{-H}{2}}^{\frac{+H}{2}} z\sigma_y dz = D_{16}\kappa_x^o + D_{26}\kappa_y^o + D_{66}\kappa_{xy}^o - M_{xy}^P .
\end{aligned}
\tag{3.13}
$$

In the above,

$$
\begin{aligned}
N_x^P &= \int_{\frac{-H}{2}}^{\frac{+H}{2}} \sigma_x^P dz = \int_{\frac{-H}{2}}^{\frac{+H}{2}} \left(\overline{Q}_{11}\varepsilon_x^P + \overline{Q}_{12}\varepsilon_y^P + \overline{Q}_{16}\gamma_{xy}^P\right)dz \\
N_y^P &= \int_{\frac{-H}{2}}^{\frac{+H}{2}} \sigma_y^P dz = \int_{\frac{-H}{2}}^{\frac{+H}{2}} \left(\overline{Q}_{12}\varepsilon_x^P + \overline{Q}_{22}\varepsilon_y^P + \overline{Q}_{26}\gamma_{xy}^P\right)dz \\
N_{xy}^P &= \int_{\frac{-H}{2}}^{\frac{+H}{2}} \tau_{xy}^P dz = \int_{\frac{-H}{2}}^{\frac{+H}{2}} \left(\overline{Q}_{16}\varepsilon_x^P + \overline{Q}_{26}\varepsilon_y^P + \overline{Q}_{66}\gamma_{xy}^P\right)dz \\
M_x^P &= \int_{\frac{-H}{2}}^{\frac{+H}{2}} z\sigma_x^P dz = \int_{\frac{-H}{2}}^{\frac{+H}{2}} \left(\overline{Q}_{11}\varepsilon_x^P + \overline{Q}_{12}\varepsilon_y^P + \overline{Q}_{16}\gamma_{xy}^P\right)zdz \\
M_y^P &= \int_{\frac{-H}{2}}^{\frac{+H}{2}} z\sigma_y^P dz = \int_{\frac{-H}{2}}^{\frac{+H}{2}} \left(\overline{Q}_{12}\varepsilon_x^P + \overline{Q}_{22}\varepsilon_y^P + \overline{Q}_{26}\gamma_{xy}^P\right)zdz \\
M_{xy}^P &= \int_{\frac{-H}{2}}^{\frac{+H}{2}} z\tau_{xy}^P dz = \int_{\frac{-H}{2}}^{\frac{+H}{2}} \left(\overline{Q}_{16}\varepsilon_x^P + \overline{Q}_{26}\varepsilon_y^P + \overline{Q}_{66}\gamma_{xy}^P\right)zdz.
\end{aligned}
\tag{3.14}
$$

These are the equivalent preloading stress resultants.

The notation

$$\pi = \pi\left(u^o, v^o, w^o\right) \tag{3.15}$$

is being used to indicate that the total potential energy is a function of the displacements and that variations in the total potential energy will be taken with respect to these kinematic quantities. To this end, consider the increment, or variation, in the total potential energy due to increments in the displacements. Specifically,

$$u^o \to u^o + \varepsilon u_1^o \ ; \quad v^o \to v^o + \varepsilon v_1^o \ ; \quad w^o \to w^o + \varepsilon w_1^o. \tag{3.16}$$

The variables u_1^o, v_1^o, and w_1^o are functions of x and y which satisfy the kinematic constraints of the reference surface displacements u^o, v^o, and w^o, respectively, and ε is a small scalar parameter. The infinitesimal scale associated with variations can be considered to be associated with the parameter ε The following interpretation can be given:

$$\begin{aligned}\delta u^{o} &= \varepsilon u_1^{o}\\ \delta v^{o} &= \varepsilon v_1^{o}\\ \delta w^{o} &= \varepsilon w_1^{o},\end{aligned} \tag{3.17}$$

where δ denotes the traditional variational operator. The increments in strain are given by substituting the increments in displacements into the basic definitions of strain. Specifically,

$$\varepsilon_x^{o} + \Delta\varepsilon_x^{o} = \frac{\partial(u^{o} + \varepsilon u_1^{o})}{\partial x} + \frac{1}{2}(\beta_x^{o} + \varepsilon\beta_{x_1}^{o})^2, \tag{3.18}$$

with

$$\beta_{x_1}^{o} = -\frac{\partial w_1^{o}}{\partial x}. \tag{3.19}$$

As a result of gathering powers of ε,

$$\Delta\varepsilon_x^{o} = \varepsilon\varepsilon_{x_1}^{o} + \varepsilon^2\varepsilon_{x_2}^{o}, \tag{3.20}$$

where

$$\varepsilon_{x_1}^{o} = \frac{\partial u_1^{o}}{\partial x} + \beta_x^{o}\beta_{x_1}^{o} \ ; \quad \varepsilon_{x_2}^{o} = \frac{1}{2}\beta_{x_1}^{o\,2}. \tag{3.21}$$

Similarly,

$$\begin{aligned}\Delta\varepsilon_y^{o} &= \varepsilon\varepsilon_{y_1}^{o} + \varepsilon^2\varepsilon_{y_2}^{o}\\ \Delta\gamma_{xy}^{o} &= \varepsilon\gamma_{xy_1}^{o} + \varepsilon^2\gamma_{xy_2}^{o},\end{aligned} \tag{3.22}$$

with

$$\varepsilon^o_{y_1} = \frac{\partial v^o_1}{\partial y} + \beta^o_y \beta^o_{y_1} \;;\quad \varepsilon^o_{y_2} = \frac{1}{2}\,\beta^{o\,2}_{y_1} \;;\quad \text{with } \beta^o_{y_1} = -\frac{\partial w^o_1}{\partial y}$$

and

$$\gamma^o_{xy_1} = \frac{\partial u^o_1}{\partial x} + \frac{\partial v^o_1}{\partial y} + \beta^o_x \beta^o_{y_1} + \beta^o_y \beta^o_{x_1} \;;\quad \gamma^o_{xy_2} = \beta^o_{x_1}\beta^o_{y_1} \tag{3.23}$$

and

$$\kappa^o_{x_1} = \frac{\partial \beta^o_{x_1}}{\partial x} \;;\quad \kappa^o_{y_1} = \frac{\partial \beta^o_{y_1}}{\partial y} \;;\quad \kappa^o_{xy_1} = \frac{\beta^o_{x_1}}{\partial y} + \frac{\beta^o_{y_1}}{\partial x}.$$

The increments in the stress resultants follow directly from eqn. 3.13. These are

$$\begin{aligned}
\Delta N_x &= A_{11}\Delta\varepsilon_x + A_{12}\Delta\varepsilon_y + A_{16}\Delta\gamma_{xy} = \varepsilon N_{x_1} + \varepsilon^2 N_{x_2} \\
\Delta N_y &= A_{12}\Delta\varepsilon_x + A_{22}\Delta\varepsilon_y + A_{26}\Delta\gamma_{xy} = \varepsilon N_{y_1} + \varepsilon^2 N_{y_2} \\
\Delta N_{xy} &= A_{16}\varepsilon_x\Delta + A_{26}\Delta\varepsilon_y + A_{66}\Delta\gamma_{xy} = \varepsilon N_{xy_1} + \varepsilon^2 N_{xy_2} \\
\Delta M_x &= D_{11}\Delta\kappa_x + D_{12}\Delta\kappa_y + D_{16}\Delta\kappa_{xy} = \varepsilon M_{x_1} \\
\Delta M_y &= D_{12}\Delta\kappa_x + D_{22}\Delta\kappa_y + D_{26}\Delta\kappa_{xy} = \varepsilon M_{y_1} \\
\Delta M_{xy} &= D_{16}\Delta\kappa_x + D_{26}\Delta\kappa_y + D_{66}\Delta\kappa_{xy} = \varepsilon M_{xy_1},
\end{aligned} \tag{3.24}$$

where the superscript zero has been dropped for convenience. By gathering powers of ε, convenient and alternate definitions of the increments in the stress resultants can obtained. These are

$$\begin{aligned}
N_{x_1} &= A_{11}\varepsilon_{x_1} + A_{12}\varepsilon_{y_1} + A_{16}\gamma_{xy_1} \\
N_{y_1} &= A_{12}\varepsilon_{x_1} + A_{22}\varepsilon_{y_1} + A_{26}\gamma_{xy_1} \\
N_{xy_1} &= A_{16}\varepsilon_{x_1} + A_{26}\varepsilon_{y_1} + A_{66}\gamma_{xy_1} \\
N_{x_2} &= A_{11}\varepsilon_{x_2} + A_{12}\varepsilon_{y_2} + A_{16}\gamma_{xy_2} \\
N_{y_2} &= A_{12}\varepsilon_{x_2} + A_{22}\varepsilon_{y_2} + A_{26}\gamma_{xy_2} \\
N_{xy_2} &= A_{16}\varepsilon_{x_2} + A_{26}\varepsilon_{y_2} + A_{66}\gamma_{xy_2} \\
M_{x_1} &= D_{11}\kappa_{x_1} + D_{12}\kappa_{y_1} + D_{16}\kappa_{xy_1} \\
M_{y_1} &= D_{12}\kappa_{x_1} + D_{22}\kappa_{y_1} + D_{26}\kappa_{xy_1} \\
M_{xy_1} &= D_{16}\kappa_{x_1} + D_{26}\kappa_{y_1} + D_{66}\kappa_{xy_1}.
\end{aligned} \tag{3.25}$$

With the increment in the displacements, there is a variation, or increment, in the total potential energy of the form

$$\pi + \Delta\pi = \pi\left(u^{o} + \varepsilon u_1^{o}, v^{o} + \varepsilon v_1^{o}, w^{o} + \varepsilon w_1^{o}\right). \tag{3.26}$$

By gathering powers of the parameter ε, the variation in the total potential energy, $\Delta\pi$, can be expressed as

$$\Delta\pi = \varepsilon\pi_1 + \varepsilon^2\pi_2 + \varepsilon^3\pi_3 + \varepsilon^4\pi_4. \tag{3.27}$$

The terms π_i, $i = 1,4$ are the first, second, third and fourth variations in the total potential energy. From these variations come the conditions for prebuckling, buckling, and postbuckling.

The conditions which govern prebuckling and postbuckling are given by

$$\pi_1\left(u_1^{o}, v_1^{o}, w_1^{o}\right) = 0. \tag{3.28}$$

This equation states that the displacements u^{o}, v^{o}, and w^{o} are made stationary with respect to the variations u_1^{o}, v_1^{o}, and w_1^{o}. The first variation of the total potential energy can be written as

$$\begin{aligned}\pi_1 = \int\int\Big\{ & N_x\varepsilon_{x_1}^{o} + N_y\varepsilon_{y_1}^{o} + N_{xy}\gamma_{xy_1}^{o} + M_x\kappa_{x_1}^{o} \\ & + M_y\kappa_{y_1}^{o} + M_{xy}\kappa_{xy_1}^{o}\Big\}dxdy.\end{aligned} \tag{3.29}$$

For buckling studies the Trefftz criterion,

$$\delta\pi_2\left(u_1^{o}, v_1^{o}, w_1^{o}\right) = 0 \tag{3.30}$$

is used. This equation states that the second variation of the total potential energy is stationary with respect to variations of the displacements u_1^{o}, v_1^{o}, and w_1^{o}, when transition from stable to unstable equilibrium occurs. The first variation of the second variation of the total potential energy is given by

$$\delta\pi_2 = \int\int\Big\{N_x\delta\varepsilon^o_{x_2} + N_y\delta\varepsilon^o_{y_2} + N_{xy}\delta\gamma^o_{xy_2} + N_{x_1}\delta\varepsilon^o_{x_1} + N_{y_1}\delta\varepsilon^o_{y_1} + N_{xy_1}\delta\gamma^o_{xy_1} + M_{x_1}\delta\kappa^o_{x_1} + M_{y_1}\delta\kappa^o_{y_1} + M_{xy_1}\delta\kappa^o_{xy_1}\Big\}dxdy. \tag{3.31}$$

The Rayleigh-Ritz method will be used in conjunction with the first variation and the first variation of the second variation to study plate response. In either case, with a Rayleigh-Ritz approach, the variational process focuses on the variations of the amplitudes of the assumed functions used to approximate response. These variational steps lead to algebraic equations. For the prebuckling and buckling problems these equations are linear. For the buckling problem, these linear equations form the basis for eigentemperature extraction. For the postbuckling problem the equations are nonlinear and must be solved numerically for the response of the plate as a function of temperature. For determining the response in the presence of imperfections, the algebraic equations are also nonlinear.

4.0 Buckling Response

Due to the presence of edge restraints, the thermally-induced expansion of a composite plate may cause the plate to buckle. The thermal buckling problem consists, primarily, of finding the temperature at which this phenomenon occurs. In this chapter the buckling problem is discussed in detail. Inherent in this discussion is a more detailed investigation of the prebuckling problem and its role in the buckling problem. The details of the various boundary conditions and temperature distributions are first discussed, then numerical results for the various cases are presented.

4.1 Formulation

For the buckling problem, the preloading effects are assumed to be due only to thermally induced deformations. In this case

$$
\begin{aligned}
\varepsilon_x^P &= \varepsilon_x^T = \alpha_x \Delta T \\
\varepsilon_y^P &= \varepsilon_y^T = \alpha_y \Delta T \\
\gamma_{xy}^P &= \gamma_{xy}^T = \alpha_{xy} \Delta T,
\end{aligned}
\tag{4.1}
$$

where α_x, α_y, and α_{xy} are the coefficients of thermal expansion in the x-y-z coordinate system and the superscript "T" denotes the fact that the preloading effects are thermally induced. Likewise, the equivalent preloading stress resultants become equivalent thermal stress resultants:

$$
\begin{aligned}
N_x^P = N_x^T &= \int_{\frac{-H}{2}}^{\frac{+H}{2}} \sigma_x^T dz = \int_{\frac{-H}{2}}^{\frac{+H}{2}} \{\overline{Q}_{11}\alpha_x + \overline{Q}_{12}\alpha_y + \overline{Q}_{16}\alpha_{xy}\}\Delta T dz \\
N_y^P = N_y^T &= \int_{\frac{-H}{2}}^{\frac{+H}{2}} \sigma_y^T dz = \int_{\frac{-H}{2}}^{\frac{+H}{2}} \{\overline{Q}_{12}\alpha_x + \overline{Q}_{22}\alpha_y + \overline{Q}_{26}\alpha_{xy}\}\Delta T dz \\
N_{xy}^P = N_{xy}^T &= \int_{\frac{-H}{2}}^{\frac{+H}{2}} \tau_{xy}^T dz = \int_{\frac{-H}{2}}^{\frac{+H}{2}} \{\overline{Q}_{16}\alpha_x + \overline{Q}_{26}\alpha_y + \overline{Q}_{66}\alpha_{xy}\}\Delta T dz \\
M_x^P = M_x^T &= \int_{\frac{-H}{2}}^{\frac{+H}{2}} \sigma_x^T z dz = \int_{\frac{-H}{2}}^{\frac{+H}{2}} \{\overline{Q}_{11}\alpha_x + \overline{Q}_{12}\alpha_y + \overline{Q}_{16}\alpha_{xy}\}\Delta T z dz \\
M_y^P = M_y^T &= \int_{\frac{-H}{2}}^{\frac{+H}{2}} \sigma_y^T z dz = \int_{\frac{-H}{2}}^{\frac{+H}{2}} \{\overline{Q}_{12}\alpha_x + \overline{Q}_{22}\alpha_y + \overline{Q}_{26}\alpha_{xy}\}\Delta T z dz \\
M_{xy}^P = M_{xy}^T &= \int_{\frac{-H}{2}}^{\frac{+H}{2}} \tau_{xy}^T z dz = \int_{\frac{-H}{2}}^{\frac{+H}{2}} \{\overline{Q}_{16}\alpha_x + \overline{Q}_{26}\alpha_y + \overline{Q}_{66}\alpha_{xy}\}\Delta T z dz.
\end{aligned}
\tag{4.2}
$$

In the above σ_x^T, σ_y^T and τ_{xy}^T are the thermal stresses. These are the stresses at a point if the composite is fully constrained from any deformation. For these buckling studies it is further assumed that the temperature distribution is uniform through the thickness of the plate, i.e., $\Delta T = \Delta T(x, y)$. For a symmetrically laminated plate, this implies that

$$
M_x^T = M_y^T = M_{xy}^T = 0. \tag{4.3}
$$

In addition, only initially flat plates will be considered. As the only non-zero equivalent thermal stress resultants are inplane, no prebuckling out-of-plane displacements should occur. Hence,

$$\beta_x^o = -\frac{\partial w^o}{\partial x} = 0 \quad \text{and} \quad \beta_y^o = -\frac{\partial w^o}{\partial y} = 0. \tag{4.4}$$

This simplifies considerably the expressions for $\varepsilon^o_{x_1}, \ldots, N_{xy_1}$. Specifically

$$\varepsilon^o_{x_1} = \frac{\partial u_1^o}{\partial x}; \quad \varepsilon^o_{y_1} = \frac{\partial v_1^o}{\partial y}; \quad \gamma^o_{xy_1} = \frac{\partial u_1^o}{\partial y} + \frac{\partial v_1^o}{\partial x}. \tag{4.5}$$

As a result of these simplifications, the first variation of the total potential energy equated to zero can be written as

$$\pi_1 = \int\int \left\{ N_x \frac{\partial u_1^o}{\partial x} + N_y \frac{\partial v_1^o}{\partial y} + N_{xy} \left(\frac{\partial u_1^o}{\partial y} + \frac{\partial v_1^o}{\partial x} \right) \right\} dxdy = 0, \tag{4.6}$$

for every u_1^o and v_1^o. This is the equation governing prebuckling. The first variation of the second variation of the total potential energy, when written in terms of displacements, also simplifies considerably. This simplification, equated to zero, becomes

$$\begin{aligned} \delta\pi_2 = \int\int \Bigg\{ & N_x \frac{\partial w_1^o}{\partial x}\frac{\partial \delta w_1^o}{\partial x} + N_y \frac{\partial w_1^o}{\partial y}\frac{\partial \delta w_1^o}{\partial y} + N_{xy} \left(\frac{\partial w_1^o}{\partial x}\frac{\partial \delta w_1^o}{\partial y} + \frac{\partial w_1^o}{\partial y}\frac{\partial \delta w_1^o}{\partial x} \right) \\ & + N_{x_1} \frac{\partial \delta u_1^o}{\partial x} + N_{y_1} \frac{\partial \delta v_1^o}{\partial y} + N_{xy_1} \left(\frac{\partial \delta u_1^o}{\partial y} + \frac{\partial \delta v_1^o}{\partial x} \right) \\ & - M_{x_1} \frac{\partial^2 \delta w_1^o}{\partial x^2} - M_{y_1} \frac{\partial^2 \delta w_1^o}{\partial y^2} - 2M_{xy_1} \frac{\partial^2 \delta w_1^o}{\partial x \partial y} \Bigg\} dxdy = 0. \end{aligned} \tag{4.7}$$

This expression can be further simplified by considering the quantity

$$\int\int\left\{N_{x_1}\frac{\partial\delta u_1^o}{\partial x}+N_{y_1}\frac{\partial\delta v_1^o}{\partial y}+N_{xy_1}\left(\frac{\partial\delta u_1^o}{\partial y}+\frac{\partial\delta v_1^o}{\partial x}\right)\right\}dxdy. \tag{4.8}$$

In the context of a Rayleigh-Ritz formulation, u_1^o and v_1^o will be assumed to be of the form

$$\begin{aligned} u_1^o(x,y) &= \sum_m\sum_n u_{1_{mn}}\phi_{1_{mn}}(x,y) \\ v_1^o(x,y) &= \sum_m\sum_n v_{1_{mn}}\psi_{1_{mn}}(x,y), \end{aligned} \tag{4.9}$$

where $u_{1_{mn}}$ and $v_{1_{mn}}$ are the to-be-determined constants and $\phi_{1_{mn}}$ and $\psi_{1_{mn}}$ are known functional forms. With eqn. 4.9 the expression of eqn. 4.8 becomes

$$\sum_m\sum_n\left[\int\int\left\{\left(N_{x_1}\frac{\partial\phi_{1_{mn}}}{\partial x}+N_{xy_1}\frac{\partial\phi_{1_{mn}}}{\partial y}\right)\delta u_{1_{mn}}+\left(N_{y_1}\frac{\partial\psi_{1_{mn}}}{\partial y}+N_{xy_1}\frac{\partial\psi_{1_{mn}}}{\partial x}\right)\delta v_{1_{mn}}\right\}dxdy\right]. \tag{4.10}$$

Since these are the only terms in eqn. 4.7 that involve $\delta u_{1_{mn}}$ and $\delta v_{1_{mn}}$, it is clear that the expression of eqn. 4.10 must be zero for $\delta\pi_2$ to be zero. This means

$$u_{1_{mn}}=v_{1_{mn}}=0 \quad \text{for all m and n} \tag{4.11}$$

or

$$u_1^o(x,y)=v_1^o(x,y)=0. \tag{4.12}$$

As a result, eqn. 4.7 can be reduced to

$$\delta\pi_2 = \int\int\left\{N_x \frac{\partial w_1^o}{\partial x}\frac{\partial \delta w_1^o}{\partial x} + N_y \frac{\partial w_1^o}{\partial y}\frac{\partial \delta w_1^o}{\partial y} + N_{xy}\left(\frac{\partial w_1^o}{\partial x}\frac{\partial \delta w_1^o}{\partial y} + \frac{\partial w_1^o}{\partial y}\frac{\partial \delta w_1^o}{\partial x}\right)\right.$$
$$\left. - M_{x_1}\frac{\partial^2 \delta w_1^o}{\partial x^2} - M_{y_1}\frac{\partial^2 \delta w_1^o}{\partial y^2} - 2M_{xy_1}\frac{\partial^2 \delta w_1^o}{\partial x \partial y}\right\} dxdy = 0. \tag{4.13}$$

This is the form that will be used to study buckling. To this point the equations developed are valid for any set of edge conditions, and any temperature distribution such that the thermal moments are zero. In this study, as mentioned previously, two boundary conditions, fixed and sliding simple supports, are considered. These boundary conditions were given previously and are repeated here for convenience. They are:

Fixed:

at $x = 0,\ a$:

$$\begin{aligned} &\text{i) } u^o = 0 \\ &\text{ii) } v^o = 0 \\ &\text{iii) } w^o = 0 \\ &\text{iv) } M_x = 0. \end{aligned} \tag{4.14a}$$

at $y = 0,\ b$:

$$\begin{aligned} &\text{i) } u^o = 0 \\ &\text{ii) } v^o = 0 \\ &\text{iii) } w^o = 0 \\ &\text{iv) } M_y = 0. \end{aligned} \tag{4.14b}$$

Sliding:

at $x = 0,\ a$:

$$\begin{aligned} &\text{i) } u^o = 0 \\ &\text{ii) } N_{xy} = 0 \\ &\text{iii) } w^o = 0 \\ &\text{iv) } M_x = 0. \end{aligned} \tag{4.15a}$$

$$\text{at } y=0,\ b: \quad \begin{array}{l} \text{i) } N_{xy}=0 \\ \text{ii) } v^{o}=0 \\ \text{iii) } w^{o}=0 \\ \text{iv) } M_{y}=0. \end{array} \tag{4.15b}$$

The sliding boundary condition implies that there is no resistance to the inplane shear force at the edge.

Two temperature distributions will be considered. The first, a uniform change in temperature, is actually a subclass of the second, a change in temperature which varies linearly in the x direction. These two conditions can be expressed as

$$\begin{array}{c} \Delta T = c \\ \text{and} \\ \Delta T = c + dx, \end{array} \tag{4.16}$$

c and d being constants. With the second form, the temperature change at $x=0$ is c, while the temperature change at $x=a$ is $c + da$. If $d=0$ the change in temperature is uniform. These two temperature distributions will be considered separately. Prebuckling and buckling for these temperature distributions and the various boundary conditions will be discussed next.

4.1.1 Uniform Change in Temperature: $\Delta T = c$

4.1.1.1 Fixed Simple Supports

In order to obtain solutions using the Rayleigh-Ritz method, the following forms are assumed for the prebuckling displacements u^o, v^o, and w^o in the case of fixed simple supports:

$$
\begin{aligned}
u^o(x, y) &= \sum_{i=1}^{I} \sum_{j=1}^{J} u_{ij} \sin\left(\frac{i\pi x}{a}\right) \sin\left(\frac{j\pi y}{b}\right) \\
v^o(x, y) &= \sum_{i=1}^{I} \sum_{j=1}^{J} v_{ij} \sin\left(\frac{i\pi x}{a}\right) \sin\left(\frac{j\pi y}{b}\right) \\
w^o(x, y) &= 0.
\end{aligned}
\tag{4.17}
$$

These forms satisfy the kinematic boundary conditions of eqn. 4.14. These forms follow the work of Huang and Tauchert [9]. For this case, the prebuckling solution is trivial. This can be seen as follows: The prebuckling equation, 4.6, can be expanded to obtain

$$
\begin{aligned}
\pi_1 = \int\!\!\int \Bigg\{ & A_{11} \frac{\partial u^o}{\partial x} \frac{\partial \delta u^o}{\partial x} + A_{12}\left(\frac{\partial v^o}{\partial y} \frac{\partial \delta u^o}{\partial x} + \frac{\partial u^o}{\partial x} \frac{\partial \delta v^o}{\partial y} \right) + A_{22} \frac{\partial v^o}{\partial y} \frac{\partial \delta v^o}{\partial y} \\
& + A_{16}\left(\frac{\partial u^o}{\partial y} \frac{\partial \delta u^o}{\partial x} + \frac{\partial v^o}{\partial x} \frac{\partial \delta u^o}{\partial x} + \frac{\partial u^o}{\partial x} \frac{\partial \delta u^o}{\partial y} + \frac{\partial u^o}{\partial x} \frac{\partial \delta v^o}{\partial x} \right) \\
& + A_{26}\left(\frac{\partial u^o}{\partial y} \frac{\partial \delta v^o}{\partial y} + \frac{\partial v^o}{\partial x} \frac{\partial \delta v^o}{\partial y} + \frac{\partial v^o}{\partial y} \frac{\partial \delta u^o}{\partial y} + \frac{\partial v^o}{\partial y} \frac{\partial \delta v^o}{\partial x} \right) \\
& + A_{66}\left(\frac{\partial u^o}{\partial y} + \frac{\partial v^o}{\partial x} \right)\left(\frac{\partial \delta u^o}{\partial y} + \frac{\partial \delta v^o}{\partial x} \right) \\
& - N_x^T \frac{\partial u^o}{\partial x} - N_y^T \frac{\partial v^o}{\partial y} - N_{xy}^T\left(\frac{\partial u^o}{\partial y} + \frac{\partial v^o}{\partial x} \right) \Bigg\} dxdy = 0,
\end{aligned}
\tag{4.18}
$$

where eqn. 3.5 and 3.13 have been used with eqn. 4.2 and 4.5. The expression

$$
-\int\!\!\int \left\{ N_x^T \frac{\partial u^o}{\partial x} + N_y^T \frac{\partial v^o}{\partial y} + N_{xy}^T\left(\frac{\partial u^o}{\partial y} + \frac{\partial v^o}{\partial x} \right) \right\} dxdy \tag{4.19}
$$

becomes the forcing vector in the system of linear equations resulting from substitution of the assumed function of eqn 4.17 into eqn. 4.18. It is clear that u_{ij} and v_{ij} will only be non-zero when the expression of eqn. 4.19 is non-zero.

Prebuckling can be investigated more easily for each temperature distribution by first expressing the thermal stress resultants as

$$
\begin{aligned}
N_x^T &= \overline{N}_x^T \Delta T \\
N_y^T &= \overline{N}_y^T \Delta T \\
N_{xy}^T &= \overline{N}_{xy}^T \Delta T,
\end{aligned}
\tag{4.20}
$$

where the barred quantities are thermal stress resultants per unit change in temperature. These quantities are constant for a specific laminate and consist only of layer material properties and layer thicknesses. Using this scheme, it is clear that the expression of eqn. 4.19, and therefore u^o and v^o, are zero for the case of a spatially uniform change in temperature and fixed simple supports. The inplane stress resultants are then uniform within the plate and are given by

$$
\begin{aligned}
N_x &= -N_x^T = -\overline{N}_x^T \Delta T \\
N_y &= -N_y^T = -\overline{N}_y^T \Delta T \\
N_{xy} &= -N_{xy}^T = -\overline{N}_{xy}^T \Delta T.
\end{aligned}
\tag{4.21}
$$

Once the prebuckling problem has been solved, the buckling problem can be addressed. The inplane stress resultants of eqn. 4.21 are substituted into eqn. 4.13. This results in the following form for the first variation of the second variation:

$$
\begin{aligned}
\delta\pi_2 = \int\int \Bigg\{ & -\overline{N}_x^T \Delta T \frac{\partial w_1^o}{\partial x}\frac{\partial \delta w_1^o}{\partial x} - \overline{N}_y^T \Delta T \frac{\partial w_1^o}{\partial y}\frac{\partial \delta w_1^o}{\partial y} - \overline{N}_{xy}^T \Delta T \left(\frac{\partial w_1^o}{\partial x}\frac{\partial \delta w_1^o}{\partial y} + \frac{\partial w_1^o}{\partial y}\frac{\partial \delta w_1^o}{\partial x} \right) \\
& - M_{x_1} \frac{\partial^2 \delta w_1^o}{\partial x^2} - M_{y_1} \frac{\partial^2 \delta w_1^o}{\partial y^2} - 2M_{xy_1} \frac{\partial^2 \delta w_1^o}{\partial x \partial y} \Bigg\} dxdy,
\end{aligned}
\tag{4.22}
$$

where, again, $\overline{N}_x^T$, $\overline{N}_y^T$, and $\overline{N}_{xy}^T$ are known constants, and ΔT is the to-be-determined buckling temperature. A double sine series is then assumed for the buckling displacement, w_1^o. This series is

$$w_1^o(x, y) = \sum_{m=1}^{M} \sum_{n=1}^{N} w_{mn} \sin\left(\frac{m\pi x}{a}\right) \sin\left(\frac{n\pi y}{b}\right). \tag{4.23}$$

Note that while this satisfies the geometric boundary conditions of eqn. 4.14, it does not satisfy the moment boundary conditions. Substituting the expression of eqn. 4.23 into eqn. 4.22, and performing the spatial integration results in a set of M × N linear simultaneous homogeneous equations in w_{mn} . Eigentemperature extraction is then performed to find the values of ΔT for which the coefficient matrix becomes singular. The smallest value of ΔT for which this occurs is the critical buckling temperature.

4.1.1.2 Sliding Simple Supports

Following the work of Huang and Tauchert [9] as before, the following forms are assumed for the prebuckling displacements in the case of sliding simple supports:

$$\begin{aligned} u^o(x, y) &= \sum_{i=1}^{I} \sum_{j=0}^{J} u_{ij} \sin\left(\frac{i\pi x}{a}\right) \cos\left(\frac{j\pi y}{b}\right) \\ v^o(x, y) &= \sum_{i=0}^{I} \sum_{j=1}^{J} v_{ij} \cos\left(\frac{i\pi x}{a}\right) \sin\left(\frac{j\pi y}{b}\right) \\ w^o(x, y) &= 0. \end{aligned} \tag{4.24}$$

Note that these assumed solutions satisfy identically the geometric boundary conditions, but not the force boundary conditions of eqn. 4.15. Again using eqn. 4.18 and considering the expression given in eqn. 4.19, it can be seen that, for plates with sliding simple supports, if the laminate is such that the material property $\overline{N}_{xy}^T = 0$, the prebuckling solution is trivial. This is the situation, for instance, for quasi-isotropic laminates. For these cases then, the prebuckling inplane stress resultants are given, as before, by eqn. 4.21. However for laminates such as the off-axis orthotropic laminate, for which $\overline{N}^T_{xy}$ is not zero, the prebuckling solution is not so simple. In these cases the inplane displacements, hence the prebuckling stress resultants, vary throughout the laminate. This nontrivial prebuckling problem is solved by substituting the assumed solution form of eqn. 4.24 into the expression for the first variation, eqn. 4.18. Performing the spatial integration leads to a linear set of algebraic equations for u_{ij} and v_{ij}. With these solved for, the stress resultants can be determined for use in eqn. 4.13. The stress resultants, as stated previously, vary with x and y. Also they are linearly proportional to the temperature change, ΔT. Thus they are of the form

$$\begin{aligned} N_x(x, y) &= \overline{N}_x(x, y)\Delta T \\ N_y(x, y) &= \overline{N}_y(x, y)\Delta T \\ N_{xy}(x, y) &= \overline{N}_{xy}(x, y)\Delta T. \end{aligned} \tag{4.25}$$

The second variation of eqn. 4.22 now takes the form

$$\begin{aligned} \delta\pi_2 = \int\int\Bigg\{ & \overline{N}_x\Delta T\frac{\partial w_1^o}{\partial x}\frac{\partial \delta w_1^o}{\partial x} + \overline{N}_y\Delta T\frac{\partial w_1^o}{\partial y}\frac{\partial \delta w_1^o}{\partial y} + \overline{N}_{xy}\Delta T\left(\frac{\partial w_1^o}{\partial x}\frac{\partial \delta w_1^o}{\partial y} + \frac{\partial w_1^o}{\partial y}\frac{\partial \delta w_1^o}{\partial x}\right) \\ & - M_{x_1}\frac{\partial^2 \delta w_1^o}{\partial x^2} - M_{y_1}\frac{\partial^2 \delta w_1^o}{\partial y^2} - 2M_{xy_1}\frac{\partial^2 \delta w_1^o}{\partial x \partial y}\Bigg\}dxdy. \end{aligned} \tag{4.26}$$

The double series of eqn. 4.23 is again assumed for the buckling displacement $w_1^o(x, y)$. With this form substituted into eqn. 4.26, and with the functional form of $\overline{N}_x$, $\overline{N}_y$ and $\overline{N}_{xy}$ now known, the spatial integral can be carried out. An eigenvalue problem for ΔT results. It is important to note that since the assumed solution for w_1^o and the prebuckling solution are the same for both fixed and sliding simple supports when the laminate is such that $\overline{N}^T_{xy} = 0$, these plates have the same buckling solution for both sets of boundary conditions when buckling is due to a uniform change in temperature.

4.1.2 Linearly Varying Change in Temperature: $\Delta T = c + dx$

4.1.2.1 Fixed Simple Supports

For a linearly varying temperature distribution, the inplane thermal stress resultants can be written as

$$
\begin{aligned}
N_x^T &= \bar{N}_x^T \Delta T = \bar{N}_x^T (c + dx) \\
N_y^T &= \bar{N}_y^T \Delta T = \bar{N}_y^T (c + dx) \\
N_{xy}^T &= \bar{N}_{xy}^T \Delta T = \overline{N_{xy}^T} (c + dx).
\end{aligned}
\tag{4.27}
$$

Using eqn. 4.27, the expression in eqn. 4.19 can be expanded as follows

$$
\begin{aligned}
&-\int\int \left\{ N_x^T \frac{\partial u^o}{\partial x} + N_y^T \frac{\partial v^o}{\partial y} + N_{xy}^T \left(\frac{\partial u^o}{\partial y} + \frac{\partial v^o}{\partial x} \right) \right\} dxdy \\
&\quad = -c\int\int \left\{ \bar{N}_x^T \frac{\partial u^o}{\partial x} + \bar{N}_y^T \frac{\partial v^o}{\partial y} + \bar{N}_{xy}^T \left(\frac{\partial u^o}{\partial y} + \frac{\partial v^o}{\partial x} \right) \right\} dxdy \\
&\quad -d\int\int \left\{ \bar{N}_x^T \frac{\partial u^o}{\partial x} + \bar{N}_y^T \frac{\partial v^o}{\partial y} + \bar{N}_{xy}^T \left(\frac{\partial u^o}{\partial y} + \frac{\partial v^o}{\partial x} \right) \right\} xdxdy.
\end{aligned}
\tag{4.28}
$$

The series solutions for the prebuckling displacements are assumed to be the same for this case as for the case of fixed simple supports and a uniform change in temperature, given in eqn. 4.17. As a result, the coefficient of c has already been determined to be zero. The coefficient of d, however, is nonzero. Because of the forms of eqn. 4.17 and 4.28, the assumed solutions for u^o and v^o can be expressed as linear functions of d, i.e.,

$$\begin{aligned} u^o(x, y) &= d\bar{u}^o(x, y) \\ v^o(x, y) &= d\bar{v}^o(x, y). \end{aligned} \tag{4.29}$$

The functional forms assumed for $\bar{u}^o(x, y)$ and $\bar{v}^o(x, y)$ are as in eqn. 4.17, namely

$$\begin{aligned} \bar{u}^o(x, y) &= \sum_{i=1}^{I} \sum_{j=1}^{J} \bar{u}_{ij} \sin\left(\frac{i\pi x}{a}\right) \sin\left(\frac{j\pi y}{b}\right) \\ \bar{v}^o(x, y) &= \sum_{i=1}^{I} \sum_{j=1}^{J} \bar{v}_{ij} \sin\left(\frac{i\pi x}{a}\right) \sin\left(\frac{j\pi y}{b}\right). \end{aligned} \tag{4.30}$$

Substituting eqn. 4.30 into eqn. 4.28, and those results into eqn. 4.18, and performing the spatial integration leads to a set of linear algebraic equations for $\bar{u}_{ij}$ and $\bar{v}_{ij}$. Note, at this point d is not involved.

With $\bar{u}_{ij}$ and $\bar{v}_{ij}$ known, the prebuckling stress resultants are now known to within the parameters c and d and are given by

$$\begin{aligned} N_x &= d\left(A_{11}\frac{\partial \bar{u}^o}{\partial x} + A_{12}\frac{\partial \bar{v}^o}{\partial y} + A_{16}\left(\frac{\partial \bar{u}^o}{\partial y} + \frac{\partial \bar{v}^o}{\partial x}\right)\right) - \bar{N}_x^T(c + dx) \\ N_y &= d\left(A_{12}\frac{\partial \bar{u}^o}{\partial x} + A_{22}\frac{\partial \bar{v}^o}{\partial y} + A_{26}\left(\frac{\partial \bar{u}^o}{\partial y} + \frac{\partial \bar{v}^o}{\partial x}\right)\right) - \bar{N}_y^T(c + dx) \\ N_{xy} &= d\left(A_{16}\frac{\partial \bar{u}^o}{\partial x} + A_{26}\frac{\partial \bar{v}^o}{\partial y} + A_{66}\left(\frac{\partial \bar{u}^o}{\partial y} + \frac{\partial \bar{v}^o}{\partial x}\right)\right) - \bar{N}_{xy}^T(c + dx). \end{aligned} \tag{4.31}$$

To determine the buckling characteristics, these quantities must be substituted into eqn. 4.13 along with the assumed solution for the buckling displacement, w_1^o. The buckling displacements are again taken to be of the form of eqn. 4.23. When the spatial integrals in eqn. 4.13 are carried out, an eigenvalue problem involving c and d results. For this situation, it is necessary to find the relation between c and d which will cause buckling. Operationally this means that either d is specified and the eigentemperature problem is solved for the lowest value of c necessary to cause buckling, or vice versa.

4.1.2.2 Sliding Simple Supports

The case of a linearly varying temperature and sliding simple supports is the most complicated buckling condition studied. Equation 4.28 is again the key equation. For this case the first term on the right hand side of eqn. 4.28 is not zero and thus the prebuckling displacements are linear functions of both c and d, namely

$$
\begin{aligned}
u^o(x, y) &= c\hat{u}^o(x, y) + d\bar{u}^o(x, y) \\
v^o(x, y) &= c\hat{v}^o(x, y) + d\bar{v}^o(x, y).
\end{aligned}
\tag{4.32}
$$

The functional forms in this equation are assumed to be as in eqn. 4.24, the form used for sliding simple supports and a uniform temperature. Specifically

$$
\begin{aligned}
\left(\hat{u}^o(x, y), \bar{u}^o(x, y)\right) &= \sum_{i=1}^{I} \sum_{j=0}^{J} (\hat{u}_{ij}, \bar{u}_{ij}) \sin\left(\frac{i\pi x}{a}\right) \cos\left(\frac{j\pi y}{b}\right) \\
\left(\hat{v}^o(x, y), \bar{v}^o(x, y)\right) &= \sum_{i=0}^{I} \sum_{j=1}^{J} (\hat{v}_{ij}, \bar{v}_{ij}) \cos\left(\frac{i\pi x}{a}\right) \sin\left(\frac{j\pi y}{b}\right).
\end{aligned}
\tag{4.33}
$$

These functional forms are substituted into eqn. 4.18 and a set of linear equations for $\hat{u}_{ij}$, $\bar{u}_{ij}$, $\hat{v}_{ij}$, and $\bar{v}_{ij}$ result. The inplane stress resultants are now known and are of the form

$$
\begin{aligned}
N_x &= c\left(A_{11}\frac{\partial \hat{u}^o}{\partial x} + A_{12}\frac{\partial \hat{v}^o}{\partial y} + A_{16}\left(\frac{\partial \hat{u}^o}{\partial y} + \frac{\partial \hat{v}^o}{\partial x}\right) - \bar{N}_x^T\right) \\
&\quad + d\left(A_{11}\frac{\partial \bar{u}^o}{\partial x} + A_{12}\frac{\partial \bar{v}^o}{\partial y} + A_{16}\left(\frac{\partial \bar{u}^o}{\partial y} + \frac{\partial \bar{v}^o}{\partial x}\right) - \bar{N}_x^T x\right) \\
N_y &= c\left(A_{12}\frac{\partial \hat{u}^o}{\partial x} + A_{22}\frac{\partial \hat{v}^o}{\partial y} + A_{26}\left(\frac{\partial \hat{u}^o}{\partial y} + \frac{\partial \hat{v}^o}{\partial x}\right) - \bar{N}_y^T\right) \\
&\quad + d\left(A_{12}\frac{\partial \bar{u}^o}{\partial x} + A_{22}\frac{\partial \bar{v}^o}{\partial y} + A_{26}\left(\frac{\partial \bar{u}^o}{\partial y} + \frac{\partial \bar{v}^o}{\partial x}\right) - \bar{N}_y^T x\right) \\
N_{xy} &= c\left(A_{16}\frac{\partial \hat{u}^o}{\partial x} + A_{26}\frac{\partial \hat{v}^o}{\partial y} + A_{66}\left(\frac{\partial \hat{u}^o}{\partial y} + \frac{\partial \hat{v}^o}{\partial x}\right) - \bar{N}_{xy}^T\right) \\
&\quad + d\left(A_{16}\frac{\partial \bar{u}^o}{\partial x} + A_{26}\frac{\partial \bar{v}^o}{\partial y} + A_{66}\left(\frac{\partial \bar{u}^o}{\partial y} + \frac{\partial \bar{v}^o}{\partial x}\right) - \bar{N}_{xy}^T x\right).
\end{aligned}
\tag{4.34}
$$

The assumed solution for w_1^o is again eqn. 4.23. Substituting eqn. 4.34 and eqn. 4.28 into 4.13, and carrying out the spatial integrals, results in another eigenvalue problem involving c and d. The buckling characteristics are studied by solving, numerically, for a relation between c and d, either by specifying d and solving for the lowest value of c to cause buckling, or vice versa.

This completes the formulation of the buckling problems studied. As can be seen, some problems are quite involved, while others are simpler. In the next section, numerical results will be presented which illustrate the influence of lamination sequence, skewing angle, plate aspect ratio, boundary conditions, and temperature gradient on buckling. Convergence of the prebuckling and buckling solutions will be discussed, as will the sensitivity of the results to material properties. This latter study is useful because the material properties required for a buckling analysis are not always known with certainty.

4.2 Numerical Results

Numerical results are given to illustrate the influence of various factors on the thermal buckling of symmetric composite plates. The material properties used in the following results represent a graphite-reinforced composite. These properties are:

$$\begin{gathered} E_1 = 22.5 \text{ Msi} \quad E_2 = 1.17 \text{ Msi} \quad G_{12} = 0.66 \text{ Msi} \quad \nu_{12} = 0.22 \\ \alpha_1 = -0.04 \text{ ppm/°F} \quad \alpha_2 = 16.7 \text{ ppm/°F} \end{gathered} \tag{4.35}$$

These properties are defined in the principal material system of a layer and follow the usual notation. Lamina thickness is 0.005 inches. The laminates that will be discussed in particular are a quasi-isotropic $(\pm 45/0/90)_s$ and an orthotropic $(\pm 45/0_2)_s$. Off-axis skew angles for the material axes are in the range $-30° \leq \alpha \leq 30°$.

4.2.1 Uniform Change in Temperature: $\Delta T = c$

4.2.1.1 Convergence Characteristics: Trivial Prebuckling Solution

Since the Rayleigh-Ritz method is used here to obtain approximate solutions, the first issue to be addressed is that of convergence. In order to study convergence in the buckling solution, the case of fixed simple supports is considered first. This is because the prebuckling solutions for this case are already known to be trivial. Thus only convergence of the series representing the buckling displacement w_1^0 needs to be considered. As an example, the convergence characteristic of the solution for the buckling of a square, $(\pm 45/0_2)_s$ plate with fixed simple supports is given in Table 1. The other laminates considered here required the same number, or fewer, terms to be taken to obtain convergence of the buckling solution. This case is thus used as an example. To obtain numerical results for this table, a 6 in. by 6 in. laminate is considered. The conclusions from the table are not limited by these specific dimensions. These dimensions are chosen based on future experimental considerations. In Table 1, $M \times N$ is the number of terms taken in the series for w_1^0, ΔT_1 is the first eigentemperature (the critical buckling temperature), and ΔT_2 is the second eigentemperature. In all cases, N is taken to be equal to M, and the product of these numbers is reported. The product represents the actual number of terms in the series for w_1^0. Both ΔT_1 and ΔT_2 are examined because when using the Rayleigh-Ritz method, the lower eigenvalues tend to converge more rapidly than the higher eigenvalues [19]. Thus ΔT_1 should be well converged at the point where ΔT_2 shows convergence. By the same reasoning, because the eigenvectors tend to converge more slowly than the eigenvalues, the largest elements in the first eigenvector, w_{11} and w_{22}, are also given as an indication of convergence. The eigensolver subroutine (IMSL math library subroutine G2CRG [20]) used in this study normalizes the eigenvector by its largest element, thus the largest term, w_{11} in this case, is always set to one. Attention should thus focus on w_{22}, the second element in the first eigenvector. As can be seen from Table 1, for this case of fixed simple supports reasonably accurate convergence is achieved for $M \times N = 49$. Using $M \times N = 49$ results in a buckling temperature of 69.4°F. This will be considered the answer for the case. In addition, the value of $\Delta T = 69.4$°F will be referred to as ΔT^* in the remainder of the text.

The convergence characteristic of quasi-isotropic $(\pm 45/0/90)_s$ plates with either fixed or sliding simple supports and any material axis skew angle, and of orthotropic $(\pm 45/0_2)_s$ plates for the case of no material axis skewing ($\alpha = 0°$) with sliding simple supports is also given by Table 1. As discussed previously, these cases have a trivial prebuckling solution, and the same series for w_1^0 is used to represent buckling. Thus the convergence of these cases follows Table 1.

Table 1. BUCKLING CONVERGENCE STUDY FOR THE UNIFORM TEMPERATURE CASE: $(\pm 45/0_2)_S$ PLATE, SQUARE, $\alpha = 0°$, FIXED SIMPLE SUPPORTS.

$M \times N^{(1)}$	$\Delta T_1^{(2)}$	$\Delta T_2^{(2)}$	W_{11}	W_{22}
1	1.029	—	—	—
4	1.009	116.6	1.000	0.0400
9	1.007	114.2	1.000	0.0420
16	1.004	114.0	1.000	0.0412
25	1.003	113.7	1.000	0.0417
36	1.001	113.6	1.000	0.0414
49	1.000	113.5	1.000	0.0415
64	1.000	113.4	1.000	0.0416

(1) $M \times N$ is the number of terms taken in the series for w_1^o.

(2) Results normalized by $\Delta T^* = 69.4°F$, the temperature considered here as the converged value. This represents the buckling temperature for a 6 in. by 6 in. plate.

4.2.1.2 *Convergence Characteristics: Nontrivial Prebuckling Solution*

To begin studying the convergence of a case for which the prebuckling solution is spatially nonuniform. it is natural to begin by using the number of terms in the buckling solution which resulted in convergence for the previous case. There are two approaches that may be taken to study convergence. One approach is to consider the convergence of the prebuckling solution separately from the buckling solution. The other approach is to consider only the effect on the buckling solution of increasing the number of terms taken in the prebuckling solution. The first approach requires a much larger number of terms to be taken in order to reach convergence. The lack of convergence of the prebuckling solution does not seem to have a serious effect on the buckling calculations. Therefore, because the buckling solution is the primary focus in this study, and in the interest of economy, the latter approach is taken here. The effect that the number of terms taken in the prebuckling solution, $I \times J$, has on the critical buckling temperature, as well as the effect of increasing the number of terms, $M \times N$, taken in the assumed solution for w_1^o, are shown in Table 2. The specific case considered is a square $(\pm 45/0_2)_s$ laminate with it's material axes skewed by $\alpha = 30°$ and sliding simple supports. This case represents an extreme in the spatial variation of the prebuckling solution. The largest elements in the first eigenvector are again given as another indication of convergence. Table 2 indicates that the same number of terms in the assumed solution for w_1^o which provided convergence in the case of fixed simple supports and/or no material axis skewing (Table 1, $M \times N = 49$) provides sufficient convergence in this case as well. Although a relatively large number of terms must be taken in the prebuckling solution for the buckling solution to converge, there is only about an 8% difference in the buckling temperature between using a 1-term prebuckling solution and a 100-term prebuckling solution! This supports the earlier statement that lack of convergence of the prebuckling solution is not a serious problem. Henceforth, all buckling results reported for the case of sliding simple supports and a uniform temperature change will use $M \times N = 49$ and $I \times J = 81$, a well converged solution.

Table 2. PREBUCKLING CONVERGENCE STUDY FOR THE UNIFORM TEMPERATURE CASE: $(\pm 45/0_2)_S$ PLATE, SQUARE, $\alpha = 30°$, SLIDING SIMPLE SUPPORTS.

M × N = 25				M × N = 36			
I × J	$\Delta T_1^{(1)}$	w_{11}	w_{22}	I × J	$\Delta T_1^{(1)}$	w_{11}	w_{22}
1	0.719	1.000	0.0497	1	0.718	1.000	0.0496
4	0.697	1.000	0.0477	4	0.694	1.000	0.0474
9	0.679	1.000	0.0544	9	0.677	1.000	0.0540
16	0.677	1.000	0.0534	16	0.674	1.000	0.0537
25	0.671	1.000	0.0538	25	0.669	1.000	0.0533
36	0.669	1.000	0.0534	36	0.667	1.000	0.0534
49	0.667	1.000	0.0537	49	0.666	1.000	0.0531
64	0.666	1.000	0.0535	64	0.664	1.000	0.0535
81	0.662	1.000	0.0535	81	0.661	1.000	0.0530
100	0.662	1.000	0.0535	100	0.661	1.000	0.0530
M × N = 49				M × N = 64			
I × J	$\Delta T_1^{(1)}$	w_{11}	w_{22}	I × J	$\Delta T_1^{(1)}$	w_{11}	w_{22}
1	0.716	1.000	0.0496	1	0.715	1.000	0.0493
4	0.694	1.000	0.0477	4	0.693	1.000	0.0475
9	0.677	1.000	0.0542	9	0.677	1.000	0.0542
16	0.674	1.000	0.0541	16	0.673	1.000	0.0538
25	0.667	1.000	0.0535	25	0.667	1.000	0.0535
36	0.666	1.000	0.0537	36	0.666	1.000	0.0534
49	0.664	1.000	0.0535	49	0.664	1.000	0.0535
64	0.662	1.000	0.0532	64	0.662	1.000	0.0532
81	0.661	1.000	0.0533	81	0.661	1.000	0.0532
100	0.661	1.000	0.0533	100	0.661	1.000	0.0531

(1) Normalized by $\Delta T^* = 69.4°F$, 6 in. by 6 in. plate used to compute numerical results.

4.2.1.3 Sensitivity Study

Having established the convergence of the buckling solution, the next issue to be considered here is the sensitivity of the buckling solution to variations in the material properties. This gives an indication of the degree of uncertainty that may be present in the buckling solution due to uncertainty in the material properties. It also gives an indication of how the buckling temperatures of plates with slightly different material systems would compare to the buckling temperatures of the laminates considered in this study. The variation in the buckling temperatures of four laminates with fixed simple supports resulting from varying each material property, except α_1, by $\pm$ 10% is given in Table 3. The range of values given for α_1 represent the degree of uncertainty associated with a property value that is so close to zero. The resulting buckling temperatures for each laminate are normalized by the buckling temperature for that laminate which results from using the original material properties given in eqn. 4.35. This buckling temperature is denoted as ΔT^{nom}. The value of ΔT^{nom} for each laminate is noted in Table 3. This normalization allows a direct comparison of the percentage change in buckling temperature, in each case, resulting from a percentage change in the given material property. It is clear from Table 3 that the buckling temperature is most sensitive to α_2, varying by more than 10% as a result of a 10% variation in α_2. It is likely that if α_1 were a larger quantity, a similar relation might result, however, because α_1 is so small, even a change in sign results in less than an 8% variation in buckling temperature. Variations of $\pm$ 10% in E_1 result in roughly a $\pm$ 10% variation in buckling temperature, while the same variations in E_2 have the opposite effect, a +10% variation in E_2 resulting in roughly a -10% variation in buckling temperature. Variations of $\pm$ 10% in G_{12} or in ν_{12} result in a difference of 2% or less in buckling temperature. Attention now turns to the influence of geometry, material axis skewing, support conditions, and lamination sequence on the buckling characteristics.

Table 3. SENSITIVITY STUDY FOR THE UNIFORM TEMPERATURE CASE: SQUARE PLATE, FIXED SIMPLE SUPPORTS.

VARIABLE PROPERTY		NORMALIZED BUCKLING TEMPERATURE $(\pm 45/0/90)_s$ $\alpha = 0°$ $\Delta T^{nom} = 69.4^{(1)}$	$(\pm 45/0/90)_s$ $\alpha = 30°$ $\Delta T^{nom} = 51.3$	$(\pm 45/0_2)_s$ $\alpha = 0°$ $\Delta T^{nom} = 69.4$	$(\pm 45/0_2)_s$ $\alpha = 30°$ $\Delta T^{nom} = 49.5$
E_1	+10%	1.099	1.091	1.099	1.092
	-10%	0.904	0.909	0.904	0.908
E_2	+10%	0.909	0.911	0.909	0.910
	-10%	1.114	1.111	1.114	1.113
G_{12}	+10%	1.001	1.006	1.001	1.006
	-10%	0.999	0.994	0.999	0.994
ν_{12}	+10%	0.983	0.984	0.983	0.983
	-10%	1.020	1.016	1.020	1.018
$\alpha_1 =$	+.04E-6	0.927	0.931	0.927	0.926
	0	0.963	0.964	0.963	0.961
	-.04E-6	1.000	1.000	1.000	1.000
α_2	+10%	0.895	0.895	0.895	0.895
	-10%	1.120	1.117	1.120	1.119

(1) ΔT^{nom} = buckling temperature using the nominal material properties given in eqn. 4.35, 6 in. by 6 in. plate used to compute numerical results.

4.2.1.4 Buckling Characteristics

The buckling temperatures of the two laminates as a function of principal material axis skewing angle, α, are shown in Fig. 2 for aspect ratio a/b = 1 and both sets of boundary conditions. These results are based on 6 in. square plates and have been normalized by ΔT^*, the buckling temperature of the quasi-isotropic $(\pm 45/0/90)_s$ laminate when $\alpha = 0°$. The actual buckling temperature for this 8-layer 6 in. square laminate is $\Delta T^* = 69.4°F$. It is important to note that this buckling temperature is quite high as compared to the buckling temperatures of steel and aluminum plates for the same dimensions. For these materials the buckling temperatures are $\Delta T = 8.7°F$ and $\Delta T = 4.2°F$, respectively. Several interesting features regarding the buckling of the various cases are evident in Fig. 2. First, both laminates under either boundary condition experience a decrease in buckling temperature when the material axes are skewed, i. e., $\alpha \neq 0$. For the so-called quasi-isotropic laminate, the fact that the buckling temperature varies with α serves as a reminder that the term quasi-isotropic really refers only to inplane properties of the laminate. The out-of-plane properties are not quasi-isotropic and this results in a dependence of the buckling temperature on skew angle in much the same way that the buckling temperature of a $(\pm 45/0_2)_s$ laminate depends on skew angle. As mentioned above, the buckling response for the quasi-isotropic laminate is the same for both fixed and sliding simple supports. This is due to the fact that for this laminate the material property $\overline{N}^T_{xy} = 0$ is independent of α. Differences in the buckling temperatures due to the two types of edge conditions exist only for the orthotropic $(\pm 45/0_2)_s$ laminate with $\alpha \neq 0°$. This is because $\overline{N}^T_{xy} \neq 0$ for these cases, hence there is a non-zero prebuckling solution for N_{xy} for the sliding simple support case. Indeed, the differences between the buckling solutions for the orthotropic plates with fixed and with sliding boundary conditions increase as the magnitude of α, and hence $\overline{N}^T_{xy}$, increases. However, even at $\alpha = 30°$ the difference between the buckling temperatures for the two sets of boundary conditions is only about 10%. Due to the influence of the prebuckling solution on the buckling problem, there is a greater difference between the buckling temperatures of the orthotropic laminate with fixed simple supports and the

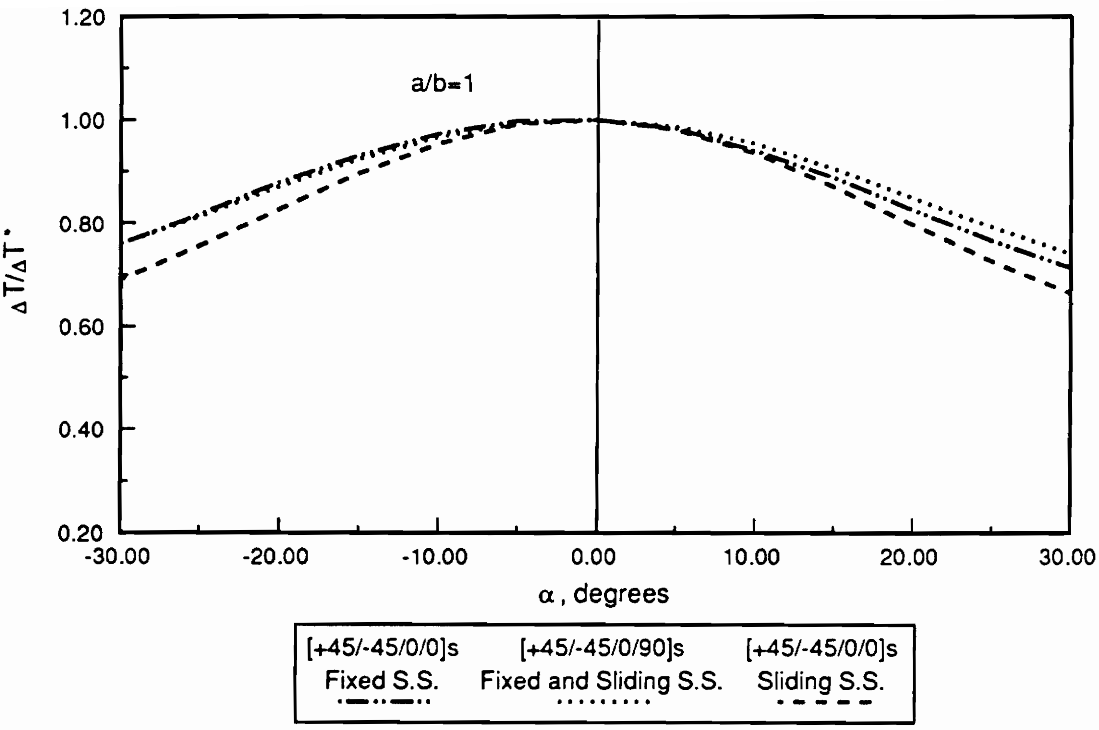

Fig. 2. The influence of skew angle, boundary conditions, and lamination on the buckling temperature of square plates.

supports and the orthotropic laminate with sliding simple supports than there is between the buckling temperatures of the quasi-isotropic laminate and the orthotropic laminate, both with fixed simple supports. That all cases vary in roughly the same fashion with α is largely due to similarities in their D matrices. In fact, by examining the algebra associated with the eigenvalue problem, it can be seen that the buckling temperature of a square laminate with fixed simple supports depends strongly on the quantity

$$D = D_{11} + 2(D_{12} + 2D_{66}) + D_{22}. \tag{4.36}$$

This quantity has the same value for both laminates for all values of α. In Fig. 3 the variation with skew angle of this quantity normalized by D^*, the value of this quantity at $\alpha = 0°$, is illustrated. It is seen that the variation of the above quantity with skew angle and the variation of the buckling temperatures of the fixed simple support plates with skew angle are very similar. The quantity defined in eqn. 4.36 is actually the the numerator in the expression for ΔT in the 1-term buckling solution for a square plate, i. e., $M \times N = 1$. By using the normalized values, the quantity D can often give an estimate of the buckling temperatures of these plates at various skew angles as good, or better, than that obtained from the 1-term buckling solution. This estimate, like the 1-term solution [11], is less accurate for laminates in which D_{16}, D_{26} and $\overline{N}^T_{xy}$ are larger, and becomes more accurate as these terms become small when compared with D, and $\overline{N}^T_x$ and $\overline{N}^T_y$, respectively. The small differences that do exist between the quasi-isotopic and orthotropic laminates with fixed simple supports are due largely to differences in D_{16}, D_{26} and $\overline{N}^T_{xy}$ for the two laminates at various values of α. At $\alpha = 0°$, where $\overline{N}^T_{xy} = 0$ and D_{16} and D_{26} are the same for both laminates, the buckling temperatures are the same to three significant digits for both square laminates.

Plates with rectangular planforms, $a/b = 2$, are compared with square plates in Fig. 4. These results are based on a plate width of $b = 6$ in.. It is seen that rectangular planform plates have lower buckling temperatures than square plates. For rectangular geometry and zero skew angle the two laminates do not give identical results. This is in contrast to the identical results for square laminates. In addition, in each case for the rectangular plates the

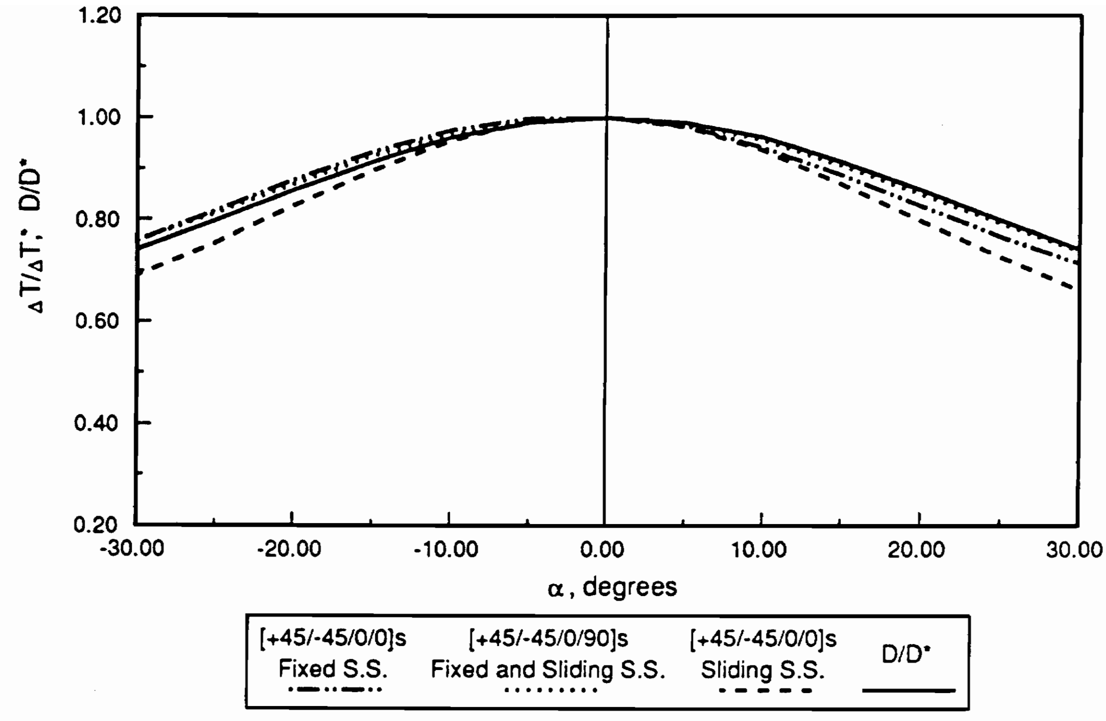

Fig. 3. The influence of skew angle on the buckling temperature and D for square plates.

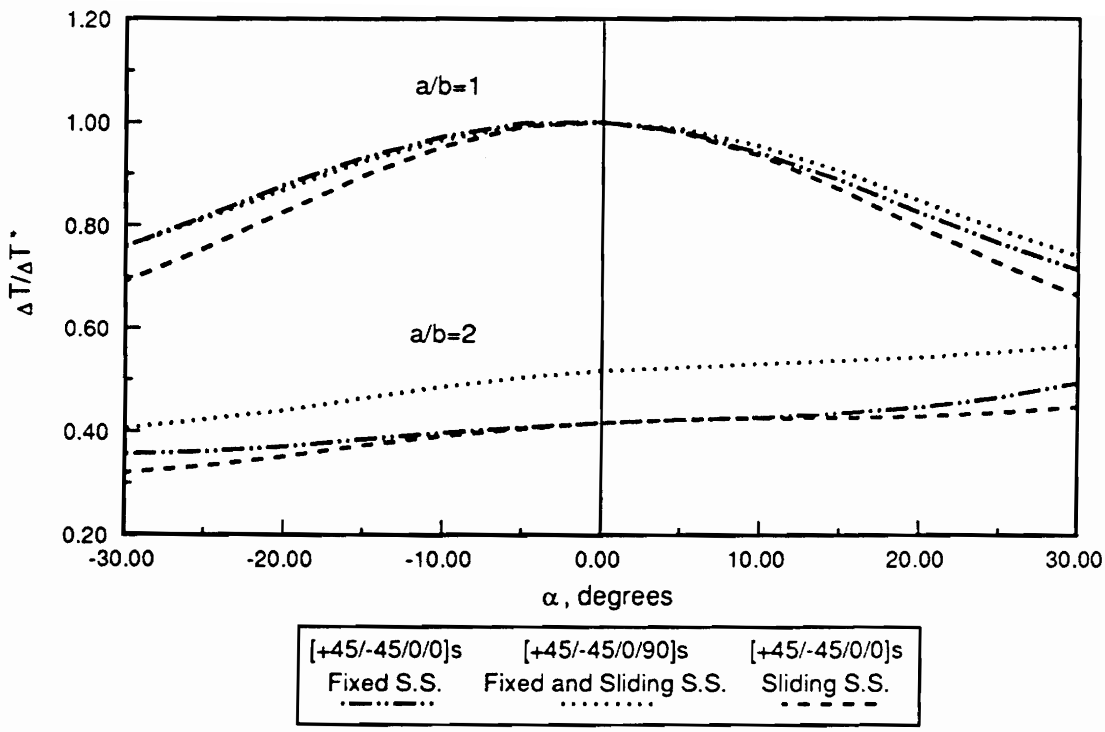

Fig. 4. The influence of skew angle and plate geometry on the buckling temperature.

buckling temperature is monotonically increasing with skew angle. The quasi-isotropic plate, as before, has the same buckling solution for both sets of boundary conditions, while for the orthotropic laminate the buckling temperatures corresponding to the two edge conditions differ for $\alpha \neq 0°$. Differences between the buckling temperatures of the orthotropic laminates with the two different boundary conditions increase with the magnitude of α. These differences are smaller for the rectangular plates than for the square plates.

The out-of-plane buckling displacements for (a) quasi-isotropic, and (b) orthotropic square laminates with $\alpha = 0°$ are given in Fig. 5. These displacements are equally valid for fixed or sliding simple support conditions. Although it is not readily apparent, because the laminates are not identical, the eigenvectors associated with each are slightly different. Thus their buckling displacements are not quite the same. Note that the buckling displacements are slightly asymmetric with respect to the square geometry of the plate. The displacements are not symmetric with respect to the lines x = a/2 or y = b/2. This asymmetry to the deformation is due to the D_{16} and D_{26} bending stiffness terms. If these terms are artificially set to zero, the buckling temperature is given by the 1-term solution and the asymmetry of the deformation disappears, as shown in Fig. 6. For $\alpha = 30°$ this asymmetry is somewhat more pronounced, owing to the dependence of the bending stiffnesses on the angle α. The influence of α on the asymmetry of the buckling displacements is quite evident when studying the $(\pm 45/0_2)_s$ laminate. A comparison of the buckling deformations at $\alpha = 0°$ and at $\alpha = 30°$ is given in Fig. 7 for the $(\pm 45/0/90)_s$ laminate, and in Fig. 8 for the $(\pm 45/0_2)_s$ laminate. The asymmetry is also slightly more dramatic for the orthotropic laminate when $\alpha = 30°$ due to the presence of the nonzero shear stress resultant $N_{xy} = -\overline{N}^T_{xy}$.

Figure 7 is valid for either set of boundary conditions, while Fig. 8 applies only to the case of fixed simple supports. The difference between the two sets of boundary conditions for the orthotropic laminate with $\alpha \neq 0°$ lies in prebuckling solutions. In comparing the deformations associated with each simple support condition, it is seen that, overall, the influence of the prebuckling solutions produces little difference in the solutions for the out-of-plane buckling displacements. These out-of-plane buckling deformations are given in Fig. 9 for the

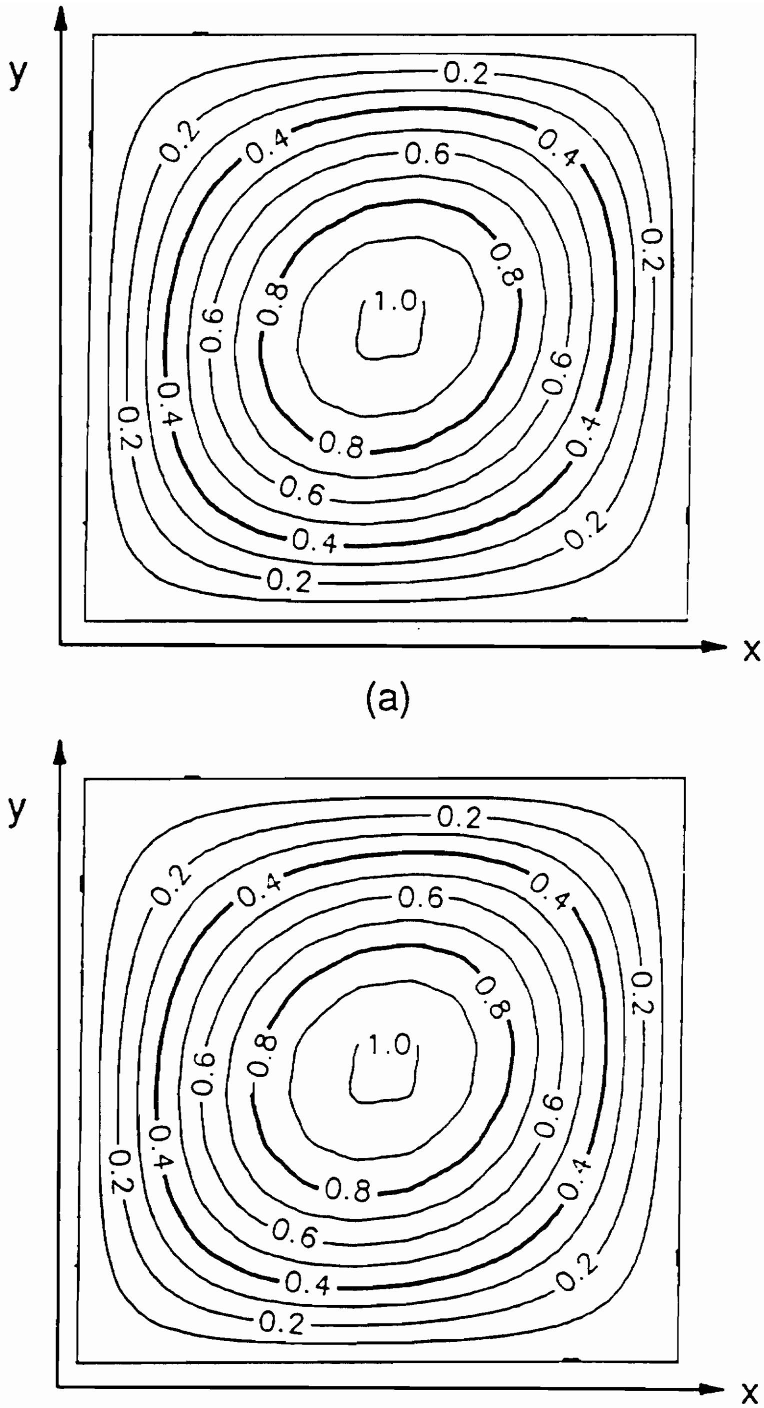

Fig. 5. Buckling displacements for (a) $(\pm 45/0/90)_s$, and (b) $(\pm 45/0_2)_s$ plates, $\alpha = 0°$.

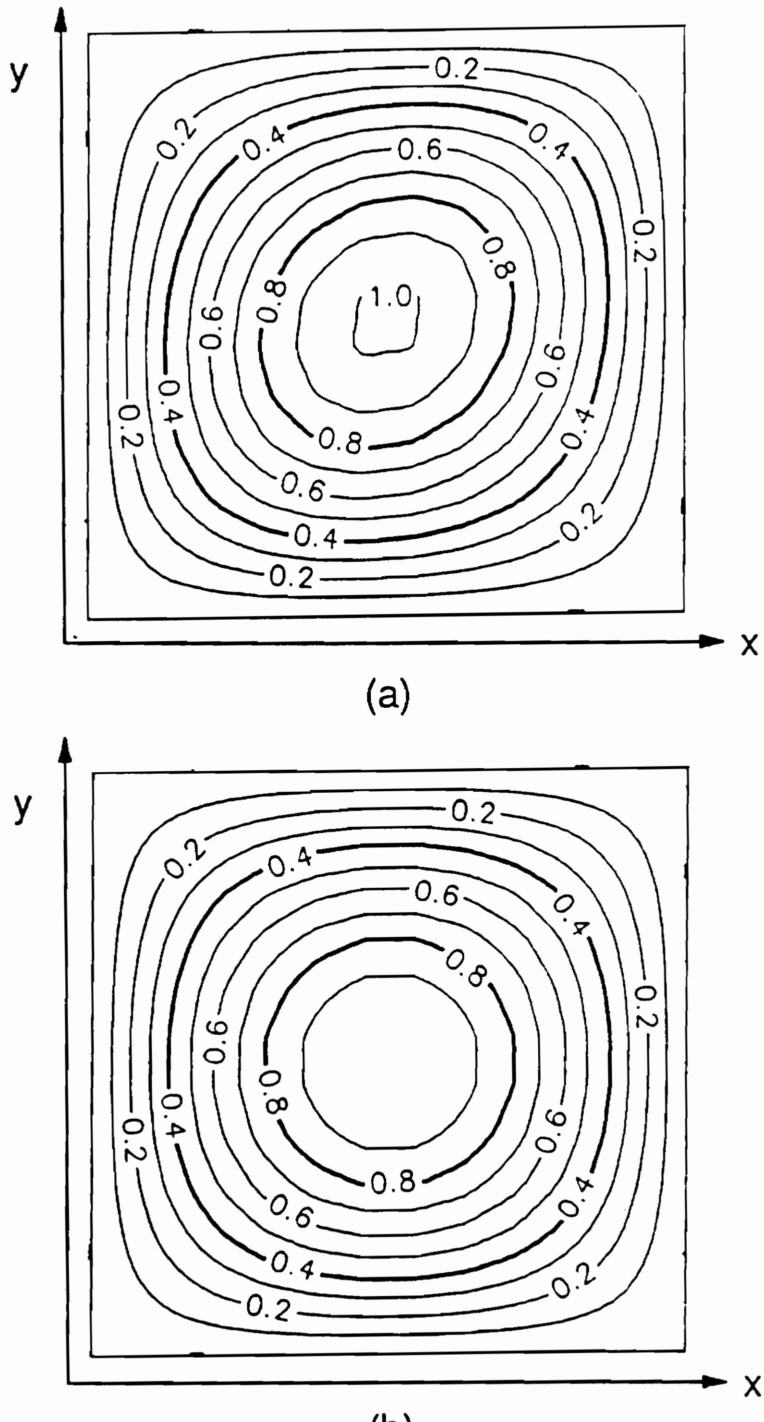

Fig. 6. Buckling displacements for (a) $(\pm45/0/90)_s$ plate, and (b) $(\pm45/0/90)_s$ plate with $D_{16}=D_{26}=0$, $\alpha=0°$.

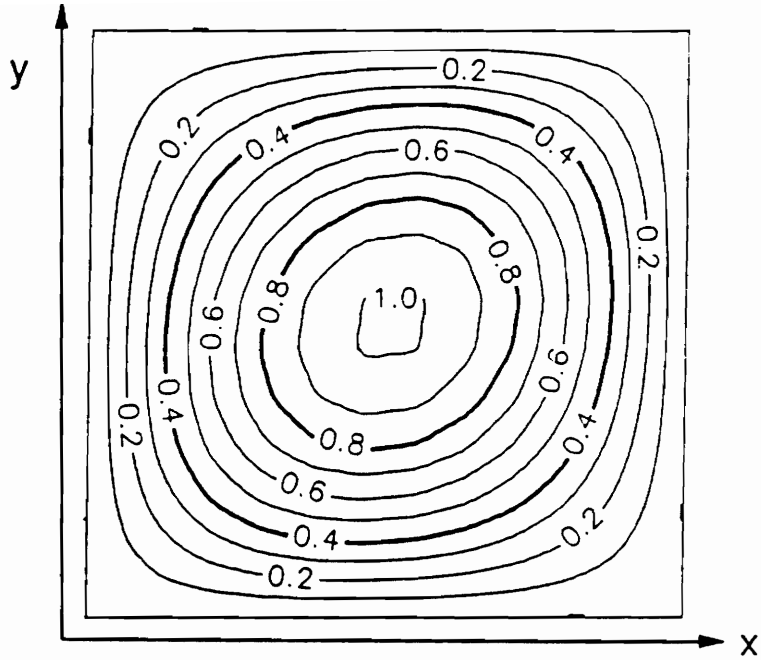

(a)

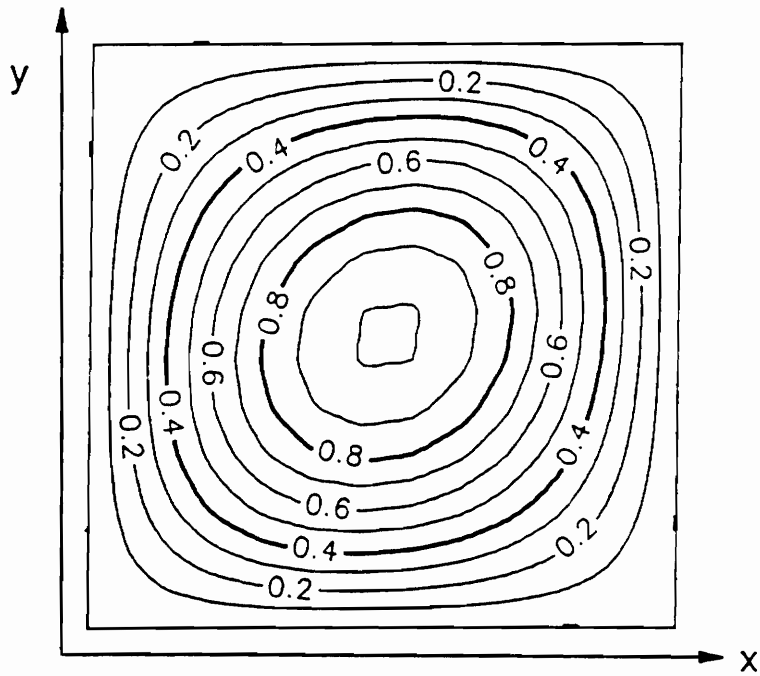

(b)

Fig. 7. Buckling displacements for $(\pm 45/0/90)_s$ plate with (a) $\alpha = 0°$, and (b) $\alpha = 30°$.

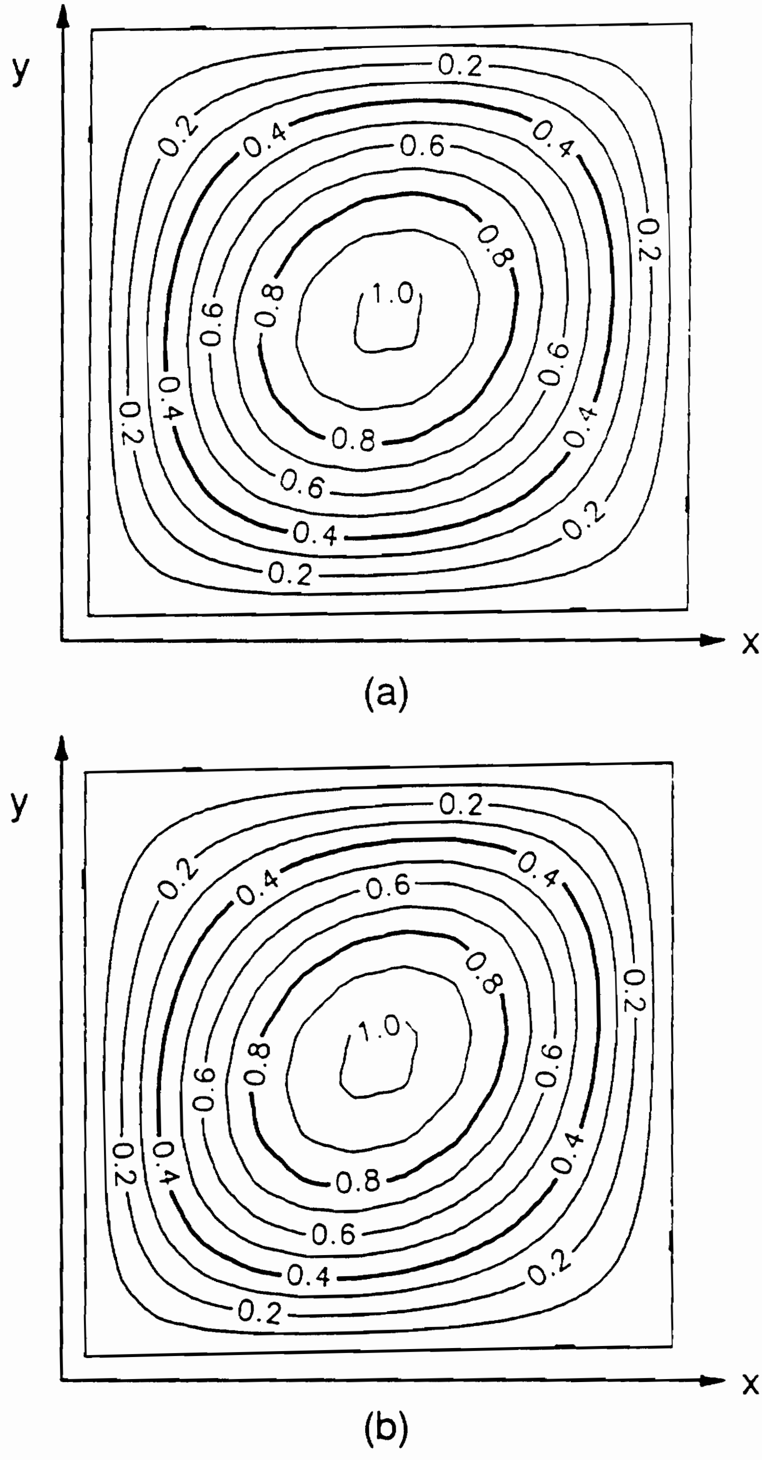

Fig. 8. Buckling displacements for $(\pm 45/0_2)_S$ plate with (a) $\alpha = 0°$, and (b) $\alpha = 30°$, and with fixed simple supports.

$(\pm 45/0_2)_s$ laminate with $\alpha = 30°$ for (a) fixed simple supports, and (b) sliding simple supports. These appear to be very similar, but the asymmetry evident in both cases is slightly less for the case of sliding simple supports.

In all cases note that neither half-plane nor quarter-plane symmetry exists for this type of problem. For all skew angles, the buckled shapes of the square laminates consist of just one half-wave in each direction. The same is true for the rectangular quasi-isotropic and orthotropic plates with either simple support boundary condition.

Although the prebuckling solution does not have a large effect on the buckling temperature or the buckled shape of a laminate, it is quite complicated itself. Contour plots are given in Fig. 10 of the prebuckling stress resultants, N_x, N_y and N_{xy}, for the $(\pm 45/0_2)_s$ at $\alpha = 30°$ with sliding simple supports. This is the only case studied with nontrivial prebuckling stress resultants. In Fig. 10 each prebuckling stress resultant has been normalized by the value of that prebuckling stress resultant for the same laminate with fixed simple supports. Since for the case of fixed simple supports all prebuckling stresses are spatially uniform, there would be no contours for that case, or, rather, there would be one contour encompassing the entire planform and the value of that contour would be unity. As can be seen from Figs. 10a and 10b, there is a large central region of the plate within which the prebuckling stress resultants N_x and N_y are quite uniform and nearly equal to their values for the fixed simple support case. In two opposite corners the values of N_x and N_y increase beyond their fixed support values, while in the two other opposite corners, the values of N_x and N_y decrease below their fixed support values. The variation of N_{xy} with spatial location is quite severe. The value of N_{xy} on the four edges for the case of sliding simple supports must be zero. On the other hand, in the center of the plate the value should approach that of fixed simple supports. The density of contours reflect this rapid change of conditions.

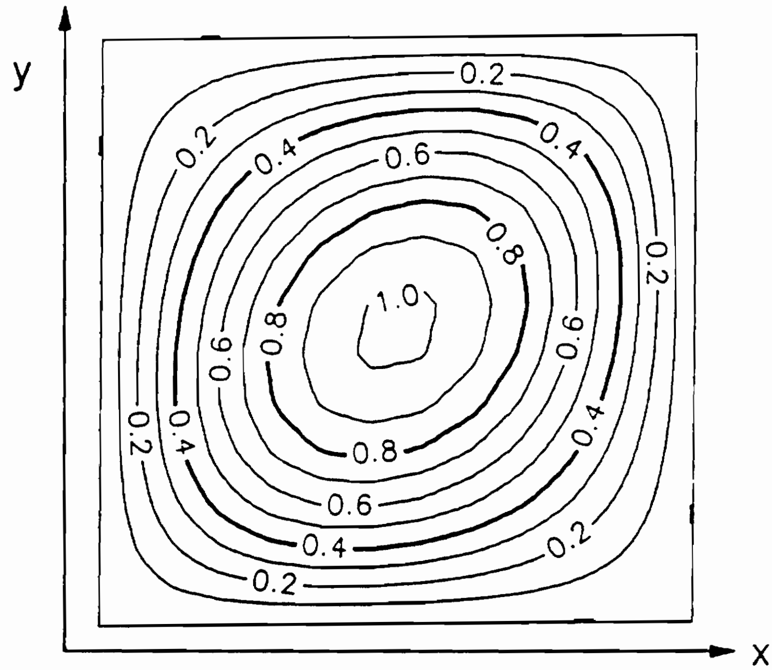

(a)

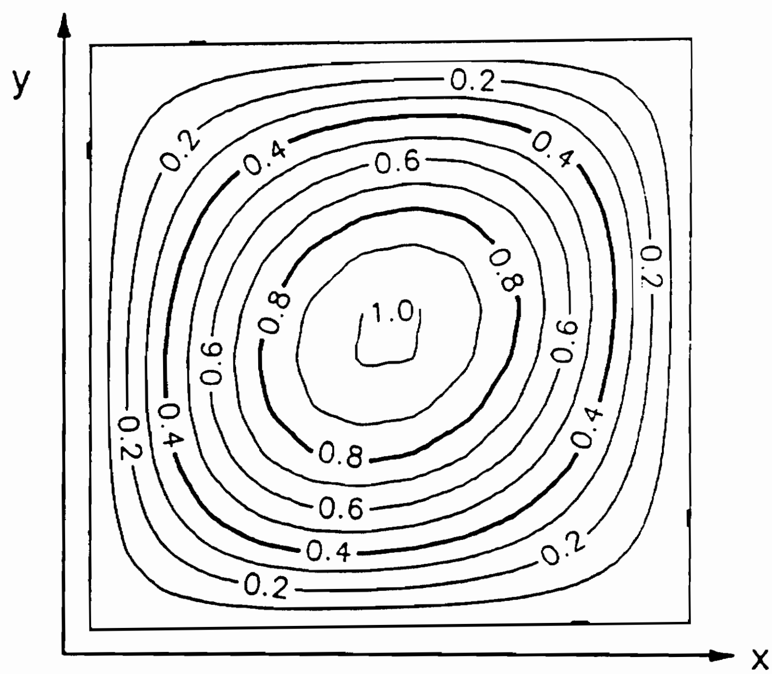

(b)

Fig. 9. Buckling displacements for $(\pm 45/0_2)_S$ plate with $\alpha = 30°$ with (a) fixed, and (b) sliding simple supports.

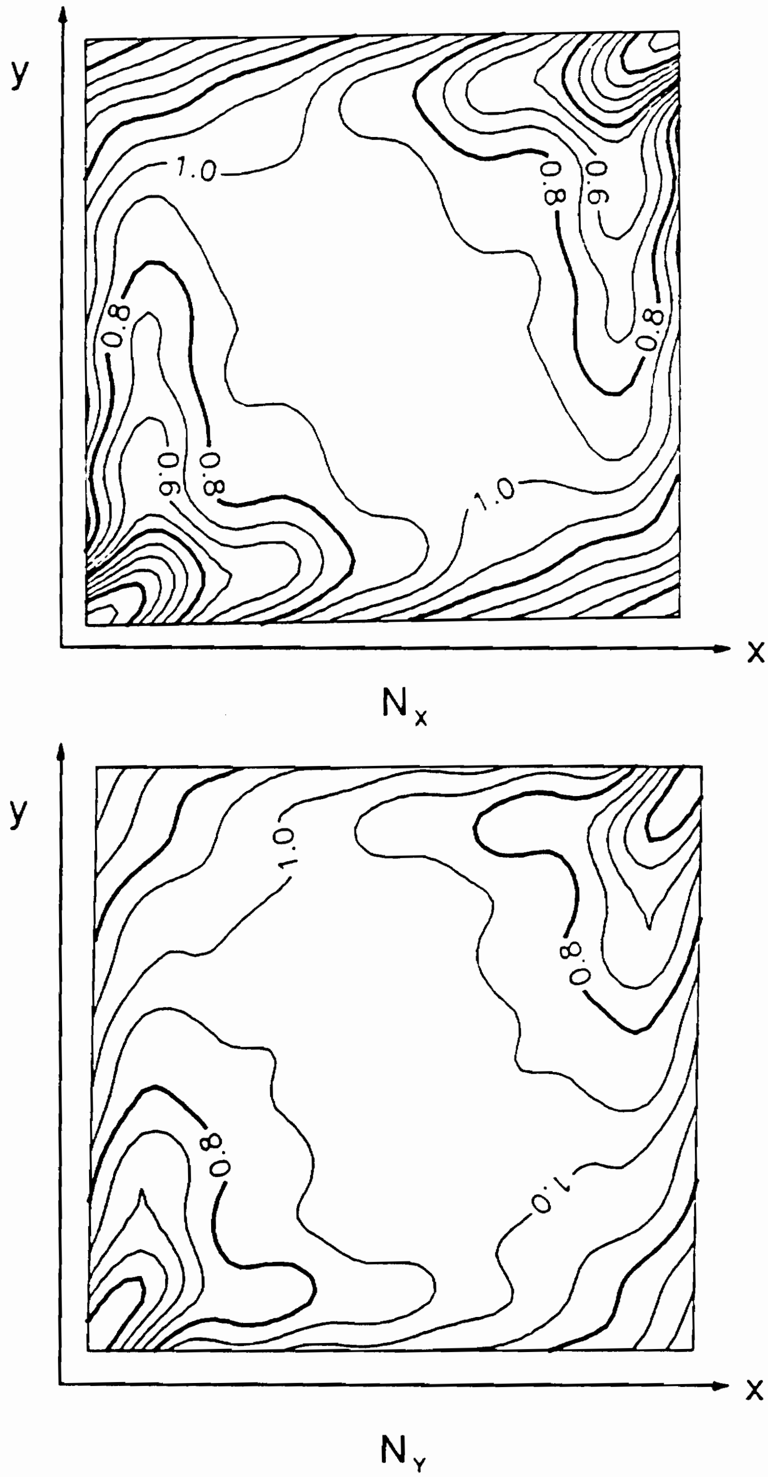

Fig. 10. Normalized prebuckling stress resultant contours for $(\pm 45/0_2)_S$ plates with $\alpha = 30°$ and sliding simple supports.

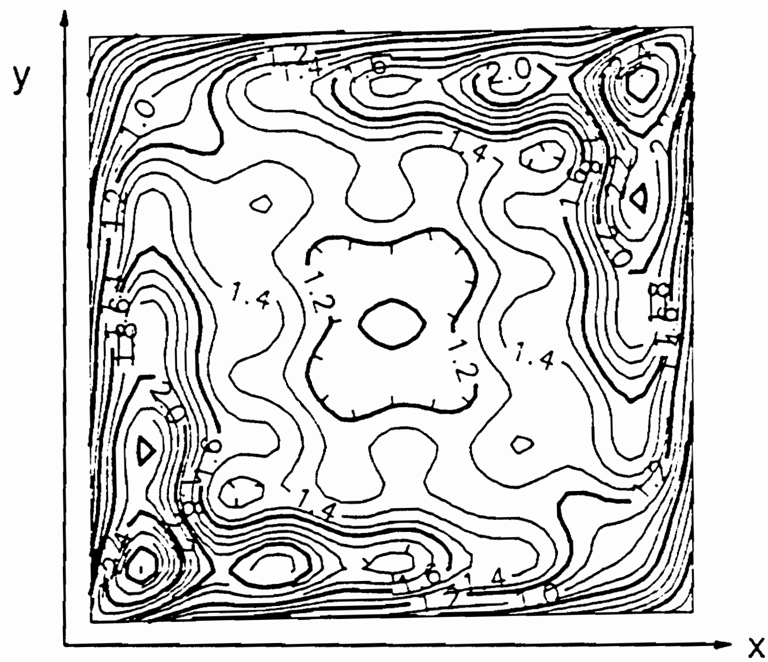

N_{XY}

Figure 10 (continued)

4.2.2 Linearly Varying Change in Temperature: $\Delta T = c + dx$

As mentioned previously, the problem of a linearly varying temperature change may be approached operationally either by specifying c and solving for the value of d to cause buckling, or by specifying d and solving for the smallest value of c necessary to cause buckling. In obtaining the following numerical results, d has been specified and the value of c is sought. The buckling of plates in the presence of a linearly varying change in temperature, $\Delta T = c + dx$, will be studied for the range of gradients

$$-1.5 \leq \frac{da}{\Delta T^*} \leq 1.5 \,. \tag{4.37}$$

The quantity da represents the difference in temperature between the two ends of the plate. The quantity ΔT^*, as has been observed, is the buckling temperature of both the quasi-isotropic and orthotropic laminates when $\alpha = 0°$ and the plate is heated uniformly. It has been a characteristic and important temperature for this study. Equation 4.37 states that the temperature difference between the two ends of the plate will be up to 150% of this characteristic temperature. The sign of the quantity $da/\Delta T^*$ will essentially dictate which end of the plate is warmer than the other.

4.2.2.1 Convergence Characteristics

Proceeding as with the case of a uniform change in temperature, the first issue to be addressed is that of convergence. The convergence of this case for $d = 0$ (the case of uniform temperature change) has already been established in the previous section and this will be used as a starting point to study the convergence of cases in which $d \neq 0$. The convergence of both the prebuckling and the buckling problem must be considered. This will be approached in the same manner as in the case of a uniform change in temperature and sliding simple supports in the previous section. Using a large gradient, $da/\Delta T^* = 1.5$, a severe situation, the convergence of a $(\pm 45/0_2)_s$ rotated by $\alpha = 30°$ for the case of fixed simple supports is considered first. Compared to the other laminates and other values of α, this situation requires as many, or more, terms in both the prebuckling and the buckling solutions as the other cases in order to reach convergence.

The effect that the number of terms taken in the prebuckling solution, $I \times J$, has on the buckling solution, as well as the effect of increasing the number of terms $M \times N$ taken in the assumed solution for w_1^o, is shown in Table 4. In Table 4 the buckling temperature, c, has again been normalized by ΔT^*. From this table, it is obvious that buckling temperature is insensitive to the details of the prebuckling solution, there being a small difference between $I \times J = 1$ terms and $I \times J = 144$ terms. The results of Table 4 indicate that solutions with $I \times J = 100$ and $M \times N = 64$ are converged. Considering the computational costs, values of $I \times J < 100$ and $M \times N < 64$ can be used with a high degree of accuracy. The numerical results of Table 4 are again based on a 6 in. by 6 in. laminate.

The convergence of the buckling and prebuckling problems are considered for a $(\pm 45/0_2)_s$ with $\alpha = 30°$ for the case of sliding simple supports in the same manner. In this case, however, $I \times J = 81$ is used as the starting point for studying the influence of prebuckling. This is the number of terms which were required in the prebuckling solution in order to reach convergence of the buckling solution in the case of uniform temperature change and sliding simple supports. The results of this convergence study are given in Table 5. Although an even larger number of terms, $I \times J = 256$, must be taken in the prebuckling solution to reach convergence of the buckling solution, the buckling temperature, c, is again seen to be fairly insensitive to the prebuckling solution. The results in Table 5 indicate that all solutions with $I \times J = 256$ and $M \times N = 100$ are converged. Series with less than these terms provide reasonably accurate answers, however.

Table 4. PREBUCKLING CONVERGENCE STUDY FOR TEMPERATURE GRADIENT CASE: $(\pm45/0_2)_S$ PLATE, SQUARE, $\alpha=30°$, FIXED SIMPLE SUPPORTS, $da/\Delta T^*=1.5$.

$M \times N = 36$				$M \times N = 49$			
$I \times J$	$\frac{c^{(1)}}{\Delta T^*}$	w_{11}	w_{21}	$I \times J$	$\frac{c^{(1)}}{\Delta T^*}$	w_{11}	w_{21}
1	-0.186	1.000	-0.2309	1	-0.176	1.000	-0.2309
4	-0.190	1.000	-0.2338	4	-0.190	1.000	-0.2339
9	-0.187	1.000	-0.2315	9	-0.187	1.000	-0.2315
16	-0.190	1.000	-0.2333	16	-0.190	1.000	-0.2333
25	-0.205	1.000	-0.2402	25	-0.207	1.000	-0.2402
36	-0.197	1.000	-0.2368	36	-0.197	1.000	-0.2378
49	-0.200	1.000	-0.2382	49	-0.203	1.000	-0.2382
64	-0.199	1.000	-0.2375	64	-0.199	1.000	-0.2374
81	-0.200	1.000	-0.2384	81	-0.196	1.000	-0.2386
100	-0.199	1.000	-0.2321	100	-0.202	1.000	-0.2306
121	-0.200	1.000	-0.2388	121	-0.202	1.000	-0.2388
144	-0.200	1.000	-0.2383	144	-0.202	1.000	-0.2383
$M \times N = 64$				$M \times N = 81$			
$I \times J$	$\frac{c^{(1)}}{\Delta T^*}$	w_{11}	w_{21}	$I \times J$	$\frac{c^{(1)}}{\Delta T^*}$	w_{11}	w_{21}
1	-0.184	1.000	-0.2310	1	-0.189	1.000	-0.2310
4	-0.192	1.000	-0.2339	4	-0.192	1.000	-0.2339
9	-0.189	1.000	-0.2316	9	-0.189	1.000	-0.2316
16	-0.192	1.000	-0.2334	16	-0.192	1.000	-0.2334
25	-0.206	1.000	-0.2403	25	-0.216	1.000	-0.2403
36	-0.199	1.000	-0.2370	36	-0.199	1.000	-0.2370
49	-0.205	1.000	-0.2383	49	-0.202	1.000	-0.2384
64	-0.200	1.000	-0.2375	64	-0.200	1.000	-0.2375
81	-0.199	1.000	-0.2385	81	-0.202	1.000	-0.2385
100	-0.203	1.000	-0.2380	100	-0.203	1.000	-0.2380
121	-0.203	1.000	-0.2389	121	-0.203	1.000	-0.2389
144	-0.203	1.000	-0.2384	144	-0.203	1.000	-0.2384

(1) Numerical results computed based on a 6 in. by 6 in. plate.

Table 5. PREBUCKLING CONVERGENCE STUDY FOR TEMPERATURE GRADIENT CASE: $(\pm 45/0_2)_s$ PLATE, SQUARE, $\alpha = 30°$, SLIDING SIMPLE SUPPORTS, $da/\Delta T^* = 1.5$.

M × N = 64				M × N = 81			
I × J	$\frac{c^{(1)}}{\Delta T^*}$	w_{11}	w_{21}	I × J	$\frac{c^{(1)}}{\Delta T^*}$	w_{11}	w_{21}
81	-0.268	1.000	-0.1839	81	-0.271	1.000	-0.1841
100	-0.271	1.000	-0.2338	100	-0.274	1.000	-0.1856
121	-0.272	1.000	-0.1861	121	-0.277	1.000	-0.1862
144	-0.273	1.000	-0.1871	144	-0.278	1.000	-0.1873
169	-0.277	1.000	-0.1877	169	-0.280	1.000	-0.1878
196	-0.278	1.000	-0.1884	196	-0.281	1.000	-0.1885
225	-0.280	1.000	-0.1888	225	-0.282	1.000	-0.1889
256	-0.281	1.000	-0.1889	256	-0.284	1.000	-0.1895
289	-0.281	1.000	-0.1891	289	-0.284	1.000	-0.1897
M × N = 100				M × N = 121			
I × J	$\frac{c^{(1)}}{\Delta T^*}$	w_{11}	w_{21}	I × J	$\frac{c^{(1)}}{\Delta T^*}$	w_{11}	w_{21}
81	-0.277	1.000	-0.1840	81	-0.280	1.000	-0.1840
100	-0.281	1.000	-0.1855	100	-0.284	1.000	-0.1855
121	-0.285	1.000	-0.1862	121	-0.285	1.000	-0.1872
144	-0.287	1.000	-0.1872	144	-0.285	1.000	-0.1878
169	-0.287	1.000	-0.1878	169	-0.287	1.000	-0.1878
196	-0.288	1.000	-0.1883	196	-0.288	1.000	-0.1886
225	-0.290	1.000	-0.1889	225	-0.290	1.000	-0.1889
256	-0.291	1.000	-0.1894	256	-0.291	1.000	-0.1895
289	-0.291	1.000	-0.1898	289	-0.291	1.000	-0.1898

(1) Numerical results computed based on using a 6 in. by 6 in. plate.

4.2.2.2 *Buckling Characteristics*

One convenient way to represent the results for the case of a linearly varying temperature gradient is shown in Fig. 11. In this figure the functional relationship between c and d is illustrated for square quasi-isotropic and orthotropic laminates with $\alpha = 0°$ and with both fixed and sliding simple supports. In this figure c is normalized by ΔT^*, and d is normalized, as explained above, using the length of the plate, a, and ΔT^*. The form of this graph is largely due to the choice of placing the origin of the coordinate system at the corner of the plate. One of the observations that can be made from this figure is that rotating the problem by 180° makes no difference to the overall buckling solution. For instance, for the $(\pm 45/0/90)_s$ plate with $\alpha = 0°$ and fixed simple supports, when $da/\Delta T^* = 1.5$, in order for the plate to buckle, at one end of the plate $c/\Delta T^* = 0.09$ while at the other end of the plate $(c + da)/\Delta T^* = 1.59$. When $da/\Delta T^* = -1.5$ for the same case, the buckling solution is that $c/\Delta T^* = 1.59$, so that, again, in order for the plate to buckle, we must have at one end $(c + da)/\Delta T^* = 0.09$ while at the other end $c/\Delta T^* = 1.59$. In other words, it does not matter which end of the plate is heated relative to the other. The case of $d = 0$ corresponds to the uniform temperature case and the values of c for this situation reiterate data shown in the previous section. As noted in the previous section, for a uniform change in temperature the buckling temperature for the quasi-isotropic and orthotropic laminates, with fixed and with sliding simple supports, is the same when $\alpha = 0°$. In the presence of a change in temperature which varies linearly with x, $d \neq 0$, the buckling temperatures for these cases are no longer the same, but are very close to one another, as is evident from the figure. In particular, the buckling solution for the quasi-isotropic laminate with fixed simple supports is not identical to the solution for the quasi-isotropic laminate with sliding simple support conditions, when $d \neq 0$. The same is true for the orthotropic laminate. This is because the prebuckling solution for either laminate with fixed simple supports is not identical to the prebuckling solution for the same laminate with sliding simple supports. The differences among solutions, though minimal, do change with α.

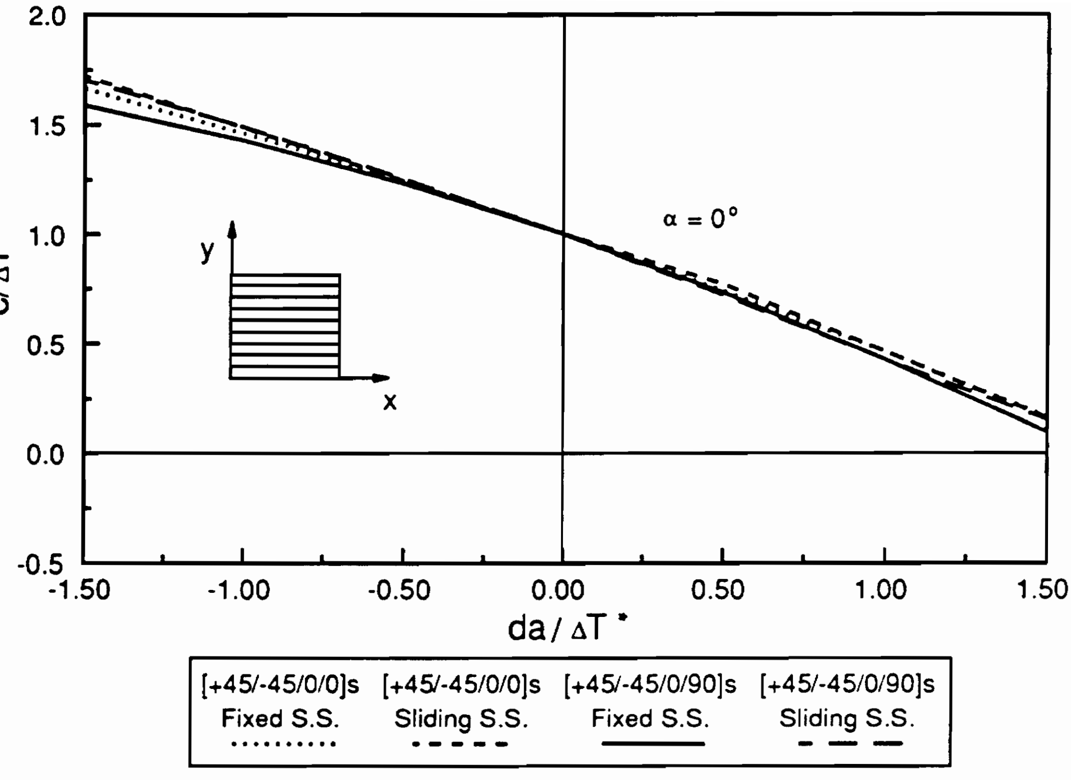

Fig. 11. The influence of a thermal gradient on buckling temperature, $\Delta T = c + dx$, square plates, $\alpha = 0°$.

The effect that skewing the material axes of these laminates by $\alpha = 30°$ has on the buckling temperatures for the case of a linearly varying change in temperature is shown in Fig. 12. For comparison, the case of $\alpha = 0°$, just discussed, is included on the figure. The buckling temperatures, c, for the $(\pm 45/0/90)_s$ and $(\pm 45/0_2)_s$ laminates with $\alpha = 30°$ and either set of boundary conditions also have values which are very close to one another for a given value of d. In the case of a uniform change in temperature, the buckling temperatures for both laminates under either boundary condition decrease when the material axes where skewed. As can be seen from this figure, the same is true for the case of a linearly varying temperature gradient. Several other observations can be made. First, for d<0, the situation where the right end of the plate is cooler than the left end, c is always positive. This is interpreted to mean the when the right end of the plate is cooler than the left end, the left end of the plate must always be heated in order for the plate to buckle. Second, for the quasi-isotropic and orthotropic laminates with no skewing, this is actually the case for any d in the range illustrated. However, for the laminates with skewing and with d positive and near the high end of the range shown, meaning the gradient is such that the right end of the plate is warmer than the left end, the left end must actually be cooled to buckle the plate, i.e., c<0.

The buckling temperatures of the orthotropic plate with no skewing and rectangular planform, a/b=2, are compared with those for the square orthotropic plate (a/b=1) with $\alpha = 0°$ in Fig. 13. As was the case for a uniform change in temperature, the rectangular plates have a lower buckling temperature, c, than the square plates. Differences between the buckling temperatures of the laminates with the two different boundary conditions are small for both the square and and rectangular plates. Unlike the square plates without skewing, however, for d positive and near the middle to high end of the range studied, the plate must be cooled on the left end to buckle, i. e., c<0. Although not shown, the results for the quasi-isotropic laminate are similar.

The effect of skewing the material axes by $\alpha = 30°$ on the rectangular orthotropic plate is shown in Fig. 14. It was seen in Fig. 12 that for square plates the cases of $\alpha = 0°$ and $\alpha = 30°$ fall into two distinct groups. In contrast to the results for square plates, for rectangular

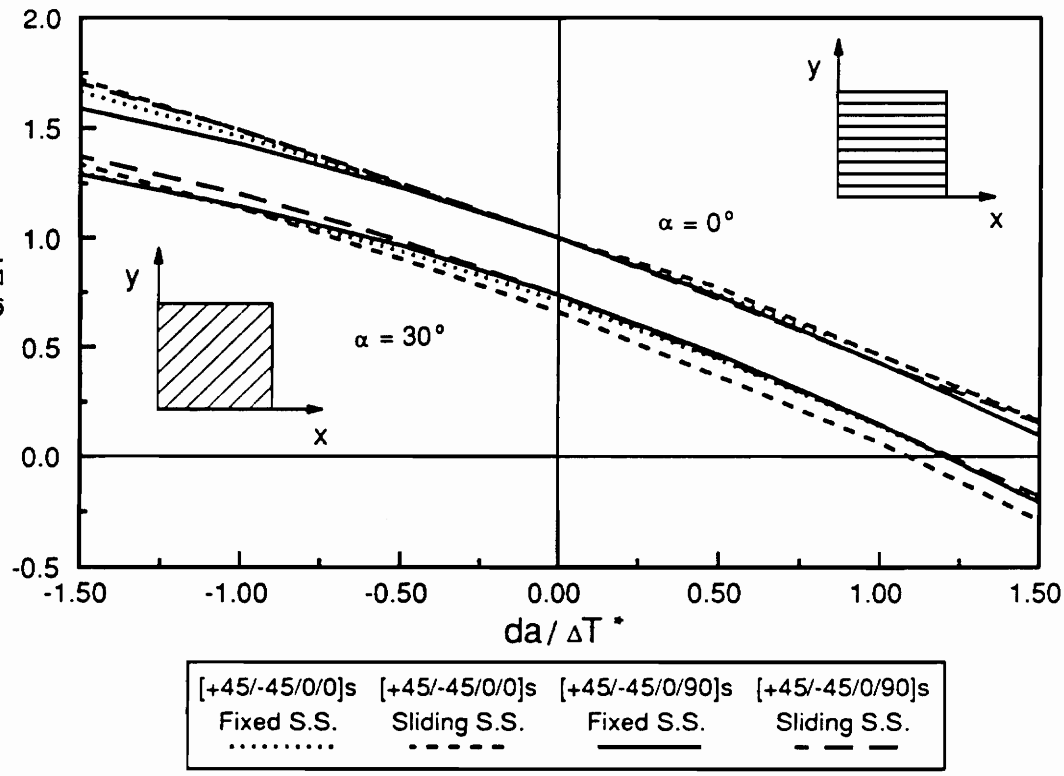

Fig. 12. The influence of a thermal gradient and skew angle on buckling temperature, $\Delta T = c + dx$, square plates.

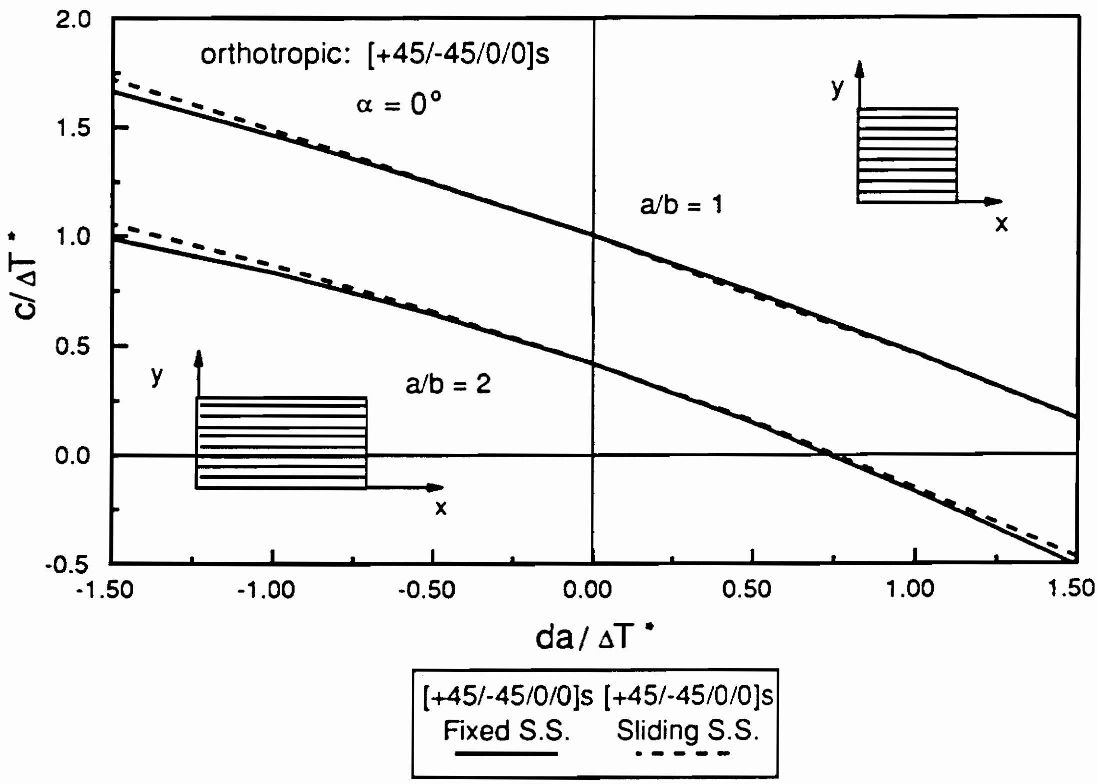

Fig. 13. The influence of a thermal gradient and plate geometry on buckling temperature, $\Delta T = c + dx$, $(\pm 45/0_2)_S$, $\alpha = 0°$.

plates, the results for the $(\pm 45/0_2)_s$ laminate with $\alpha = 0°$ and $\alpha = 30°$ and with either set of boundary conditions, are very similar. Again, although not shown, the results for rectangular quasi-isotropic laminates are similar.

Figure 15 shows the out-of-plane deflection contours for the orthotropic laminate with $\alpha = 0°$ and fixed simple supports for (a) $da/\Delta T^* = 0$, and (b) $da/\Delta T^* = 1.5$. As can be seen, the temperature gradient causes the maximum deflection to move toward the warm end of the plate, $x = a$. As was seen previously, in Fig. 5b, for the $(\pm 45/0_2)_s$ laminate, with $\alpha = 0°$ and no temperature gradient there was an asymmetry to the out-of-plane deflection due to D_{16} and D_{26}. These bending coefficients also cause an asymmetry for the nonuniform temperature case. When D_{16} and D_{26} are artificially set to zero for the case of a nonzero gradient, the deflection is symmetric about the line $y = b/2$. This is illustrated in Fig. 16 where the buckling displacements of the $(\pm 45/0_2)_s$ laminate with $\alpha = 0°$ and D_{16} and D_{26} set to zero is compared with the case where D_{16} and D_{26} are not zero.

In Fig. 17 the buckling displacements for the orthotropic laminate with fixed simple supports and (a) $\alpha = 0°$, and (b) $\alpha = 30°$, and a linear temperature gradient of $da/\Delta T^* = 1.5$ are compared. For the uniform temperature case the asymmetry of the buckled configuration was more pronounced in the $(\pm 45/0_2)_s$ plate with $\alpha = 30°$ than with $\alpha = 0°$. This was seen in Fig. 8. As can be seen from Fig. 17, this greater asymmetry is also more exaggerated in the presence of a thermal gradient. Thus it can be concluded that the presence of a temperature gradient exaggerates the asymmetry caused by D_{16} and D_{26}. For the case of the $(\pm 45/0_2)_s$ plate with $\alpha = 30°$, however, part of this asymmetry is also due to the presence of a nonzero $\overline{N}^T_{xy}$, as was discussed for the uniform temperature case (Fig. 8).

A comparison of the buckling displacements of the $(\pm 45/0_2)_s$ plate when $\alpha = 30°$ (a) with fixed simple supports, and (b) with sliding simple supports, is given in Fig. 18 for $da/\Delta T^* = 1.5$. For the case of a uniform temperature change these deflections were very similar, although the asymmetry was slightly more for the case of sliding simple supports. As can be seen from this figure, for the case of a gradient in temperature, the asymmetry is much more pronounced for the case of sliding simple supports.

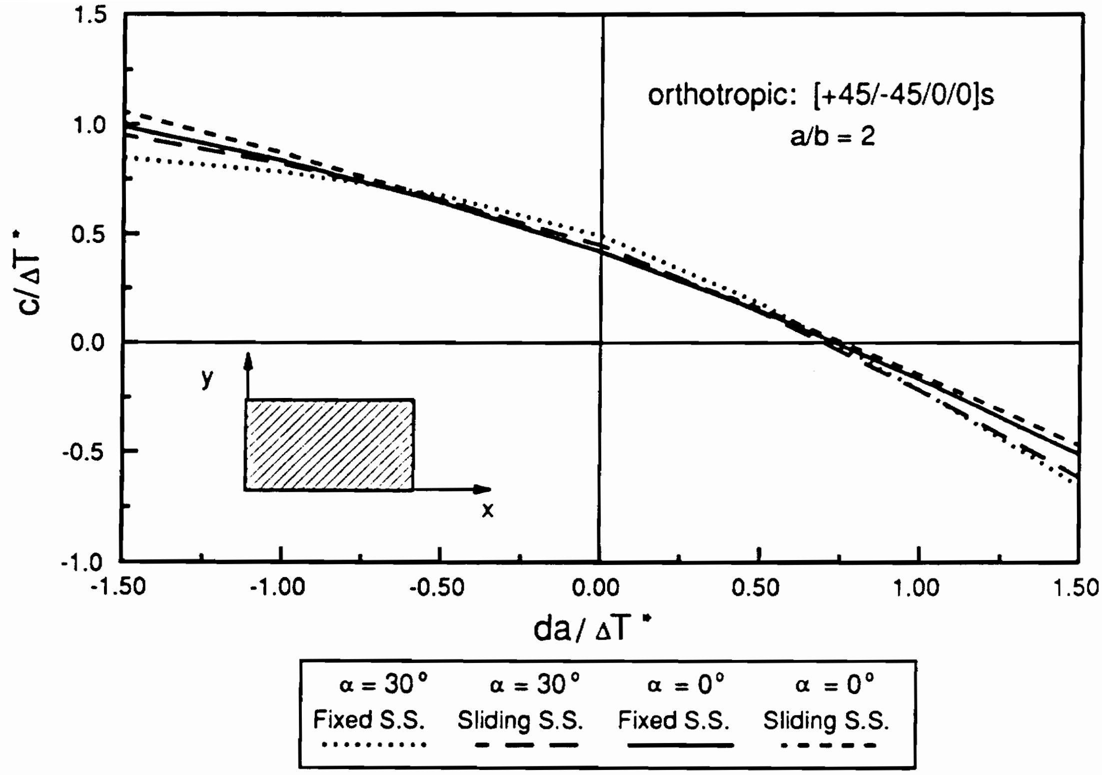

Fig. 14. The influence of thermal gradient, support conditions, and skew angle on buckling temperature, $\Delta T = c + dx$, $(\pm 45/0_2)_S$ plates.

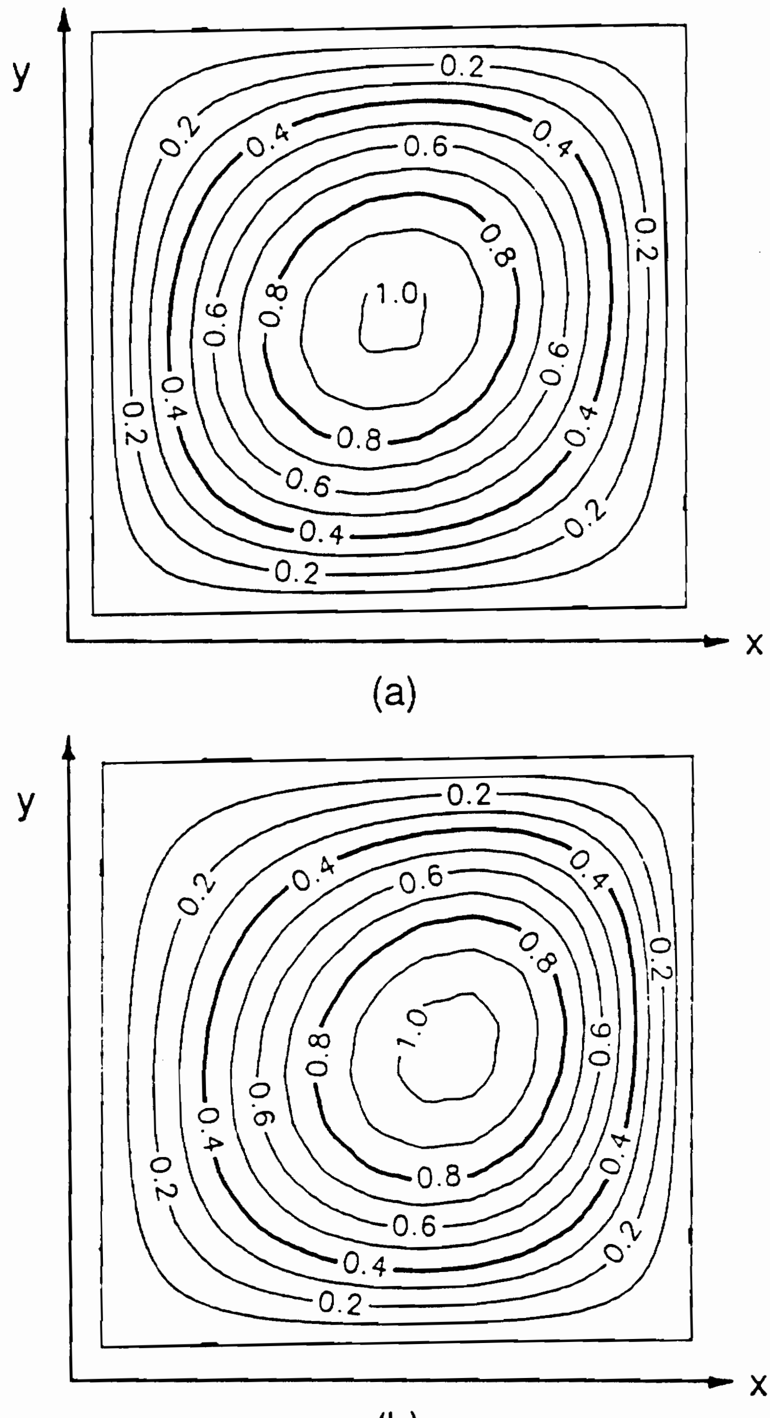

Fig. 15. Buckling displacements for $(\pm 45/0_2)_s$ plates with $\alpha = 0°$ and fixed simple supports (a) no gradient, and (b) $da/\Delta T^{*} = 1.5$.

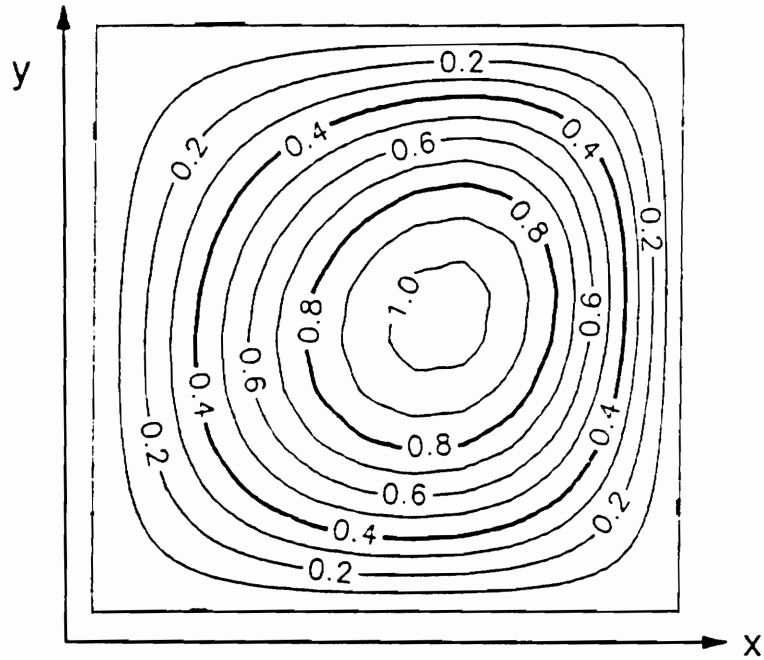

(a)

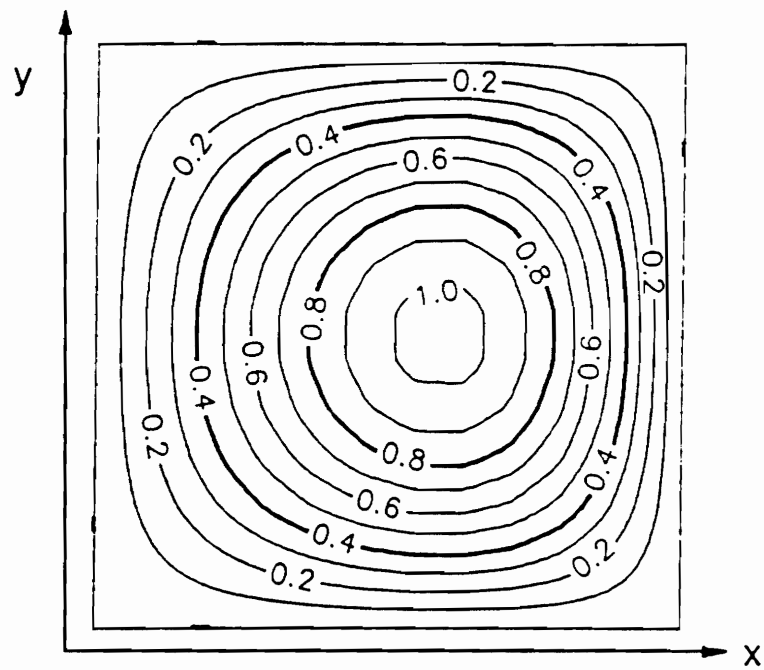

(b)

Fig. 16. Buckling displacements for (a) $(\pm 45/0_2)_s$ plate, and (b) $(\pm 45/0_2)_s$ plate with $D_{16} = D_{26} = 0$, $\alpha = 0°$, fixed simple supports, $da/\Delta T^* = 1.5$.

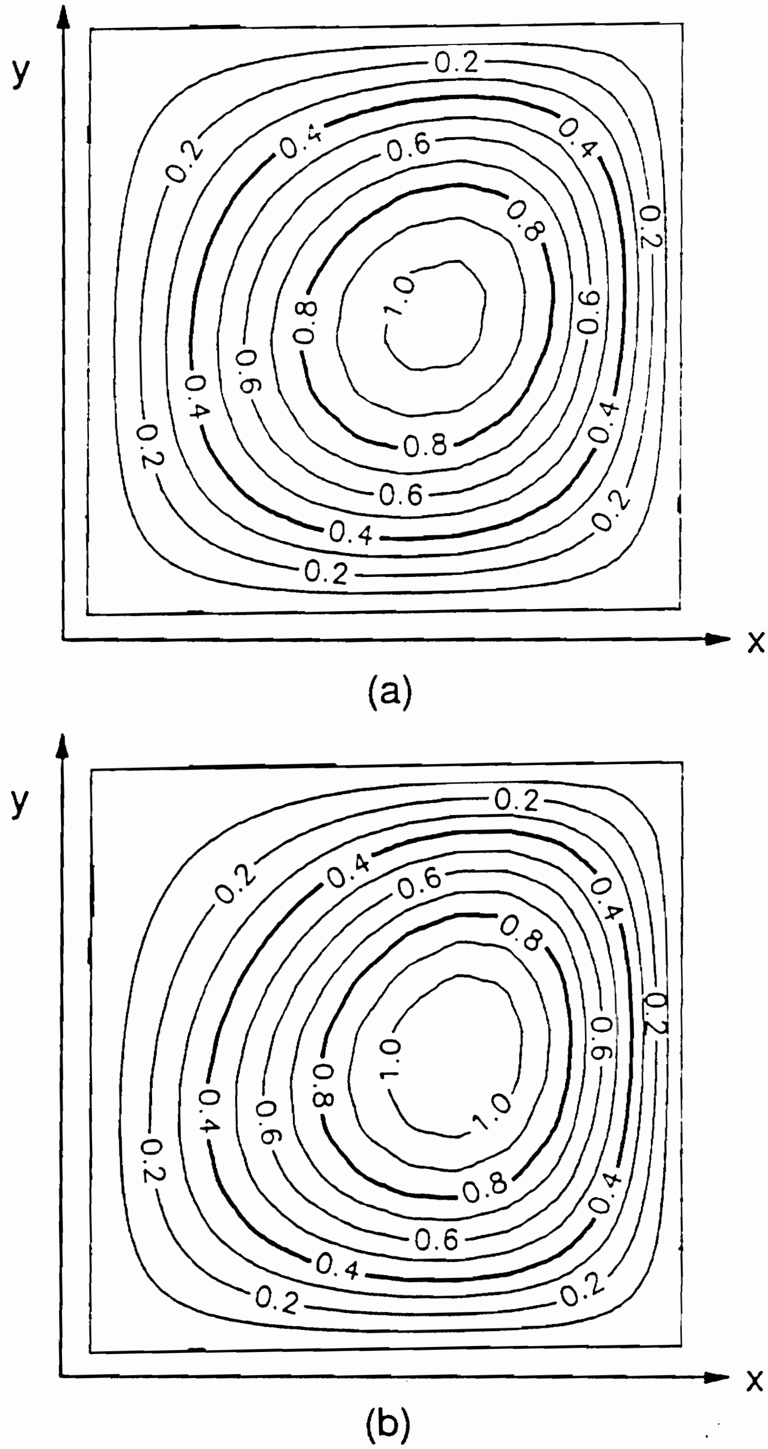

Fig. 17. Buckling displacements for $(\pm 45/0_2)_S$ plate with (a) $\alpha = 0°$ and (b) $\alpha = 30°$, fixed simple supports, $da/\Delta T^* = 1.5$.

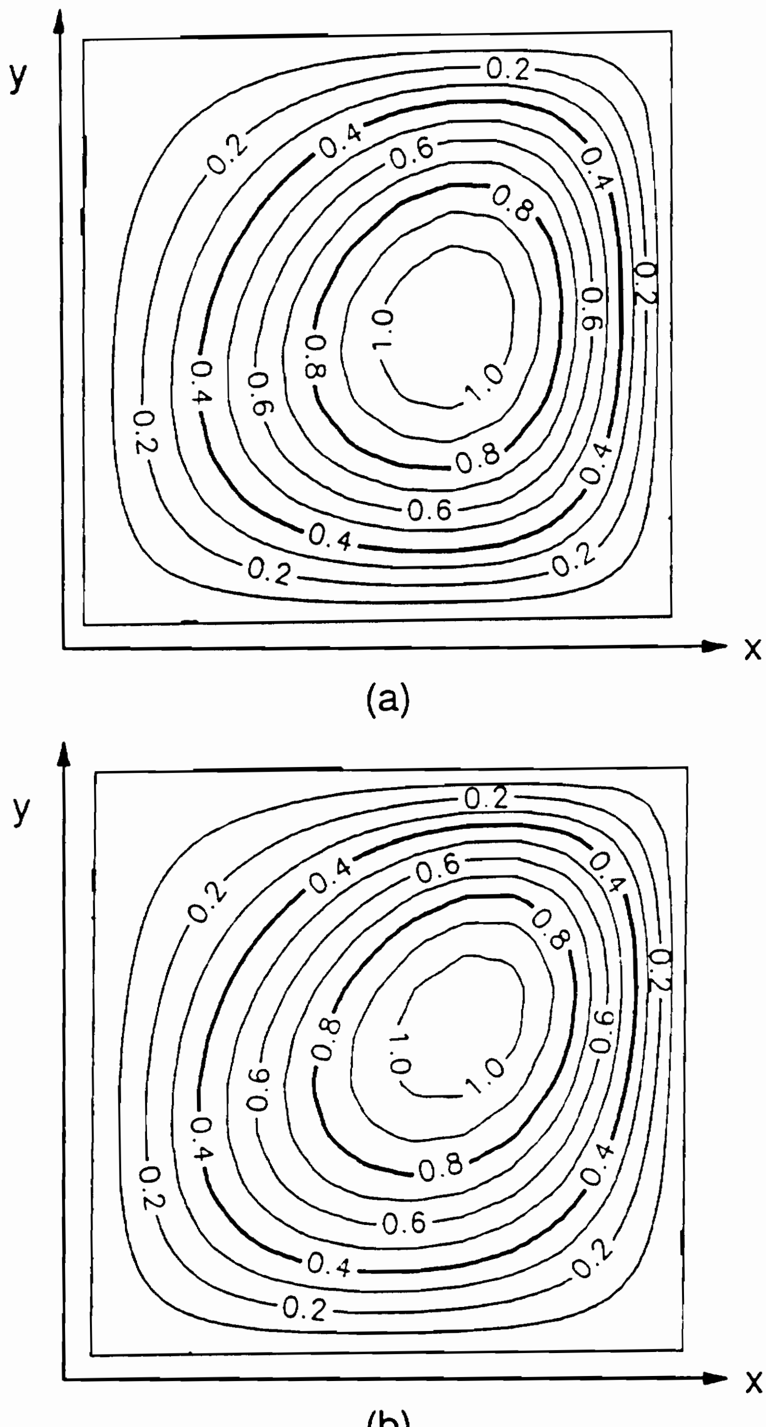

Fig. 18. Buckling displacements for $(\pm45/0_2)_S$ plates with $\alpha=30°$and (a) fixed simple supports, and (b) sliding simple supports, $da/\Delta T^* = 1.5$.

Although the prebuckling solutions do not have a large effect on the buckling temperatures of these laminates for the case of a thermal gradient, the prebuckling solutions are themselves quite complicated. Contour plots are given of the prebuckling stress resultants, N_x, N_y and N_{xy}, for the $(\pm 45/0_2)_s$ plate for $\alpha = 30°$ when $da/\Delta T^* = 1.5$ in Fig. 19 for the case of fixed simple supports and in Fig. 20 for the case of sliding simple supports. In both figures, each prebuckling stress resultant has been normalized by the value of that prebuckling stress resultant for the same laminate with fixed simple supports and no temperature gradient. For the case of fixed simple supports, Fig. 19, the values of N_x and N_y increase from the cooler to the warmer edge of the plate, while the variation of N_{xy} with spatial location is quite severe. Specifically, the point $x/a=0$, $y/b=0.5$ has $N_x = 0$. The locus of points for N_x forms an 'S'-shaped contour from that point. The normalized value of N_x exceeds 3 on the opposite, warmer, edge. The normalized value of N_y is close to unity on the line $x/a=0.5$ and the zero contour is to the left of that. It reaches about 1.8 on the warmer edge. The locus for $N_{xy} = 0$ covers a large area of the plate, the normalized value of N_{xy} covering the approximate range ± 5. For the case of sliding simple supports, Fig. 20, the value of N_y increases rather uniformly from the cooler to the warmer edge of the plate. The resultant N_{xy} varies rapidly on the left, cooler edge, varies less rapidly and quite uniformly on the central 80% of the plate, then varies rapidly again on the right, warmer edge. For N_{xy} there are what might be termed boundary layers at the left and right edges. The resultant N_x exhibits rapid changes in the corners, particularly near the corner $x/a=1$, $y/b=1$.

This concludes the investigation of thermal buckling and prebuckling in this study. These linear analyses have provided insight into the influence of boundary conditions, material axis skewing, degree of orthotropy, and aspect ratio on thermal buckling for both a uniform change in temperature and a change in temperature which varies linearly across the plate. The nonlinear problem of determining the plate response as the temperature increases beyond the buckling temperature, thermal postbuckling, is discussed in the next chapter.

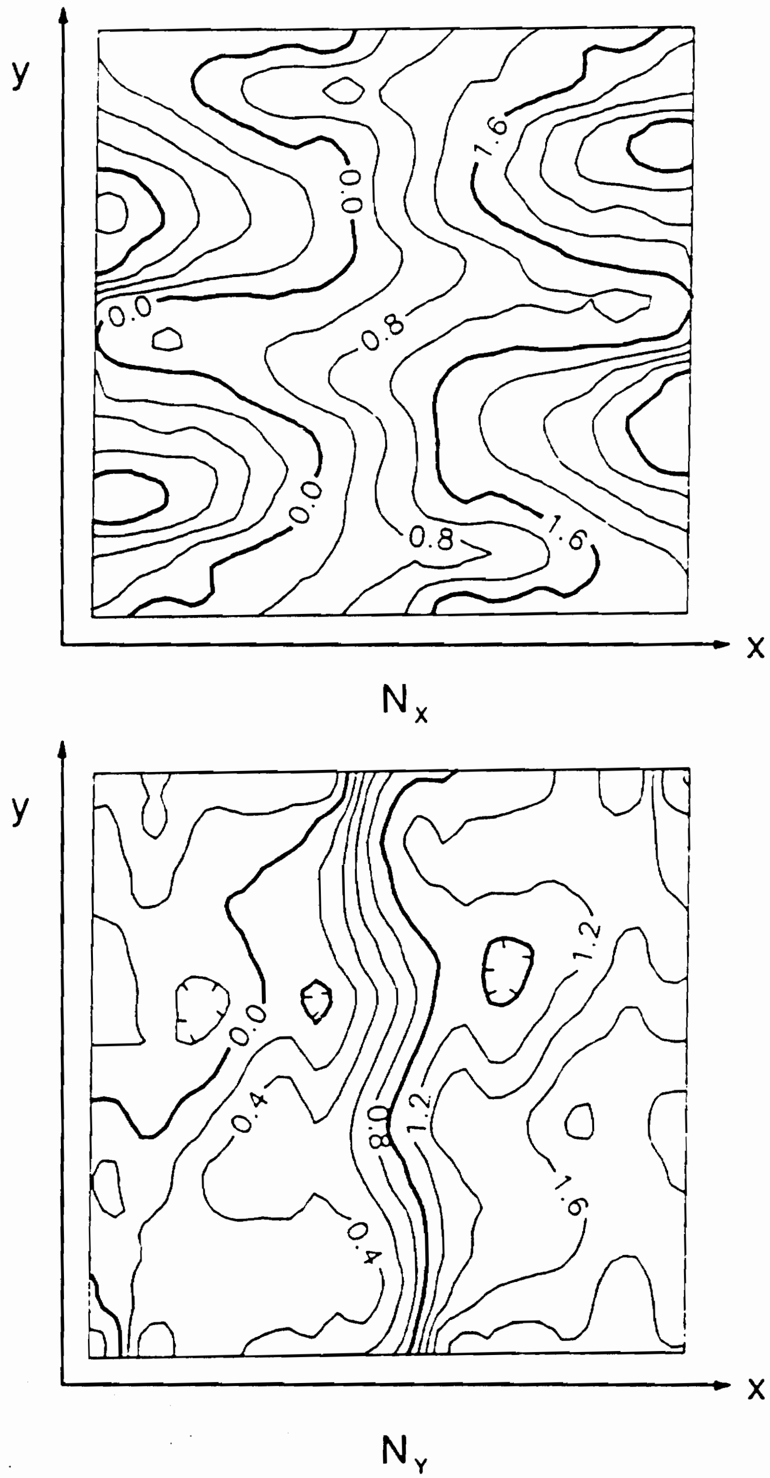

Fig. 19. Normalized prebuckling stress resultant contours for $(\pm 45/0_2)_S$ plate with $\alpha = 30°$ and fixed simple supports, $da/\Delta T^* = 1.5$.

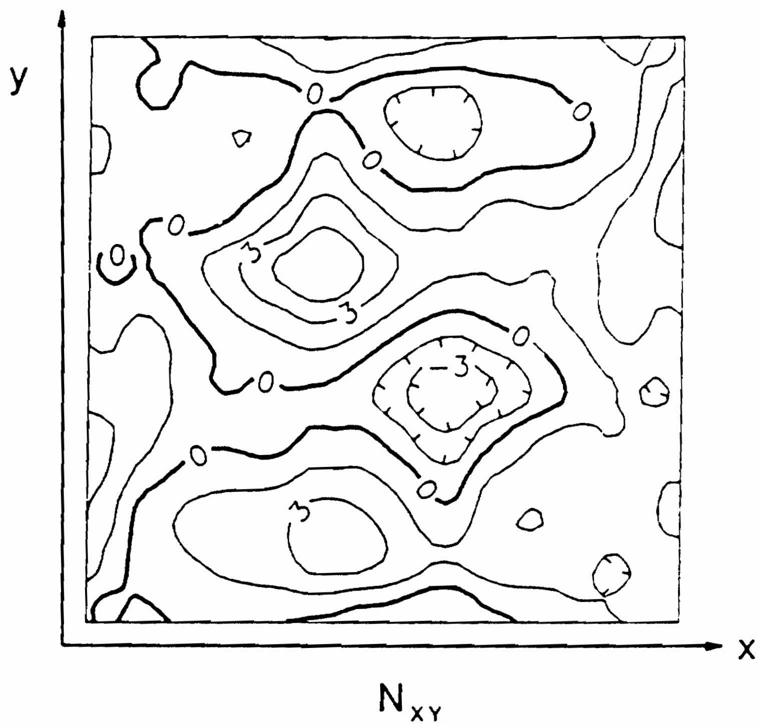

Figure 19 (continued)

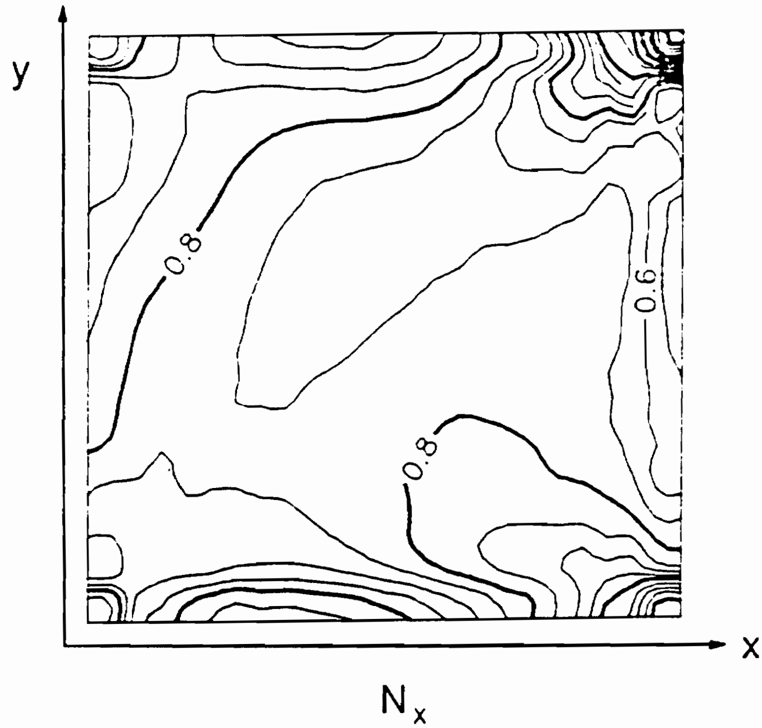

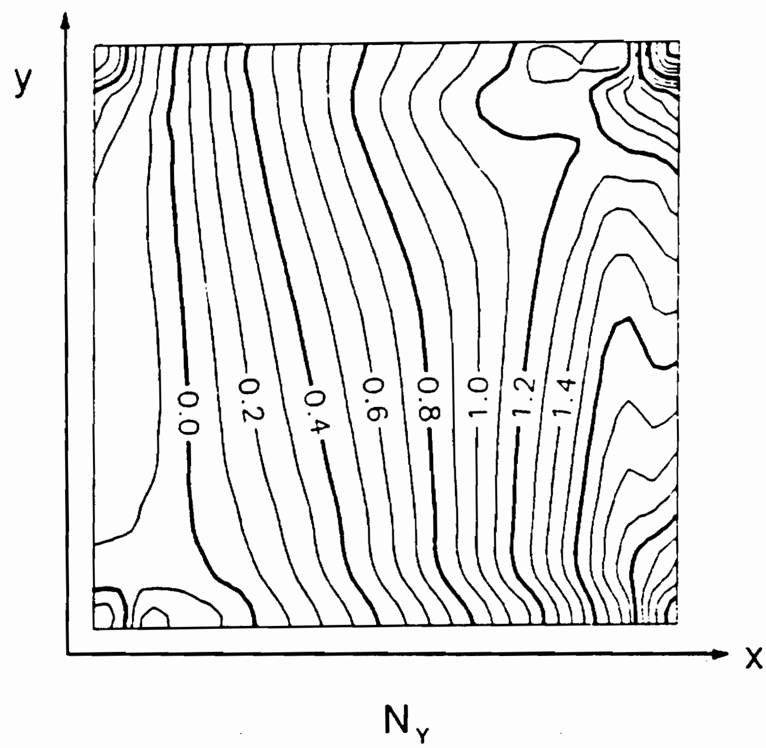

Fig. 20. Normalized prebuckling stress resultant contours for $(\pm 45/0_2)_S$ plate with $\alpha = 30°$ and sliding simple supports, $da/\Delta T^* = 1.5$.

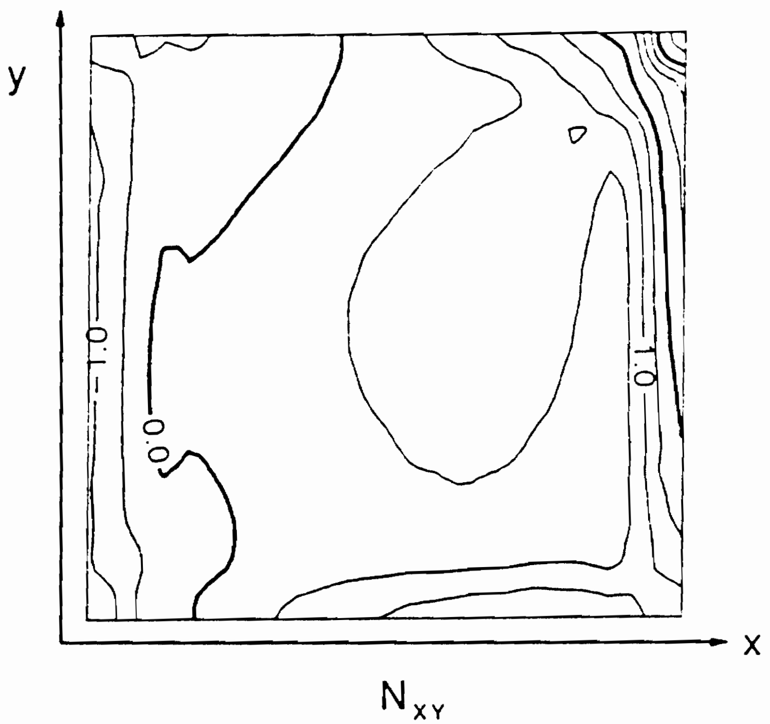

Figure 20 (continued)

5.0 Postbuckling Response

Plates are usually able to resist increasing loads subsequent to the onset of buckling [21]. The ability to resist loads beyond the buckling load is an asset in that the buckling load is not as critical, and it is possible to utilize the postbuckling load capacity to improve structural efficiency. Because plates may also be able to resist deflections at temperatures beyond the critical buckling temperature, thermal postbuckling is investigated. In this chapter the thermal postbuckling problem is formulated, a solution scheme presented, and numerical results discussed.

5.1 Formulation

As in the buckling problem, in the postbuckling problem, as it is studied here, the so-called preloading effects, σ_x^p, σ_y^p and τ_{xy}^p, in eqn. 3.10 are assumed to be due only to thermally-induced deformations, and the temperature distribution is assumed to be spatially uniform. As a result, eqns. 4.1 - 4.3 apply. However, although the plates are still assumed to be initially flat, the effects of moderate rotations can no longer be neglected in the expressions for the reference surface strains. Thus, from eqns. 3.5 and 3.6, the reference surface strains are given by

$$\varepsilon_x^o = \frac{\partial u^o}{\partial x} + \frac{1}{2}\left(\frac{\partial w^o}{\partial x}\right)^2 \; ; \; \varepsilon_y^o = \frac{\partial v^o}{\partial y} + \frac{1}{2}\left(\frac{\partial w^o}{\partial y}\right)^2$$
$$\gamma_{xy}^o = \frac{\partial u^o}{\partial y} + \frac{\partial v^o}{\partial x} + \frac{\partial w^o}{\partial x}\frac{\partial w^o}{\partial y}. \tag{5.1}$$

The equations governing the postbuckling are obtained by setting the first variation of the total potential energy equal to zero. Using eqn. 5.1, the first variation of the total potential energy, eqn. 3.29, using the notation of eqn. 3.17, is given by

$$\begin{aligned}\delta\pi = \int\int\Bigg\{ & N_x\left(\frac{\partial \delta u^o}{\partial x} + \frac{\partial w^o}{\partial x}\frac{\partial \delta w^o}{\partial x}\right) + N_y\left(\frac{\partial \delta v^o}{\partial y} + \frac{\partial w^o}{\partial y}\frac{\partial \delta w^o}{\partial y}\right) \\ & + N_{xy}\left(\frac{\partial \delta u^o}{\partial y} + \frac{\partial \delta v^o}{\partial x} + \frac{\partial w^o}{\partial y}\frac{\partial \delta w^o}{\partial x} + \frac{\partial w^o}{\partial x}\frac{\partial \delta w^o}{\partial y}\right) \\ & - M_x\frac{\partial^2 \delta w^o}{\partial^2 x} - M_y\frac{\partial^2 \delta w^o}{\partial^2 y} - 2M_{xy}\frac{\partial^2 \delta w^o}{\partial x \partial y}\Bigg\}dxdy,\end{aligned} \tag{5.2}$$

where the stress resultants, expressed in terms of the reference surface displacements, are, from eqn. 3.13,

$$
\begin{aligned}
N_x &= A_{11}\left(\frac{\partial u^o}{\partial x} + \frac{1}{2}\left(\frac{\partial w^o}{\partial x}\right)^2\right) + A_{12}\left(\frac{\partial v^o}{\partial y} + \frac{1}{2}\left(\frac{\partial w^o}{\partial y}\right)^2\right) \\
&\quad + A_{16}\left(\frac{\partial u^o}{\partial y} + \frac{\partial v^o}{\partial x} + \frac{\partial w^o}{\partial y}\frac{\partial w^o}{\partial x}\right) - N_x^T \\
N_y &= A_{12}\left(\frac{\partial u^o}{\partial x} + \frac{1}{2}\left(\frac{\partial w^o}{\partial x}\right)^2\right) + A_{22}\left(\frac{\partial v^o}{\partial y} + \frac{1}{2}\left(\frac{\partial w^o}{\partial y}\right)^2\right) \\
&\quad + A_{26}\left(\frac{\partial u^o}{\partial y} + \frac{\partial v^o}{\partial x} + \frac{\partial w^o}{\partial y}\frac{\partial w^o}{\partial x}\right) - N_y^T \\
N_{xy} &= A_{16}\left(\frac{\partial u^o}{\partial x} + \frac{1}{2}\left(\frac{\partial w^o}{\partial x}\right)^2\right) + A_{26}\left(\frac{\partial v^o}{\partial y} + \frac{1}{2}\left(\frac{\partial w^o}{\partial y}\right)^2\right) \\
&\quad + A_{66}\left(\frac{\partial u^o}{\partial y} + \frac{\partial v^o}{\partial x} + \frac{\partial w^o}{\partial y}\frac{\partial w^o}{\partial x}\right) - N_{xy}^T \\
M_x &= -D_{11}\frac{\partial^2 w^o}{\partial^2 x} - D_{12}\frac{\partial^2 w^o}{\partial^2 y} - 2D_{16}\frac{\partial^2 w^o}{\partial x \partial y} \\
M_y &= -D_{12}\frac{\partial^2 w^o}{\partial^2 x} - D_{22}\frac{\partial^2 w^o}{\partial^2 y} - 2D_{26}\frac{\partial^2 w^o}{\partial x \partial y} \\
M_{xy} &= -D_{16}\frac{\partial^2 w^o}{\partial^2 x} - D_{26}\frac{\partial^2 w^o}{\partial^2 y} - 2D_{66}\frac{\partial^2 w^o}{\partial x \partial y} .
\end{aligned}
\tag{5.3}
$$

In the above expressions, the thermal stress resultants are

$$
\begin{aligned}
N_x^T &= \overline{N}_x^T \Delta T \\
N_y^T &= \overline{N}_y^T \Delta T \\
N_{xy}^T &= \overline{N}_{xy}^T \Delta T,
\end{aligned}
\tag{5.4}
$$

where the barred quantities were defined in Ch. 4 as the thermal stress resultants due to a unit temperature change. Substitution of the expressions of eqn. 5.3 into eqn. 5.2 leads to a rather complex equation for the first variation of the total potential energy. Closed-form solutions are difficult to obtain. As an alternative, using the Rayleigh-Ritz method, substitution into eqn. 5.2 of the assumed forms for the displacements u^o, v^o and w^o results in a coupled set of nonlinear algebraic equations. These coupled equations can be solved numerically for the coefficients of the assumed displacement functions in order to obtain the response of the plate as a function of temperature. Here the assumed forms for u^o, v^o, and w^o for the case of fixed simple supports are given by

$$
\begin{aligned}
u^o(x, y) &= \sum_{i=1}^{I} \sum_{j=1}^{J} u_{ij} \sin\left(\frac{i\pi x}{a}\right) \sin\left(\frac{j\pi y}{b}\right) \\
v^o(x, y) &= \sum_{i=1}^{I} \sum_{j=1}^{J} v_{ij} \sin\left(\frac{i\pi x}{a}\right) \sin\left(\frac{j\pi y}{b}\right) \\
w^o(x, y) &= \sum_{m=1}^{M} \sum_{n=1}^{N} w_{mn} \sin\left(\frac{m\pi x}{a}\right) \sin\left(\frac{n\pi y}{b}\right).
\end{aligned}
\tag{5.5}
$$

The assumed forms for the case of sliding simple supports are given by

$$
\begin{aligned}
u^o(x, y) &= \sum_{i=1}^{I} \sum_{j=0}^{J} u_{ij} \sin\left(\frac{i\pi x}{a}\right) \cos\left(\frac{j\pi y}{b}\right) \\
v^o(x, y) &= \sum_{i=0}^{I} \sum_{j=1}^{J} v_{ij} \cos\left(\frac{i\pi x}{a}\right) \sin\left(\frac{j\pi y}{b}\right) \\
w^o(x, y) &= \sum_{m=1}^{M} \sum_{n=1}^{N} w_{mn} \sin\left(\frac{m\pi x}{a}\right) \sin\left(\frac{n\pi y}{b}\right).
\end{aligned}
\tag{5.6}
$$

The form for $w^o(x, y)$ follows from the form used for studying the buckling response. The forms for $u^o(x, y)$ and $v^o(x, y)$ follow from the forms used for the prebuckling computations. Despite this similarity between the prebuckling and postbuckling problems, the postbuckling problem is computationally more involved. Substitution of either eqn. 5.5 or 5.6 into eqn. 5.3 and eqn. 5.2 leads to the nonlinear coupled equations for u_{ij}, v_{ij}, and w_{ij}.

Due to the complexity of this problem, the specific issues discussed here will be more limited than for the buckling problem. Specifically, only square plates undergoing a uniform change in temperature will be considered. However, the influence of both sets of boundary conditions, material axis skewing, and quasi-isotropic and orthotropic stacking arrangements on the thermal postbuckling response will be discussed.

5.2 Numerical Results

The nonlinear, coupled equations for the postbuckling response of a laminate are solved using a nonlinear equation solver (IMSL subroutine N2QNF [20]). A continuously increasing change in temperature from an ambient temperature is represented by a sequence of incremental temperature changes. At each increment in temperature a new solution must be found such that each nonlinear equation is equal to zero. This is equivalent to solving for $\delta\pi(u^o, v^o, w^o) = 0$. At each step the search for a new solution is begun by taking as an initial guess the solution calculated for the preceding temperature step. Because derivatives of u^o and v^o are added to squares of derivatives of w^o, in order to allow a full amount of coupling, more terms need to be taken in the series for u^o and v^o than in the series for w^o. To determine the relation between the number of terms taken in u^o and v^o and the number of terms taken in w^o the following trigonometric relations are considered:

$$\begin{aligned} \sin^2\theta &= \frac{1}{2}(1 - \cos 2\theta) \\ \cos^2\theta &= \frac{1}{2}(1 + \cos 2\theta) \\ \sin\theta\cos\theta &= \frac{1}{2}\sin 2\theta. \end{aligned} \tag{5.7}$$

In light of these relations and the expressions in eqns. 5.5 and 5.6, in order to allow the highest harmonic in u^o and v^o to match the highest harmonic in w^{o2}, we must have $I = 2M$ and $J = 2N$, where I and J are the upper limits in the series for u^o and v^o, and M and N are the upper limits in the series representing w^o.

5.2.1 Convergence

To study the convergence of these series solutions to the postbuckling problem, the response of a $(\pm 45/0_2)_s$ laminate with $\alpha = 30°$ is calculated using different numbers of terms in the series expressions for u^o, v^o and w^o. As with the buckling response, this particular situation requires as many, or more, terms in the postbuckling solution, compared to the other cases, in order to reach convergence. In the figures to follow, the relationship between the deflections at the center of the plate, normalized by the plate thickness, and $\Delta T/\Delta T^*$ are illustrated. Recall from Ch. 4 that ΔT^* is defined to be the buckling temperature of a quasi-isotropic plate with fixed simple supports, $\alpha = 0°$, and a uniform temperature distribution. The numerical value of ΔT^* is 69.4°F. In Fig. 21 the convergence characteristics for the fixed simple support case are illustrated. The temperature-deflection relationship as a function of the number of terms in the series are shown. Note that the plate remains flat until the buckling temperature for this particular plate configuration is reached, $\Delta T/\Delta T^* = 0.71$. From this figure it can be concluded that the use of $M \times N = 9$ leads to a converged solution. In fact, the use of $M \times N = 1$ provides an excellent estimate of the postbuckling response. The results of Fig. 21 show that at temperatures five times the buckling temperature, plate deflections less than twice the thickness of the plate occur. In Fig. 22 the convergence characteristics for the case of sliding simple supports are illustrated. Convergence for this case is not quite as rapid as for the case of fixed simple supports. The cases of $M \times N = 1$ and $M \times N = 4$ are not good estimates of the response as they were for the fixed boundaries. However, $M \times N = 9$ appears to lead to a converged solution. It is important to note that compared to the fixed simple support case, the postbuckling deflections for this case are not as large. The results in these figures are again based on a 6 in. by 6 in. laminate.

With convergence issues addressed, the next section focuses on some of the postbuckling responses for various physical situations. For these cases $M \times N = 9$ will be used.

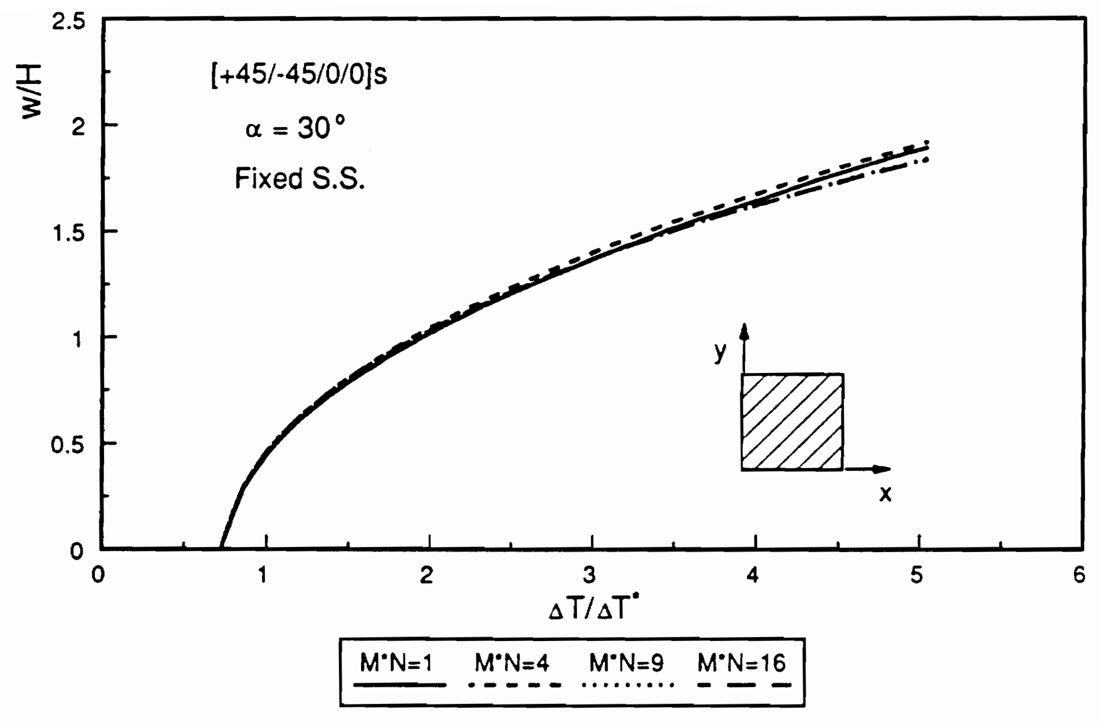

Fig. 21. Postbuckling convergence study: $(\pm 45/0_2)_S$ plate with $\alpha = 30°$ and fixed simple supports.

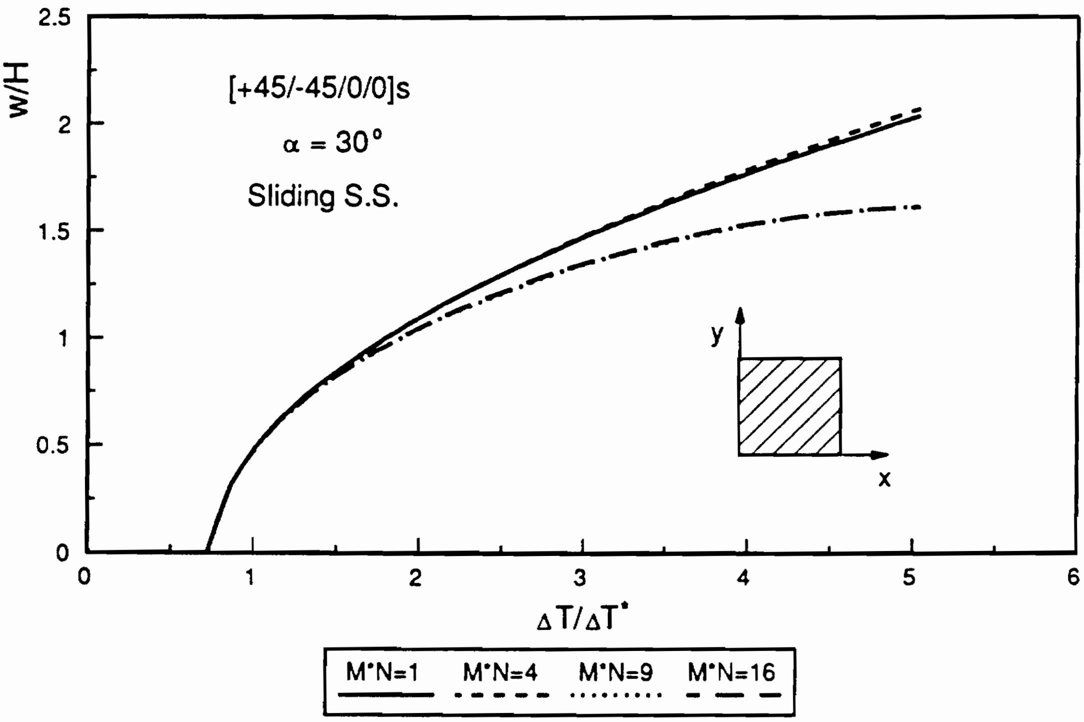

Fig. 22. Postbuckling convergence study: $(\pm 45/0_2)_s$ plate with $\alpha = 30°$ and sliding simple supports.

5.2.2 Postbuckling Characteristics

The postbuckling deflections at the center of the plate, normalized by plate thickness, versus $\Delta T/\Delta T^*$ for the quasi-isotropic laminate with $\alpha = 0°$ and fixed simple supports are illustrated in Fig. 23. As would be expected, the laminate begins to deflect out-of-plane at the critical buckling temperature predicted by the buckling solution, $\Delta T/\Delta T^* = 1$. Beyond this point the deflection increases rapidly until nearly twice the buckling temperature, ΔT^*, and then increases more slowly with increasing temperature. Although the slope of the temperature-deflection relation appears to be somewhat steep, even at five times the buckling temperature the deflection of the laminate is less than two plate thicknesses! It should be noted that the negative of these deflections is a possible postbuckling solution, as is the case $w^o = 0$. Though stability of the postbuckling configurations was not addressed in this study, the case of $w^o = 0$ is not believed to be stable.

The normalized postbuckling deflection at the center of the plate for the quasi-isotropic laminate with $\alpha = 30°$ and fixed simple supports is shown in Fig. 24. A comparison with the previous case, shown by a dotted line, shows that the postbuckling responses of the quasi-isotropic laminate with $\alpha = 0°$ and the quasi-isotropic laminate with $\alpha = 30°$ are distinct. The buckling temperature for the $(\pm 45/0/90)_s$ laminate with $\alpha = 30°$ is lower than the buckling temperature for the $(\pm 45/0/90)_s$ laminate with $\alpha = 0°$, so the postbuckling deflections of these laminates begin at different normalized temperatures. However, even if the postbuckling response for the $\alpha = 30°$ case were shifted to the right so that its starting point coincided with that for the $\alpha = 0°$ case, the two responses would still not coincide. With $\alpha = 30°$, the postbuckling deflections are greater than with $\alpha = 0°$. This serves again as a reminder that the term 'quasi-isotropic' refers only to the inplane properties of the laminate, the laminate acting softer when $\alpha = 0°$.

The postbuckling response of the orthotropic laminate with $\alpha = 0°$ and fixed simple supports is shown in Fig. 25. Again the quasi-isotropic case is shown for comparison. Although

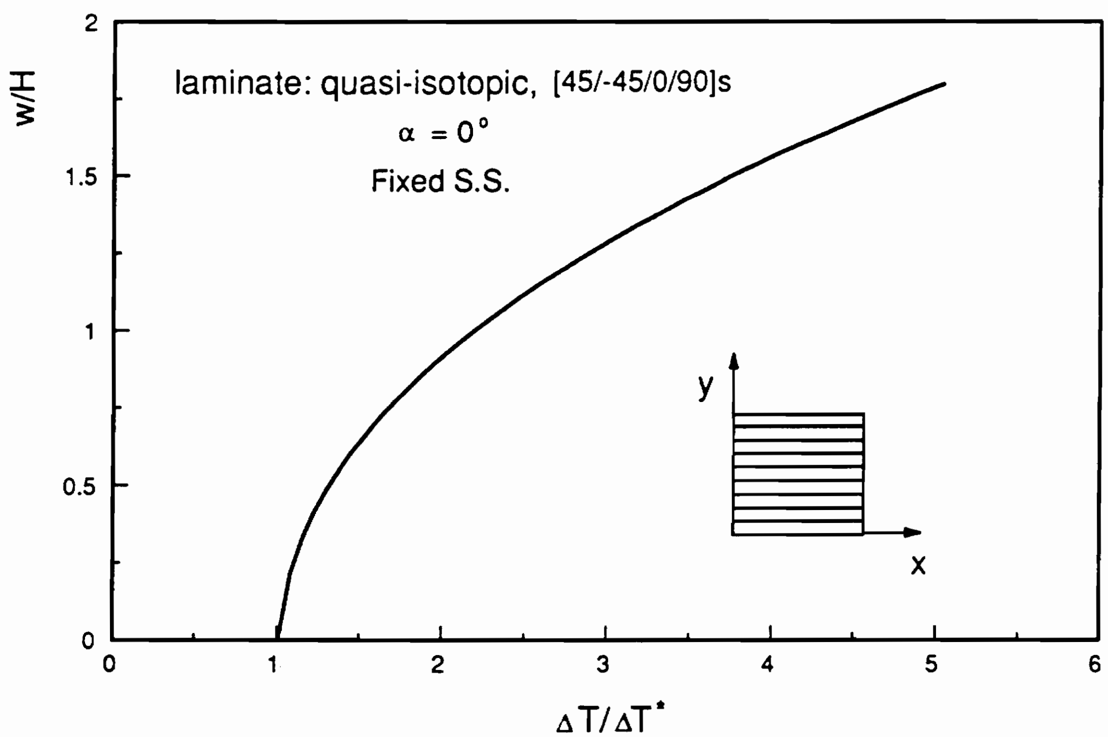

Fig. 23. Postbuckling response of a $(\pm 45/0/90)_s$ plate with $\alpha = 0°$ and fixed simple supports.

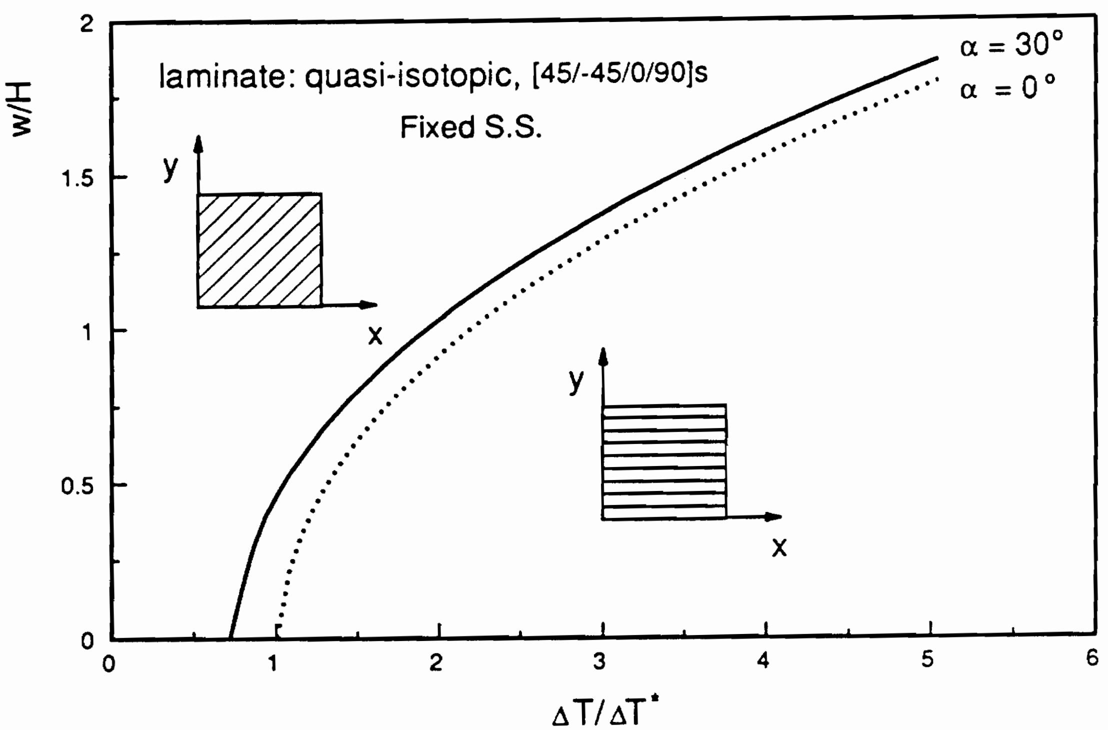

Fig. 24. Postbuckling response of a $(\pm 45/0/90)_S$ plate with $\alpha = 30°$ and fixed simple supports.

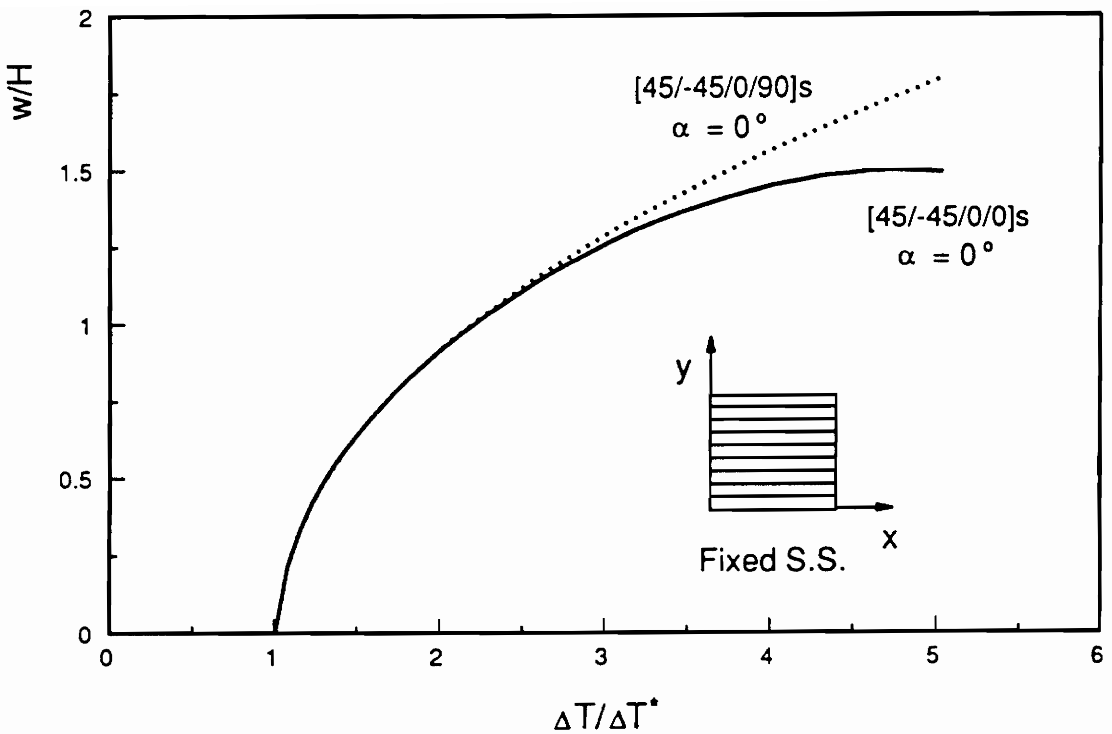

Fig. 25. Postbuckling response of a $(\pm 45/0_2)_S$ plate with $\alpha = 0°$ and fixed simple supports.

the buckling temperatures for the orthotropic and quasi-isotropic laminates with $\alpha = 0°$ are the same, the postbuckling responses of these two laminates are different. The normalized deflection-temperature relations for both laminates begin at the same point and follow similar paths until nearly twice ΔT^*, after which the deflection for the $(\pm 45/0_2)_s$ laminate with $\alpha = 0°$ increases less rapidly, reaching less than 1.5 plate thicknesses at $\Delta T/\Delta T^* = 5$.

As was seen in ch. 3, Table 3, the buckling temperatures of the $(\pm 45/0_2)_s$ laminate with $\alpha = 30°$ and the $(\pm 45/0/90)_s$ laminate with $\alpha = 30°$, both with fixed simple supports, are within a few degrees of each other. The postbuckling responses of these laminates are also very similar, as shown in Fig. 26. Indeed, referring to Fig. 24, it is observed that the postbuckling responses of the $(\pm 45/0_2)_s$ and the $(\pm 45/0/90)_s$ laminates with $\alpha = 30°$ are much more similar than are the responses of the same laminates with $\alpha = 0°$. Skewing tends to be an equalizer as regards the postbuckling responses of these two laminates.

The postbuckling response of the quasi-isotropic laminate with $\alpha = 0°$ and sliding simple supports is shown in Fig. 27. The case of fixed simple supports from Fig. 23 is included for comparison. The buckling solutions for the on-axis quasi-isotropic laminate with fixed simple supports and with sliding simple supports are identical, and thus both postbuckling responses remain flat until the normalized temperature is unity. However, while the postbuckling responses for these two cases are initially close to one another, they soon diverge. The out-of-plane deflection at the center of the plate for the quasi-isotropic laminate with sliding simple supports at $\Delta T/\Delta T^* = 5$ is about 20% less than the deflection of the quasi-isotropic laminate with fixed simple supports. Comparison of this figure with Fig. 24 shows that a change in boundary conditions can have as much influence on the postbuckling response of a laminate as skewing of the laminate's material axes.

In Fig. 28 the postbuckling response of the quasi-isotropic laminate with $\alpha = 30°$ and sliding simple supports is shown. The case of $\alpha = 0°$ is shown for comparison. Once again, it is seen that the response of the quasi-isotropic laminate with $\alpha = 30°$ is distinct from the response of the quasi-isotropic laminate with $\alpha = 0°$. This was the case for fixed simple sup-

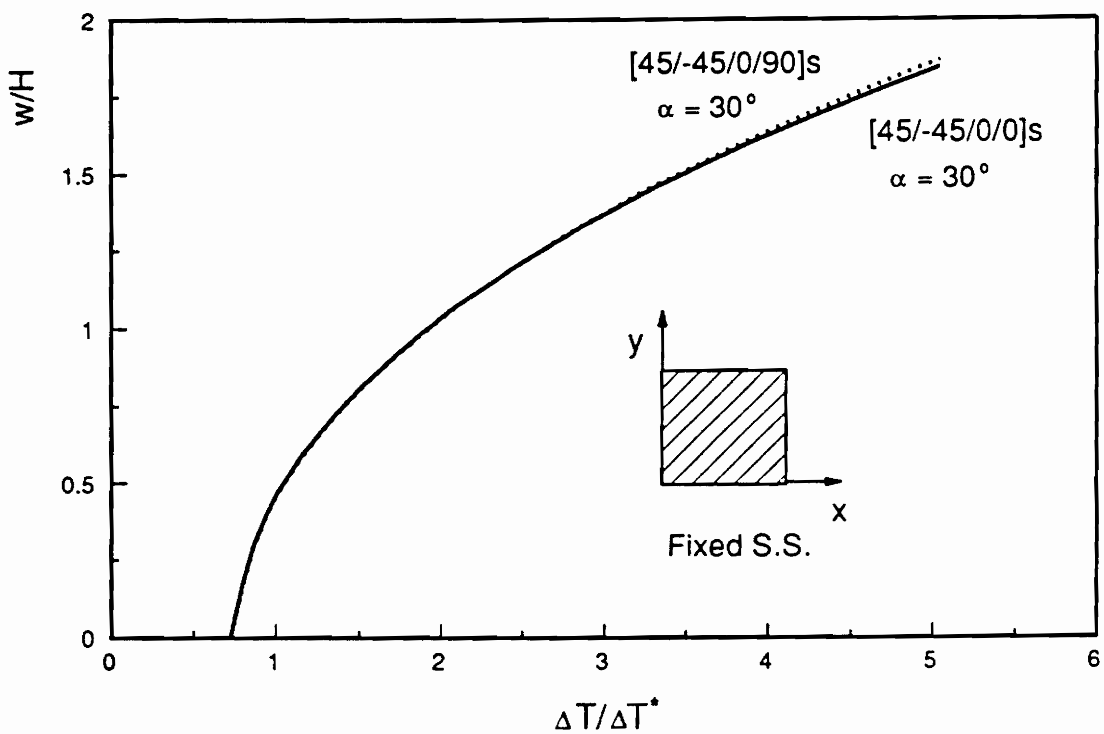

Fig. 26. Postbuckling response of a $(\pm 45/0_2)_S$ plate with $\alpha = 30°$ and fixed simple supports.

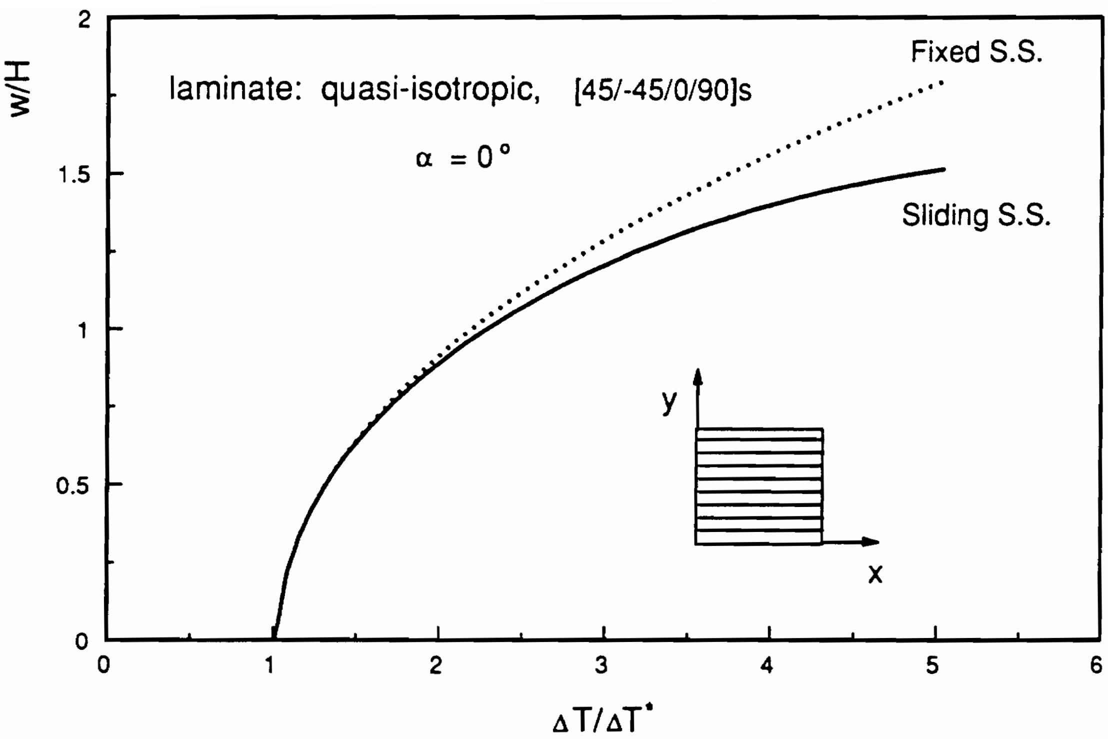

Fig. 27. Postbuckling response of a $(\pm 45/0/90)_s$ plate with $\alpha = 0°$ and sliding simple supports.

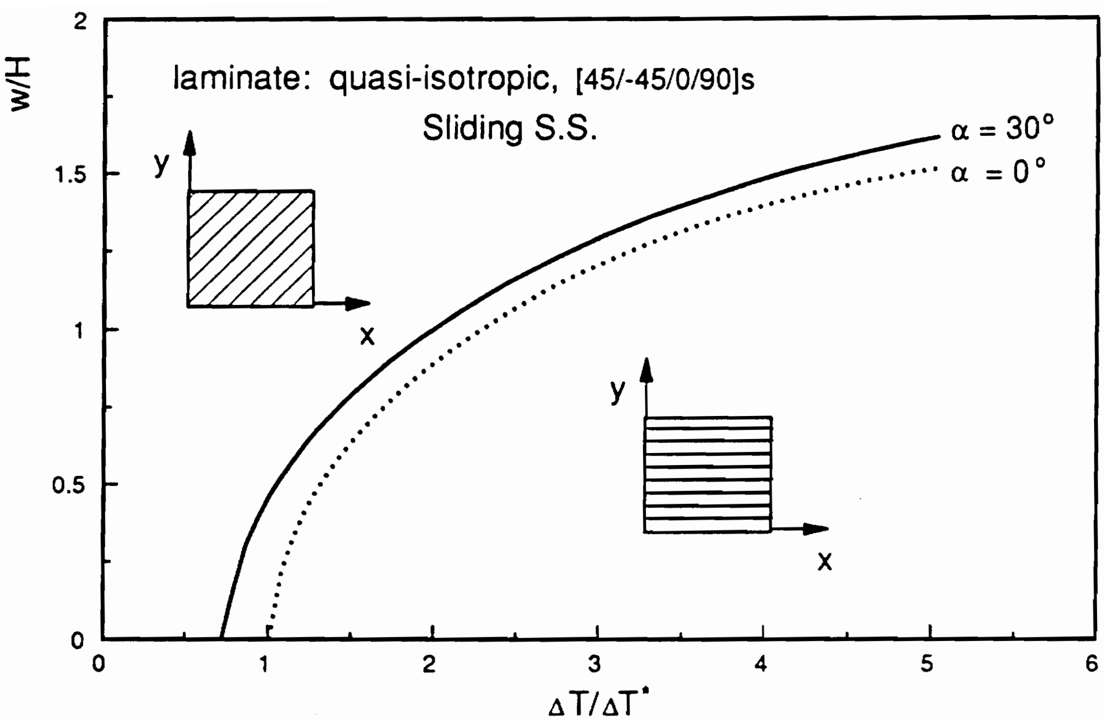

Fig. 28. Postbuckling respone of a $(\pm 45/0/90)_s$ plate with $\alpha = 30°$ and sliding simple supports.

ports, Fig. 24. That deflections for the fixed support case are greater is evident by comparison of Fig. 28 with Fig. 24.

Figure 29 shows the postbuckling response for the $(\pm 45/0_2)_s$ laminate with $\alpha = 0°$ and sliding simple supports. The postbuckling response for this case is quite different from those seen previously. While the response for this case is initially almost identical to that for the same laminate with fixed simple supports, for changes in temperature beyond $\Delta T/\Delta T^* = 3$ the out-of-plane deflection at the center of the plate actually <u>decreases</u> with increasing temperature! In all of the previous cases examined, the postbuckling response consists mainly of the deflections associated with the Rayleigh-Ritz coefficient w_{11}. In the present case, for $\Delta T/\Delta T^* > 1.5$ the deflection associated with w_{13}, and, to a lesser extent, the deflection associated with w_{31}, begin to influence the postbuckling response more and more as w_{13} and w_{31} rapidly approach the magnitude of w_{11}. The change in the character of the response with increasing ΔT can be interpreted as modal interaction, the modes being the buckling modes associated with the higher eigentemperatures in the buckling problem. This interaction can be better understood by examining contour plots of the deflection, w, normalized by the plate thickness, H, at $\Delta T/\Delta T^*$ = 2, 3, 4, and 5. These contour plots are given in Fig. 30. At $\Delta T/\Delta T^* = 2$ the postbuckling deflection is similar to the buckling deflection for this case given in Fig. 5b. The location of the maximum deflection is the center of the plate. As the temperature increases, at $\Delta T/\Delta T^* = 3$ and $\Delta T/\Delta T^* = 4$, the contours become more oval shaped, with the regions of maximum deflections moving toward the edges $y=0$ and $y=b$. At $\Delta T/\Delta T^* = 5$, this process has continued to the point that the maximum deflections no longer occur at the center of the plate. This shift in the point of maximum deflection is largely due to the fact the four 0° layers make the laminate much stiffer in the x direction than in the y direction, and the fact that $\overline{N}_x^T$ is less than one half of $\overline{N}_y^T$. This latter relationship is due to the negative value of the thermal expansion coefficient α_1. A similar but less pronounced trend can be seen for the $(\pm 45/0_2)_s$ laminate with fixed simple supports and $\alpha = 0°$. The postbuckling response for this case was shown in Fig. 25. The deflection contours at various temperatures are shown in

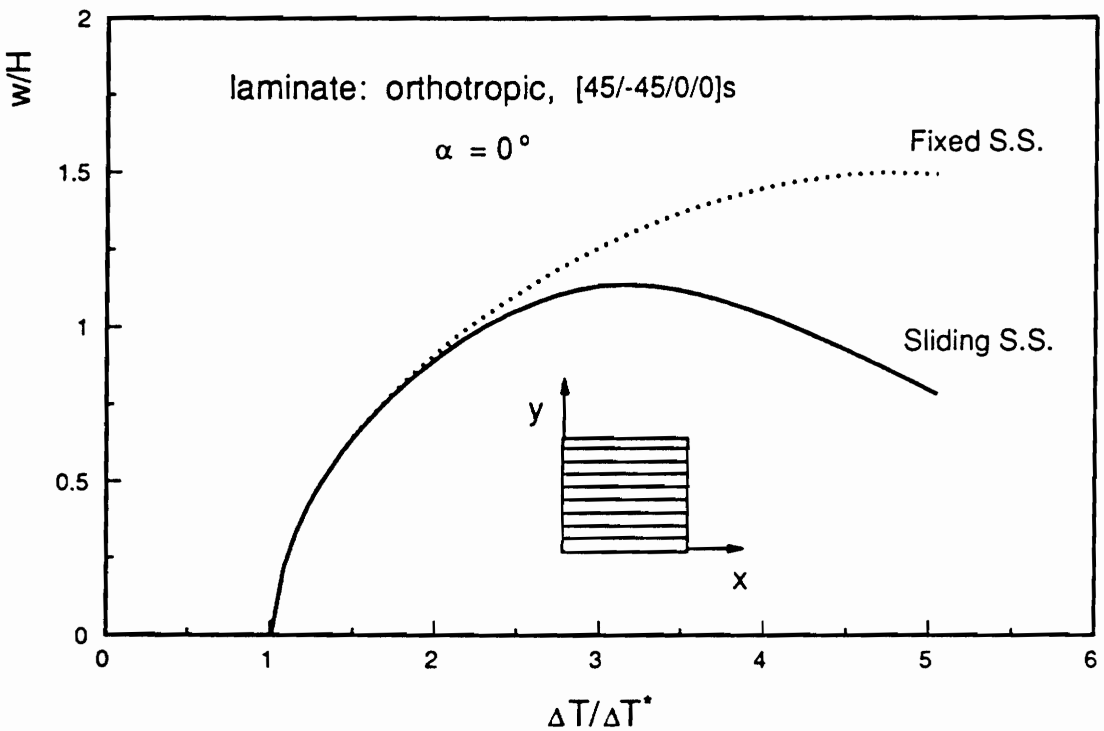

Fig. 29. Postbuckling response of a $(\pm 45/0_2)_S$ plate with $\alpha = 0°$ and sliding simple supports.

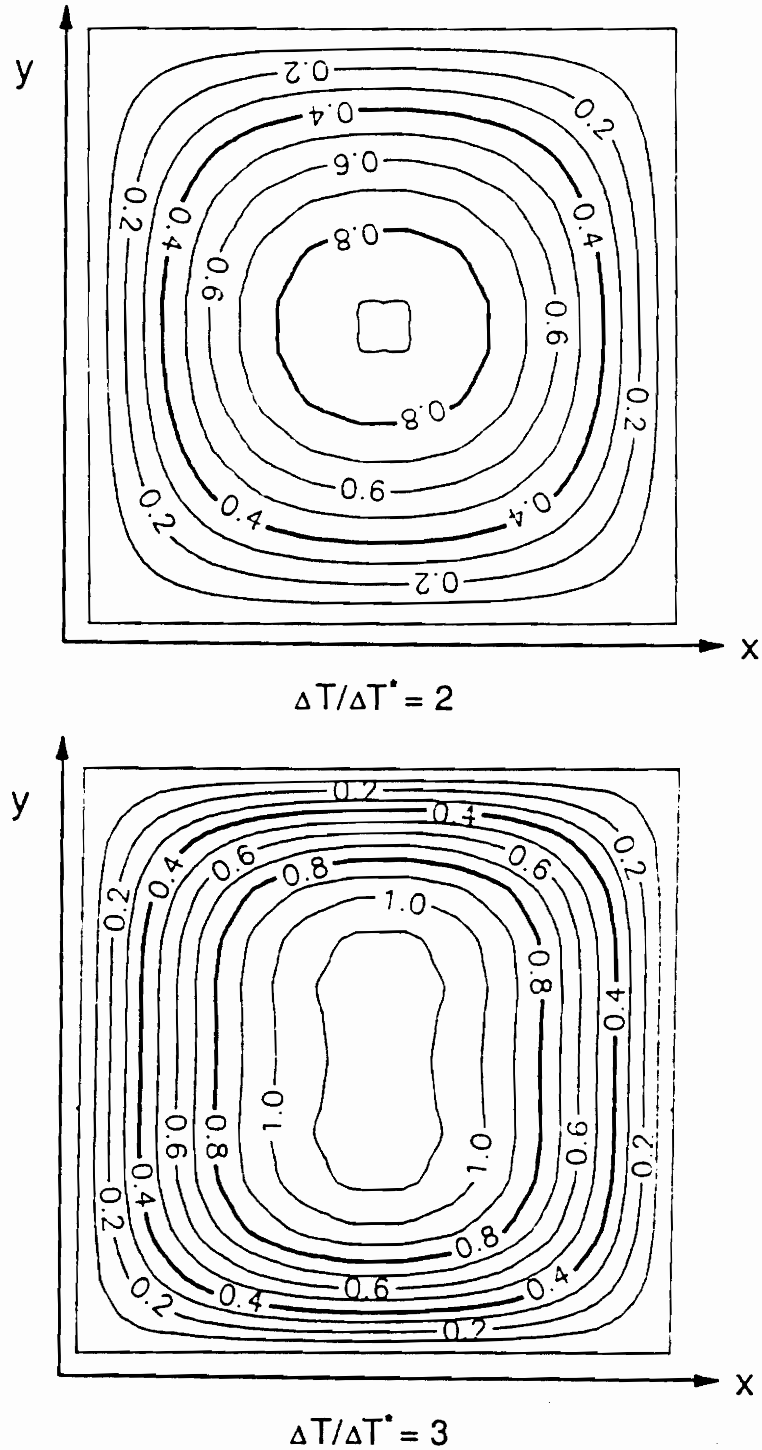

Fig. 30. Postbuckling deflections for a $(\pm45/0_2)_S$ plate with $\alpha = 0°$ and sliding simple supports at $\Delta T/\Delta T^* = 2, 3, 4,$ and 5.

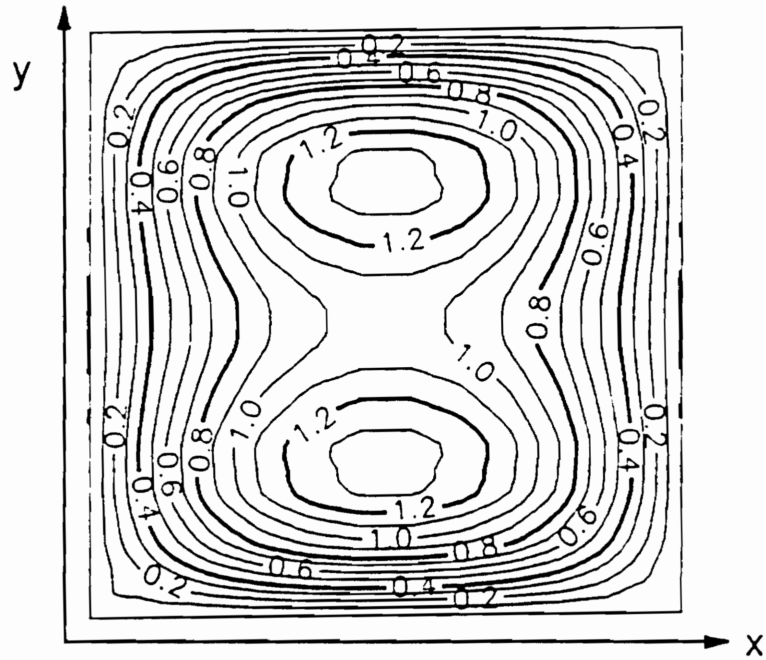

$\Delta T/\Delta T^{*}= 4$

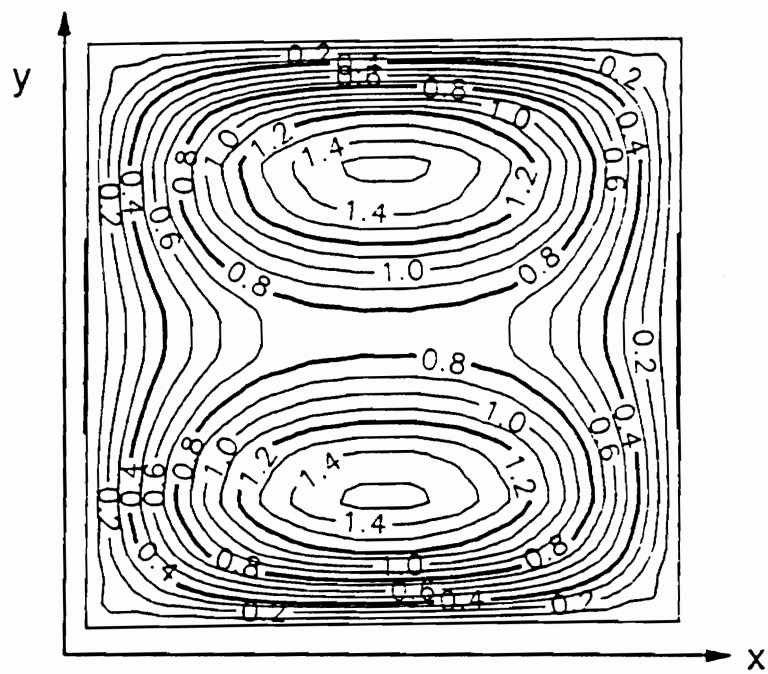

$\Delta T/\Delta T^{*}= 5$

Figure 30 (continued)

Fig. 31. It is evident that the points of maximum deflection move away from the center as the temperature increases for this case as well.

As shown in Fig. 32 when the material axes of the $(\pm 45/0_2)_s$ with sliding simple supports are skewed by $\alpha = 30°$ the postbuckling response once again is such that the deflection associated with w_{11} dominates with increasing temperature.

In conclusion, it can be stated that the thermal postbuckling response can be complex. The dramatic change of the deflection pattern with increasing temperature for certain physical conditions attests to this fact. Also it is clear that the support conditions have an influence on the thermal postbuckling response, as do the skewing angle and degree of orthotropy. While an understanding of the postbuckling response is important, as mentioned in ch. 1, it represents an ideal situation. Generally, imperfections in the plate, support conditions, and even imperfections in the temperature field prevent observation of true postbuckling response. Rather, postbuckling response is taken as the limit of behavior, imperfections causing the deflection-temperature relations to deviate from those just discussed. The next chapter addresses the influence of imperfections and compares the response in the presence of imperfections with the ideal postbuckling case.

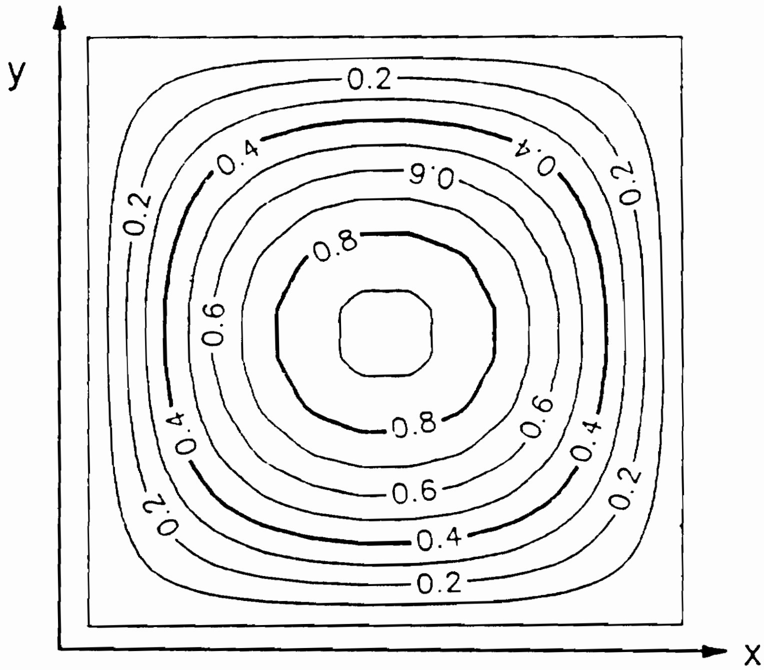

$\Delta T/\Delta T^{*} = 2$

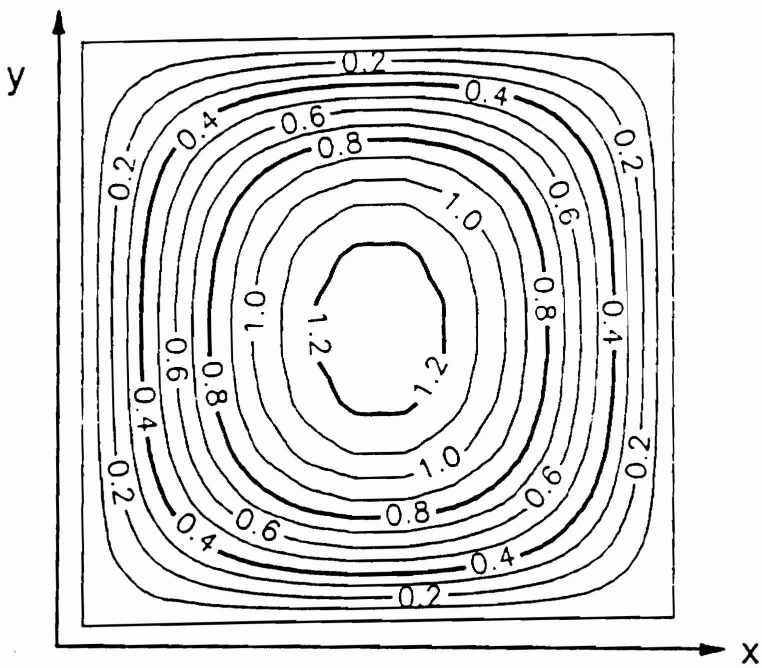

$\Delta T/\Delta T^{*} = 3$

Fig. 31. Postbuckling deflections for a $(\pm 45/0_2)_S$ plate with $\alpha = 0°$ and fixed simple supports at $\Delta T/\Delta T^{*}$ = 2, 3, 4, and 5.

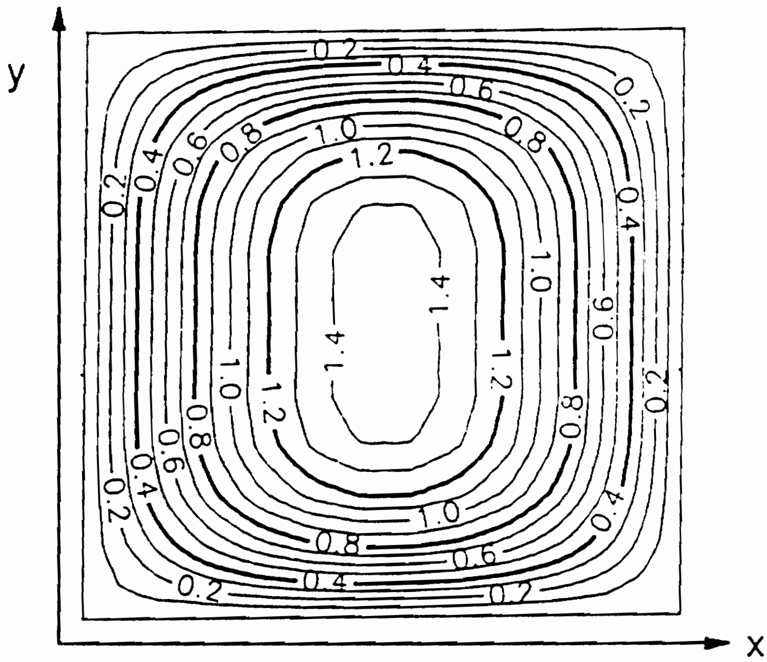

$\Delta T/\Delta T^{*} = 4$

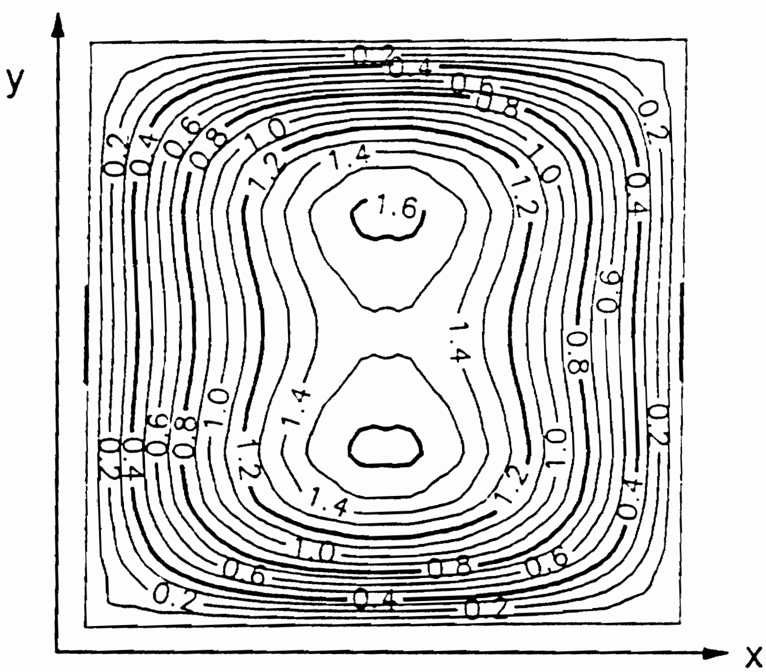

$\Delta T/\Delta T^{*} = 5$

Figure 31 (continued)

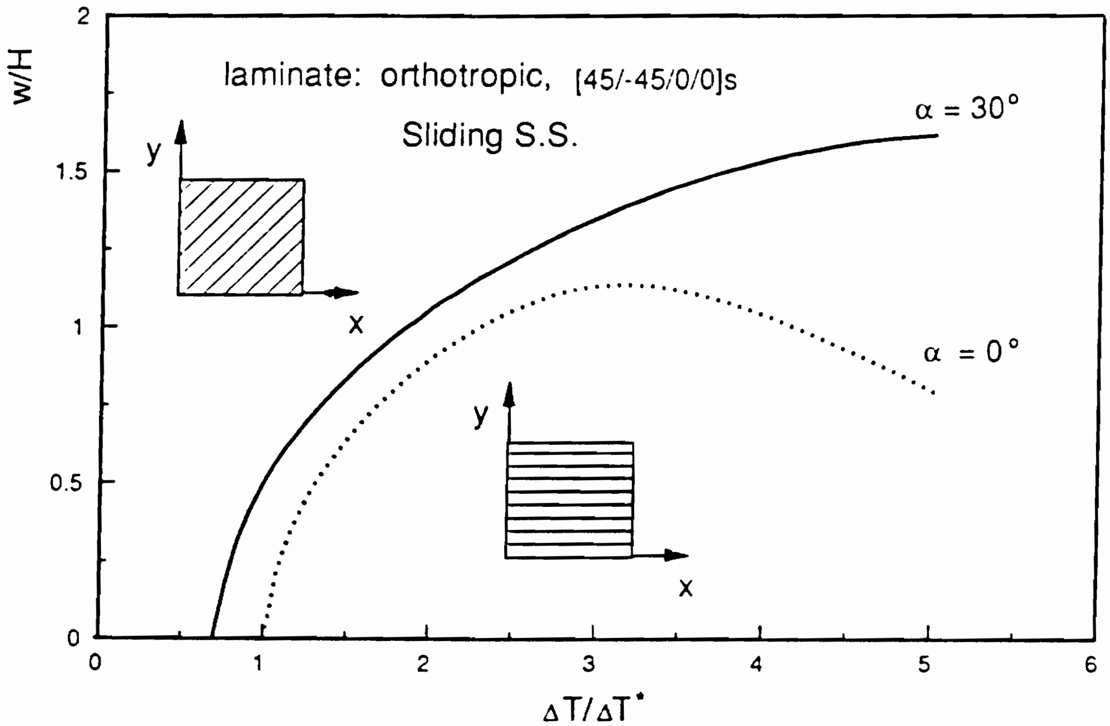

Fig. 32. Postbuckling response of a $(\pm 45/0_2)_s$ plate with $\alpha = 30°$ and sliding simple supports.

6.0 Response in the Presence of an Imperfection

In this chapter the influence of two forms of imperfections on the thermally-induced response of the plates are considered. One imperfection considered is a slight through-the-thickness temperature gradient. The other imperfection considered is a lack of initial plate flatness. Both of the imperfections represent very realistic deviations from the ideal. While they do not include all the forms of imperfections that might be encountered, a study of their influence provides insight into possible explanations of differences between observed and ideal behavior in actual experiments. Numerical results are presented for both cases.

6.1 Formulation

6.1.1 Temperature Gradient Through the Thickness of the Plate

In the testing of plates in a thermal enviroment, achieving a perfectly uniform temperature within the entire volume of the test chamber may be difficult. In a previous chapter the influence of a temperature gradient in the plane of the plate was examined. Here, the influence of a temperature gradient through the thickness of the plate on the thermal response will be examined. This is a reasonable deviation from the ideal since if a plate is tested in a horizontal position within the test chamber, convection and conduction effects may result in the top surface of the plate being a slightly different temperature than the bottom surface of the plate. Accordingly, the imperfection considered here is a temperature gradient through the thickness of the plate which is of the form

$$\Delta T = c\left(1 + \frac{e}{H} z\right). \tag{6.1}$$

In the above equation, e represents the magnitude of the gradient and H is the total thickness of the plate. Because the reference surface, $z=0$, is the midplane of the plate, c is the temperature at the midplane of the plate. Referring to the coordinate system in Fig. 1, the temperature at the top of the plate is then $c(1+e/2)$, and at the bottom of the plate the temperature is $c(1-e/2)$. Thus, if e is positive the plate is warmer on the top than on the bottom. This will cause the plate to begin to deflect out of plane as soon as the temperature is increased relative to the reference temperature.

For this form of an imperfection the preloading effects, σ_x^P, σ_y^P, and τ_{xy}^P, are again due only to thermally-induced deformations. As a result, eqn. 4.1 - 4.2 are valid. Equation 5.2 still governs the nonlinear response. However, M_x^T, M_y^T, and M_{xy}^T are no longer zero, thus the stress resultants are given by

$$\begin{aligned}
N_x &= A_{11}\varepsilon_x^o + A_{12}\varepsilon_y^o + A_{16}\gamma_{xy}^o - N_x^T \\
N_y &= A_{12}\varepsilon_x^o + A_{22}\varepsilon_y^o + A_{26}\gamma_{xy}^o - N_y^T \\
N_{xy} &= A_{16}\varepsilon_x^o + A_{26}\varepsilon_y^o + A_{66}\gamma_{xy}^o - N_{xy}^T \\
M_x &= D_{11}\kappa_x^o + D_{12}\kappa_y^o + D_{16}\kappa_{xy}^o - M_x^T \\
M_y &= D_{12}\kappa_x^o + D_{22}\kappa_y^o + D_{26}\kappa_{xy}^o - M_y^T \\
M_{xy} &= D_{16}\kappa_x^o + D_{26}\kappa_y^o + D_{66}\kappa_{xy}^o - M_{xy}^T,
\end{aligned} \tag{6.2}$$

where,

$$
\begin{aligned}
N_x^T &= c\int_{\frac{-H}{2}}^{\frac{+H}{2}} (\overline{Q}_{11}\alpha_x + \overline{Q}_{12}\alpha_y + \overline{Q}_{16}\alpha_{xy})dz \\
N_y^T &= c\int_{\frac{-H}{2}}^{\frac{+H}{2}} (\overline{Q}_{12}\alpha_x + \overline{Q}_{22}\alpha_y + \overline{Q}_{26}\alpha_{xy})dz \\
N_{xy}^T &= c\int_{\frac{-H}{2}}^{\frac{+H}{2}} (\overline{Q}_{16}\alpha_x + \overline{Q}_{26}\alpha_y + \overline{Q}_{66}\alpha_{xy})dz \\
M_x^T &= \frac{ce}{H}\int_{\frac{-H}{2}}^{\frac{+H}{2}} (\overline{Q}_{11}\alpha_x + \overline{Q}_{12}\alpha_y + \overline{Q}_{16}\alpha_{xy})z^2dz \\
M_y^T &= \frac{ce}{H}\int_{\frac{-H}{2}}^{\frac{+H}{2}} (\overline{Q}_{12}\alpha_x + \overline{Q}_{22}\alpha_y + \overline{Q}_{26}\alpha_{xy})z^2dz \\
M_{xy}^T &= \frac{ce}{H}\int_{\frac{-H}{2}}^{\frac{+H}{2}} (\overline{Q}_{16}\alpha_{+}\overline{Q}_{26}\alpha_y + \overline{Q}_{66}\alpha_{xy})z^2dz.
\end{aligned}
\tag{6.3}
$$

Using the reference surface strains and curvatures from eqns. 3.5 - 3.7, the stress resultants of eqn. 6.2 become

$$
\begin{aligned}
N_x = {} & A_{11}\left(\frac{\partial u^o}{\partial x} + \frac{1}{2}\left(\frac{\partial w^o}{\partial x}\right)^2\right) + A_{12}\left(\frac{\partial v^o}{\partial y} + \frac{1}{2}\left(\frac{\partial w^o}{\partial y}\right)^2\right) \\
& + A_{16}\left(\frac{\partial u^o}{\partial y} + \frac{\partial v^o}{\partial x} + \frac{\partial w^o}{\partial y}\frac{\partial w^o}{\partial x}\right) - N_x^T \\
N_y = {} & A_{12}\left(\frac{\partial u^o}{\partial x} + \frac{1}{2}\left(\frac{\partial w^o}{\partial x}\right)^2\right) + A_{22}\left(\frac{\partial v^o}{\partial y} + \frac{1}{2}\left(\frac{\partial w^o}{\partial y}\right)^2\right) \\
& + A_{26}\left(\frac{\partial u^o}{\partial y} + \frac{\partial v^o}{\partial x} + \frac{\partial w^o}{\partial y}\frac{\partial w^o}{\partial x}\right) - N_y^T \\
N_{xy} = {} & A_{16}\left(\frac{\partial u^o}{\partial x} + \frac{1}{2}\left(\frac{\partial w^o}{\partial x}\right)^2\right) + A_{26}\left(\frac{\partial v^o}{\partial y} + \frac{1}{2}\left(\frac{\partial w^o}{\partial y}\right)^2\right) \\
& + A_{66}\left(\frac{\partial u^o}{\partial y} + \frac{\partial v^o}{\partial x} + \frac{\partial w^o}{\partial y}\frac{\partial w^o}{\partial x}\right) - N_{xy}^T \\
M_x = {} & -D_{11}\frac{\partial^2 w^o}{\partial^2 x} - D_{12}\frac{\partial^2 w^o}{\partial^2 y} - 2D_{16}\frac{\partial^2 w^o}{\partial x \partial y} - M_x^T \\
M_y = {} & -D_{12}\frac{\partial^2 w^o}{\partial^2 x} - D_{22}\frac{\partial^2 w^o}{\partial^2 y} - 2D_{26}\frac{\partial^2 w^o}{\partial x \partial y} - M_y^T \\
M_{xy} = {} & -D_{16}\frac{\partial^2 w^o}{\partial^2 x} - D_{26}\frac{\partial^2 w^o}{\partial^2 y} - 2D_{66}\frac{\partial^2 w^o}{\partial x \partial y} - M_{xy}^T.
\end{aligned}
\tag{6.4}
$$

Substitution of eqns. 6.3 and 6.4 into eqn. 5.2 results in an expression for the first variation of the total potential energy for this case. Proceeding as in ch. 5, the Rayleigh-Ritz method is used to obtain a coupled set of nonlinear algebraic equations which can be solved numerically for the response of the plate, for a given value of e, as a function of the plate's midplane temperature, c. The assumed series of eqns. 5.5 and 5.6 are used to determine the responses for the two boundary conditions.

6.1.2 Lack of Initial Flatness

Because of the lack of ideal alignment of the fiber directions in all of the layers, the lack of uniform processing conditions, and even slight variations in the prepreg used to fabricate the plates, a composite plate rarely is perfectly flat. Generally the plate has an initial out-of-plane deflection. Here the influence of the imperfection on the thermal response of the plate will be studied. Such an imperfection will cause the thermal response to deviate from the ideal postbuckling response. Because the Rayleigh-Ritz method will again be used to solve this problem, the initial out-of-plane deflection is given by a double sine series similar to the one used to represent w° in ch. 5, namely,

$$w^{I}(x, y) = \sum_{m=1}^{M} \sum_{n=1}^{N} w^{I}_{mn} \sin\left(\frac{m\pi x}{a}\right) \sin\left(\frac{n\pi y}{b}\right). \tag{6.5}$$

This represents the deviation from initial flatness of the reference surface. The displacement, w°, as before, is the total out-of-plane deflection, including w^{I}.

For this case the preloading effects are now due to more than just thermally-induced deformations. In this case the reference surface strains of eqn. 3.5, due to the preloading effects, are

$$\begin{aligned}
\varepsilon_x^P &= \frac{1}{2}\left(\frac{\partial w^I}{\partial x}\right)^2 - z\frac{\partial^2 w^I}{\partial x^2} + \alpha_x \Delta T \\
\varepsilon_y^P &= \frac{1}{2}\left(\frac{\partial w^I}{\partial y}\right)^2 - z\frac{\partial^2 w^I}{\partial y^2} + \alpha_y \Delta T \\
\gamma_{xy}^P &= \frac{\partial w^I}{\partial x}\frac{\partial w^I}{\partial y} - 2z\frac{\partial^2 w^I}{\partial x \partial y} + \alpha_{xy} \Delta T.
\end{aligned} \tag{6.6}$$

From eqn. 3.8, the preloading effects are given by

$$\begin{aligned}\sigma_x^P &= \overline{Q}_{11}\varepsilon_x^P + \overline{Q}_{12}\varepsilon_y^P + \overline{Q}_{16}\gamma_{xy}^P\\ \sigma_y^P &= \overline{Q}_{12}\varepsilon_x^P + \overline{Q}_{22}\varepsilon_y^P + \overline{Q}_{26}\gamma_{xy}^P\\ \tau_{xy}^P &= \overline{Q}_{16}\varepsilon_x^P + \overline{Q}_{26}\varepsilon_y^P + \overline{Q}_{66}\gamma_{xy}^P.\end{aligned} \tag{6.7}$$

The stress resultants are the same as in eqn. 3.13. Namely,

$$\begin{aligned}N_x &= A_{11}\varepsilon_x^o + A_{12}\varepsilon_y^o + A_{16}\gamma_{xy}^o - N_x^P\\ N_y &= A_{12}\varepsilon_x^o + A_{22}\varepsilon_y^o + A_{26}\gamma_{xy}^o - N_y^P\\ N_{xy} &= A_{16}\varepsilon_x^o + A_{26}\varepsilon_y^o + A_{66}\gamma_{xy}^o - N_{xy}^P\\ M_x &= D_{11}\kappa_x^o + D_{12}\kappa_y^o + D_{16}\kappa_{xy}^o - M_x^P\\ M_y &= D_{12}\kappa_x^o + D_{22}\kappa_y^o + D_{26}\kappa_{xy}^o - M_y^P\\ M_{xy} &= D_{16}\kappa_x^o + D_{26}\kappa_y^o + D_{66}\kappa_{xy}^o - M_{xy}^P.\end{aligned} \tag{6.8}$$

In the present situation the preloading stress resultants are given by a combination of effects due to lack of initial flatness, and thermal effects. The preloading stress resultants are, from eqn. 3.14,

$$\begin{aligned}N_x^P &= \int_{\frac{-H}{2}}^{\frac{+H}{2}} \sigma_x^P dz = \frac{1}{2}A_{11}\left(\frac{\partial w^I}{\partial x}\right)^2 + \frac{1}{2}A_{12}\left(\frac{\partial w^I}{\partial y}\right)^2 + A_{16}\frac{\partial w^I}{\partial x}\frac{\partial w^I}{\partial y} + N_x^T\\ N_y^P &= \int_{\frac{-H}{2}}^{\frac{+H}{2}} \sigma_y^P dz = \frac{1}{2}A_{12}\left(\frac{\partial w^I}{\partial x}\right)^2 + \frac{1}{2}A_{22}\left(\frac{\partial w^I}{\partial y}\right)^2 + A_{26}\frac{\partial w^I}{\partial x}\frac{\partial w^I}{\partial y} + N_y^T\\ N_{xy}^P &= \int_{\frac{-H}{2}}^{\frac{+H}{2}} \tau_{xy}^P dz = \frac{1}{2}A_{16}\left(\frac{\partial w^I}{\partial x}\right)^2 + \frac{1}{2}A_{26}\left(\frac{\partial w^I}{\partial y}\right)^2 + A_{66}\frac{\partial w^I}{\partial x}\frac{\partial w^I}{\partial y} + N_{xy}^T\\ M_x^P &= \int_{\frac{-H}{2}}^{\frac{+H}{2}} z\sigma_x^P dz = -D_{11}\frac{\partial^2 w^I}{\partial x^2} - D_{12}\frac{\partial^2 w^I}{\partial y^2} - 2D_{16}\frac{\partial^2 w^I}{\partial x\partial y} + M_x^T\\ M_y^P &= \int_{\frac{-H}{2}}^{\frac{+H}{2}} z\sigma_y^P dz = -D_{12}\frac{\partial^2 w^I}{\partial x^2} - D_{22}\frac{\partial^2 w^I}{\partial y^2} - 2D_{26}\frac{\partial^2 w^I}{\partial x\partial y} + M_y^T\\ M_{xy}^P &= \int_{\frac{-H}{2}}^{\frac{+H}{2}} z\tau_{xy}^P dz = -D_{16}\frac{\partial^2 w^I}{\partial x^2} - D_{26}\frac{\partial^2 w^I}{\partial y^2} - 2D_{66}\frac{\partial^2 w^I}{\partial x\partial y} + M_{xy}^T.\end{aligned} \tag{6.9}$$

For this case the change in temperature will be assumed to be uniform, both with x and y, and also with z. The thermal stress resultants are thus once again given by

$$
\begin{aligned}
N_x^T &= \overline{N}_x^T \Delta T \\
N_y^T &= \overline{N}_y^T \Delta T \\
N_{xy}^T &= \overline{N}_{xy}^T \Delta T \\
M_x^T = M_y^T &= M_{xy}^T = 0.
\end{aligned}
\tag{6.10}
$$

Using the reference surface strains and curvatures, the stress resultants of eqn. 6.8 become

$$
\begin{aligned}
N_x &= A_{11}\left(\frac{\partial u^o}{\partial x} + \frac{1}{2}\left(\frac{\partial w^o}{\partial x}\right)^2\right) + A_{12}\left(\frac{\partial v^o}{\partial y} + \frac{1}{2}\left(\frac{\partial w^o}{\partial y}\right)^2\right) \\
&\quad + A_{16}\left(\frac{\partial u^o}{\partial y} + \frac{\partial v^o}{\partial x} + \frac{\partial w^o}{\partial y}\frac{\partial w^o}{\partial x}\right) - N_x^P \\
N_y &= A_{12}\left(\frac{\partial u^o}{\partial x} + \frac{1}{2}\left(\frac{\partial w^o}{\partial x}\right)^2\right) + A_{22}\left(\frac{\partial v^o}{\partial y} + \frac{1}{2}\left(\frac{\partial w^o}{\partial y}\right)^2\right) \\
&\quad + A_{26}\left(\frac{\partial u^o}{\partial y} + \frac{\partial v^o}{\partial x} + \frac{\partial w^o}{\partial y}\frac{\partial w^o}{\partial x}\right) - N_y^P \\
N_{xy} &= A_{16}\left(\frac{\partial u^o}{\partial x} + \frac{1}{2}\left(\frac{\partial w^o}{\partial x}\right)^2\right) + A_{26}\left(\frac{\partial v^o}{\partial y} + \frac{1}{2}\left(\frac{\partial w^o}{\partial y}\right)^2\right) \\
&\quad + A_{66}\left(\frac{\partial u^o}{\partial y} + \frac{\partial v^o}{\partial x} + \frac{\partial w^o}{\partial y}\frac{\partial w^o}{\partial x}\right) - N_{xy}^P \\
M_x &= -D_{11}\frac{\partial^2 w^o}{\partial^2 x} - D_{12}\frac{\partial^2 w^o}{\partial^2 y} - 2D_{16}\frac{\partial^2 w^o}{\partial x \partial y} - M_x^P \\
M_y &= -D_{12}\frac{\partial^2 w^o}{\partial^2 x} - D_{22}\frac{\partial^2 w^o}{\partial^2 y} - 2D_{26}\frac{\partial^2 w^o}{\partial x \partial y} - M_y^P \\
M_{xy} &= -D_{16}\frac{\partial^2 w^o}{\partial^2 x} - D_{26}\frac{\partial^2 w^o}{\partial^2 y} - 2D_{66}\frac{\partial^2 w^o}{\partial x \partial y} - M_{xy}^P,
\end{aligned}
\tag{6.11}
$$

where the preloading stress resultants are those of eqn. 6.9. The governing equation for this problem is again the expression for the first variation of the total potential energy, given in eqn. 5.2. However, substitution of the expressions for the stress resultants, eqn. 6.11, leads to an even more complex set of equations than before.

6.1.3 Assumed Displacements

For both the response due to a through-the-thickness temperature gradient and the response due a lack of initial flatness, the assumed displacement functions used are the same as those employed in ch. 5. These are:

for fixed simple supports,

$$\begin{aligned} u^o(x,y) &= \sum_{i=1}^{I}\sum_{j=1}^{J} u_{ij}\sin\left(\frac{i\pi x}{a}\right)\sin\left(\frac{j\pi y}{b}\right) \\ v^o(x,y) &= \sum_{i=1}^{I}\sum_{j=1}^{J} v_{ij}\sin\left(\frac{i\pi x}{a}\right)\sin\left(\frac{j\pi y}{b}\right) \\ w^o(x,y) &= \sum_{m=1}^{M}\sum_{n=1}^{N} w_{mn}\sin\left(\frac{m\pi x}{a}\right)\sin\left(\frac{n\pi y}{b}\right); \end{aligned} \tag{6.12}$$

and for sliding simple supports,

$$\begin{aligned} u^o(x,y) &= \sum_{i=1}^{I}\sum_{j=0}^{J} u_{ij}\sin\left(\frac{i\pi x}{a}\right)\cos\left(\frac{j\pi y}{b}\right) \\ v^o(x,y) &= \sum_{i=0}^{I}\sum_{j=1}^{J} v_{ij}\cos\left(\frac{i\pi x}{a}\right)\sin\left(\frac{j\pi y}{b}\right) \\ w^o(x,y) &= \sum_{m=1}^{M}\sum_{n=1}^{N} w_{mn}\sin\left(\frac{m\pi x}{a}\right)\sin\left(\frac{n\pi y}{b}\right). \end{aligned} \tag{6.13}$$

In addition, for the case of initial out-of-plane deflections, the series representation for w^i is given in eqn. 6.5.

6.2 *Numerical Results*

The nonlinear, coupled equations for the imperfection analyses are solved in the same manner as were the equations for determining postbuckling response in the previous chapter. The continuously increasing change in temperature is represented by a sequence of incremental temperatures, and, at each step, the search for a new solution is begun by taking the values of the displacement coefficients calculated in the previous step as an initial guess. Because derivatives of u^o and v^o are added to squares of derivatives of w^o, as was the case for the postbuckling response, the relation between the numbers of terms taken in the series for u^o, v^o, and w^o is the same as for postbuckling: $I = 2M$ and $J = 2N$, where I and J are the upper limits on the series representing u^o and v^o, and M and N are the upper limits on the series representing w^o.

Numerical results will be presented for two specific cases. For the case of a temperature gradient through the thickness of the plate, results will be presented for $e = 0.05$. This value of e means that the plate is 5% warmer on the top than on the bottom. The form of this temperature gradient is

$$\Delta T = c\left(1 + 0.05\frac{z}{H}\right). \tag{6.12}$$

For the case of an initial deviation from flatness, the initial deflection is taken to be

$$w^I(x, y) = 0.1H \sin\left(\frac{\pi x}{a}\right)\sin\left(\frac{\pi y}{b}\right). \tag{6.13}$$

This represents an initial deflection which has an amplitude equal to one tenth of the laminate thickness and is composed of one half wave in x direction and in the y direction.

The results to follow consider only square plates, a 6 in. by 6 in. plate being used to compute the numerical results.

6.2.1 Convergence Characteristics

the convergence characteristics of the reponse of a square $(\pm 45/0_2)_S$ laminate with $\alpha = 30°$ and with 5% temperature gradient through the thickness of the plate are given in Fig. 33 for the case of fixed simple supports, and in Fig. 34 for the case of sliding simple supports. In these figures the relation between the deflections at the center of the plate, normalized by plate thickness, and $c/\Delta T^*$ are illustrated. Likewise, convergence studies for the reponse to an initial out-of-plane deformation of a square $(\pm 45/0_2)_S$ laminate with $\alpha = 30°$ are given in Fig. 35 for the case of fixed simple supports, and in Fig. 36 for the case of sliding simple supports. In the figures relating to convergence in the presence of an initial imperfection, the deflections at the center of the plate minus the initial deformation and normalized by the plate thickness are plotted as a function of $c/\Delta T^*$. These results were calculated using different numbers of terms in the series expressions for u^o, v^o and w^o. In all four studies the case of the $(\pm 45/0_2)_S$ laminate with $\alpha = 30°$ requires as many, or more, terms in the imperfection response solution, compared to the other cases, in order to reach convergence. These figures indicate that for both imperfections and with both sets of boundary conditions, convergence is reached when $M \times N = 9$.

Attention now turns to a discussion of the influence of laminate properties, skew angle, and boundary conditions on the response.

6.2.2 Imperfection Response Characteristics

The deflection response of a square $(\pm 45/0/90)_S$ laminate in the presence of each of the two imperfections with $\alpha = 0°$ and fixed simple supports is shown in Fig. 37. The deflection at the center of the plate, minus any initial deflection and normalized by the laminate thickness, H, is plotted as a function of c, the change in temperature at the midplane of the lami-

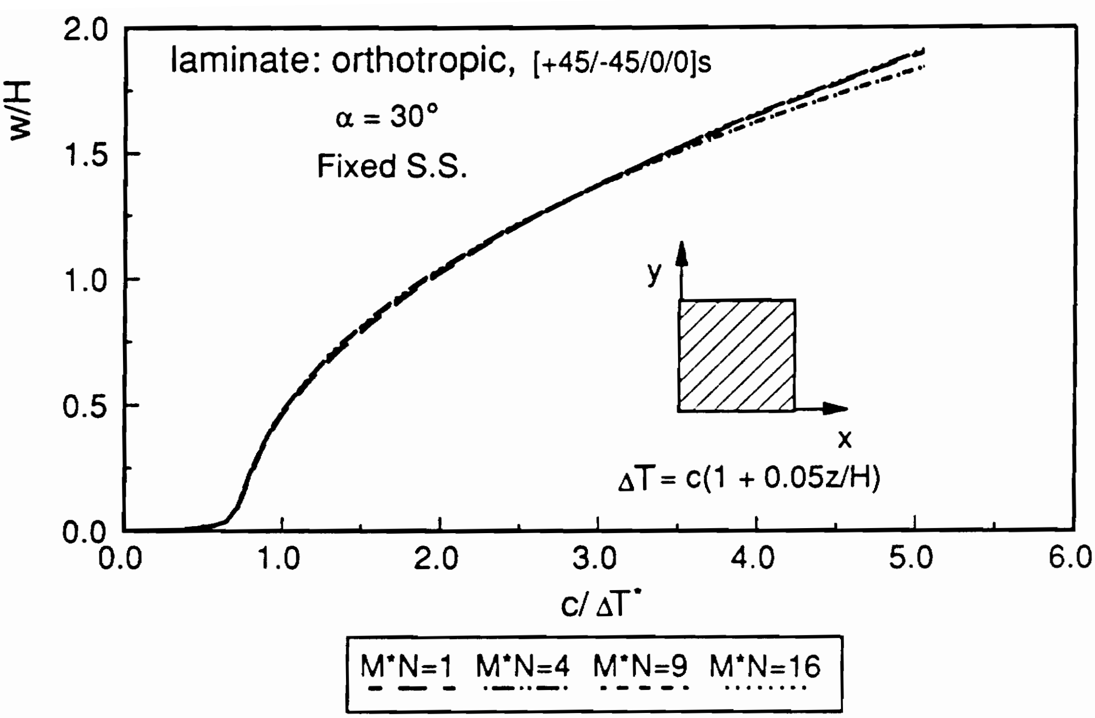

Fig. 33. Convergence study: thermal gradient imperfection, $(\pm 45/0_2)_s$ plate with $\alpha = 30°$ and fixed simple supports.

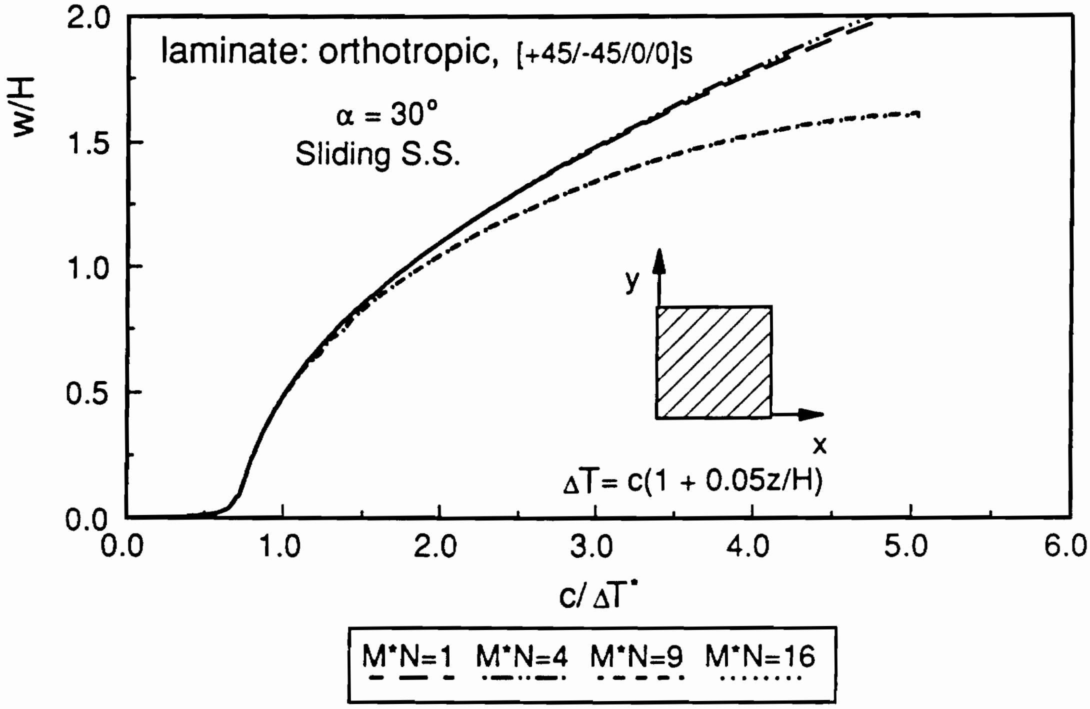

Fig. 34. Convergence study: thermal gradient imperfection, $(\pm 45/0_2)_S$ plate with $\alpha = 30°$ and sliding simple supports.

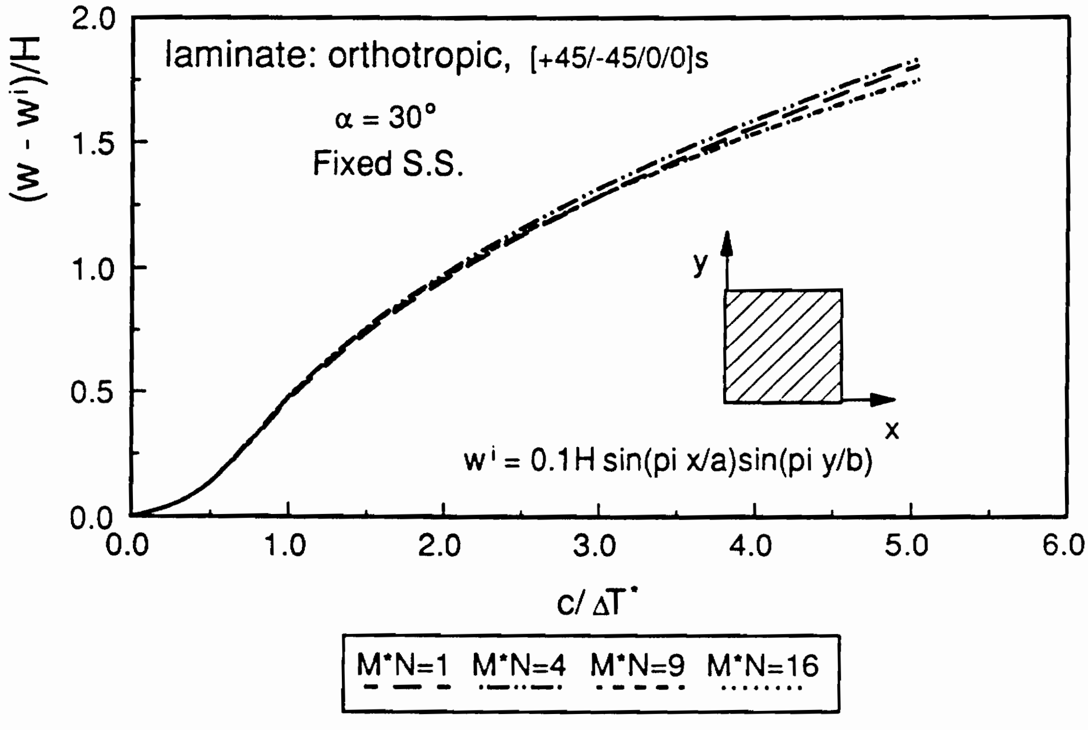

Fig. 35. Convergence study: Initial deformation, $(\pm 45/0_2)_S$ plates with $\alpha = 30°$ and fixed simple supports.

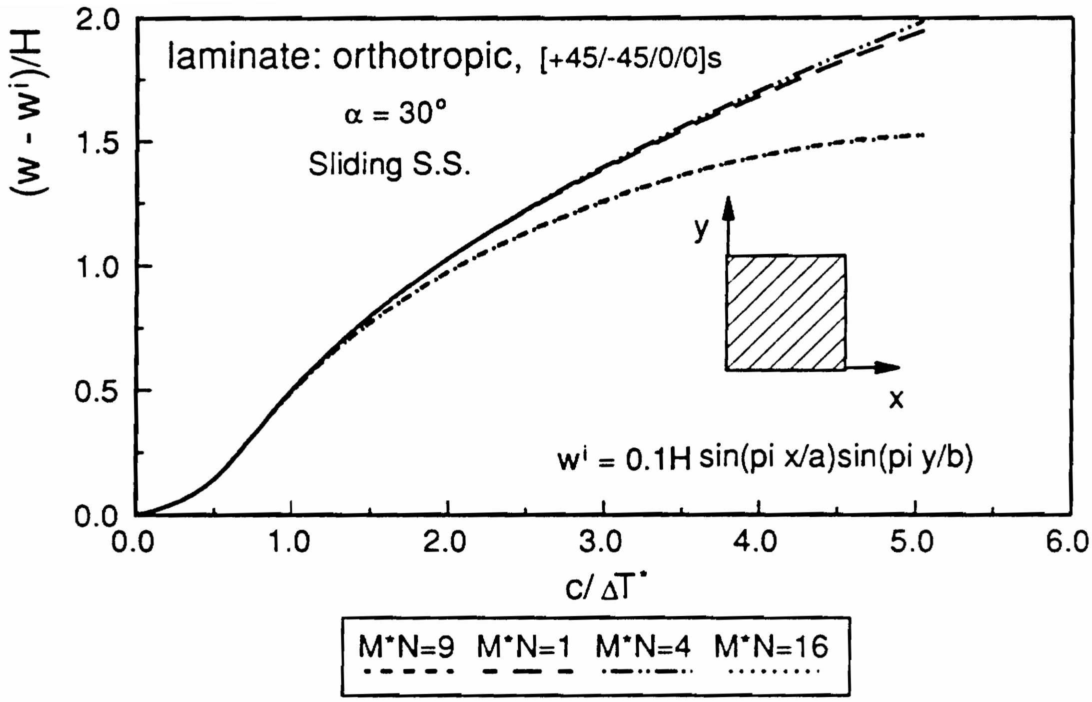

Fig. 36. Convergence study: initial deformation, $(\pm 45/0_2)_S$ plates with $\alpha = 30°$ and sliding simple supports.

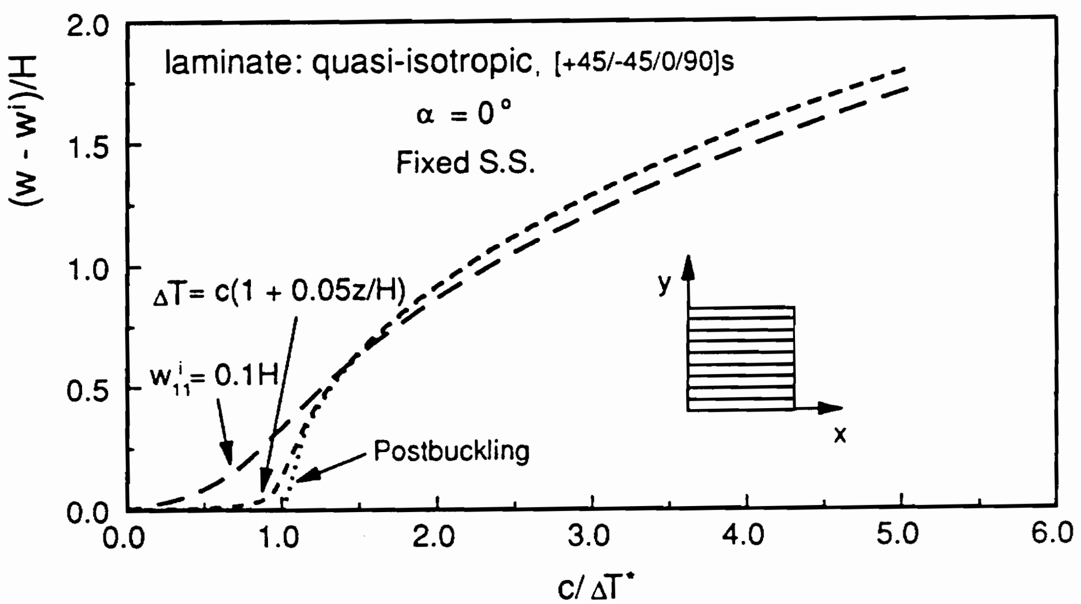

Fig. 37. Imperfection analyses: $(\pm 45/0/90)_s$ plate with $\alpha = 0°$ and fixed simple supports.

nate, normalized by ΔT^*. Note that for the case of initial out-of-plane deflection, c represents ΔT, the temperature change at every point in the plate, not just the midplane. Also, in this figure the ideal postbuckling response is indicated for comparison. Unlike the postbuckling response of a laminate under ideal conditions, the out-of-plane deflection of a laminate with an imperfection begins as soon as temperature is applied. The deflections increase slowly at first, then more quickly in the neighborhood of the critical buckling temperature, in the case of this plate, ΔT^*. Furthermore, as the deflections increase, the response of a laminate in the presence of an imperfection asymptotically approaches the postbuckling response. In the case of a temperature gradient through the thickness of the plate, the imperfection response becomes virtually indistinguishable from the postbuckling response for $c/\Delta T^* \geq 1.25$. The imperfection response in the case of an initial deflection shows much greater deflections at the outset, but then falls just below the postbuckling response of the laminate. The case of the initial out-of-plane deflection must be viewed in context, however. As was noted, it is the normalized increment in displacement, i. e., $(w - w^i)/H$, that is being plotted. If w/H were plotted, the postbuckling relation and the relation for the temperature gradient would remain unchanged from the way they appear in the figure. The relation for the case of initial lack of flatness would be shifted upward by 0.1 and beyond a certain temperature the postbuckling response and the response due to an initial out-of-plane displacement would also be indistinguishable. Thus the deflection-temperature relation for the case of an initial deformation would approach the postbuckling response from above, just as the deflection-temperature relation does for the case of a temperature gradient.

The results look very similar for all the other cases involving the quasi-isotropic laminate. Attention will thus focus on the response of the orthotropic laminate for the remainder of this chapter.

The responses of the $(\pm 45/0_2)_s$ laminate in the presence of imperfections with $\alpha = 0°$ and fixed simple supports are shown in Fig. 38. As in the case of the quasi-isotropic laminate, the deflections of the orthotropic laminate with either imperfection begin as soon as temperature is increased and they approach the postbuckling response as the increase in temperature

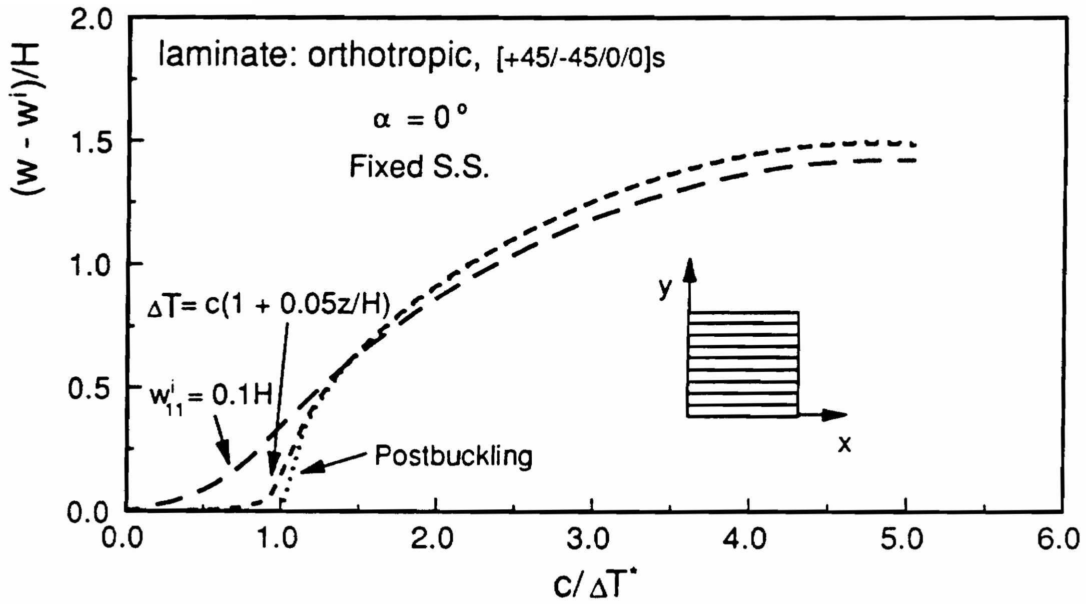

Fig. 38. Imperfection analyses: $(\pm45/0_2)_s$ plate with $\alpha = 0°$ and fixed simple supports.

continues. As the temperature is increased, the response for the case of the thermal gradient in the z direction quickly coincides with the postbuckling response, while the laminate with an initial deviation from flatness deflects much more at the outset, but then falls just below the postbuckling response. Note also how flat the relationships are, compared to the same relationships for the $(\pm 45/0/90)_s$ plate, Fig. 37, when $c/\Delta T^*$ exceeds four.

In Fig. 39 the responses of the $(\pm 45/0_2)_s$ in the presence of imperfections with $\alpha = 0°$ and sliding simple supports are given. As seen previously, the postbuckling response for this case begins primarily with the domination of the deflection associated with w_{11}, but changes when $c/\Delta T^* = 3$. At temperatures greater than this, the deflection at the center of the plate actually begins to decrease due to the influence of the deflections associated with the w_{13} and w_{31} terms. As in the previous cases, the response of the laminate with a temperature gradient through the thickness of the plate approaches the postbuckling relation very closely. It is interesting to note that even when the plate has an initial deformation including only w^i_{11}, the influence of the w_{13} and the w_{31} terms in the solution still become important and cause the deflections at the center of the plate to decrease for $c/\Delta T^* \geq 3$. The imperfection response still follows the postbuckling response. The shift in the importance of the terms w_{13} and w_{31} influences the overall deflection pattern of the plate, as was illustrated in Fig. 30.

The responses for the $(\pm 45/0_2)_s$ laminate in the presence of imperfections with $\alpha = 30°$ are shown in Fig. 40 for the case of fixed simple supports, and in Fig. 41 for the case of sliding simple supports. To avoid clutter, other boundary or skewing conditions are not shown for comparison. However, these figures should be compared with Fig. 38 and Fig. 39. For both sets of boundary conditions, with $\alpha = 30°$ the imperfection responses approach the postbuckling response more swiftly than $\alpha = 0°$. The response for the case of a thermal gradient through the thickness of the plate lies even closer to the postbuckling response for a $(\pm 45/0_2)_s$ laminate with $\alpha = 30°$ than for a $(\pm 45/0_2)_s$ laminate with $\alpha = 0°$ under either set of boundary conditions. For both sets of boundary conditons, the deflections prior to the critical buckling temperature for a $(\pm 45/0_2)_s$ with $\alpha = 30°$ in the case of an initial deformation are also smaller than those for a $(\pm 45/0_2)_s$ laminate with $\alpha = 0°$. Also to be noted is that whereas the

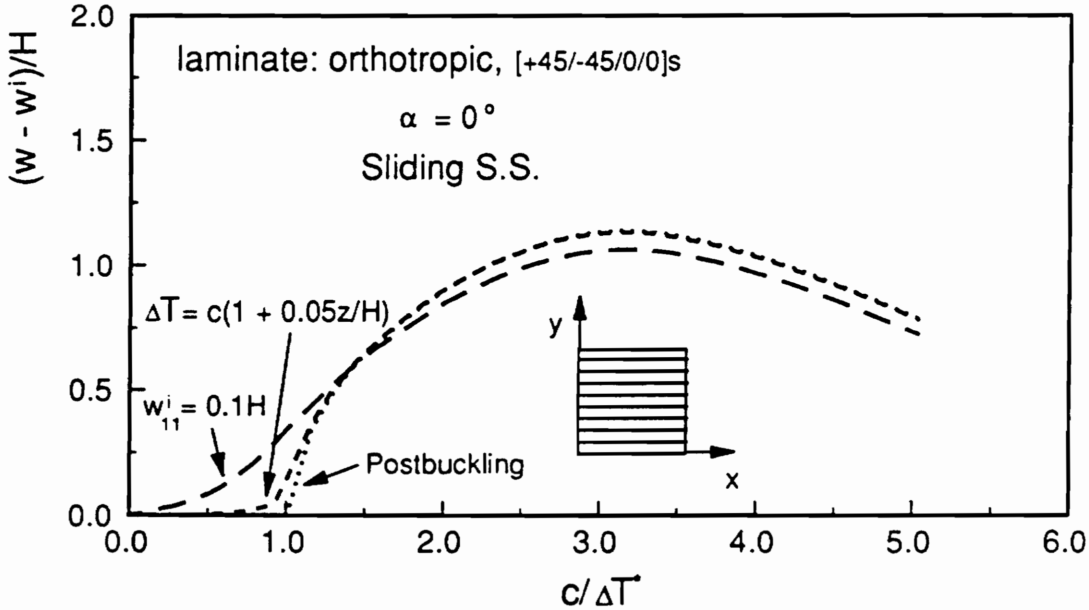

Fig. 39. Imperfection analyses: $(\pm 45/0_2)_S$ plate with $\alpha = 0°$ and sliding simple supports.

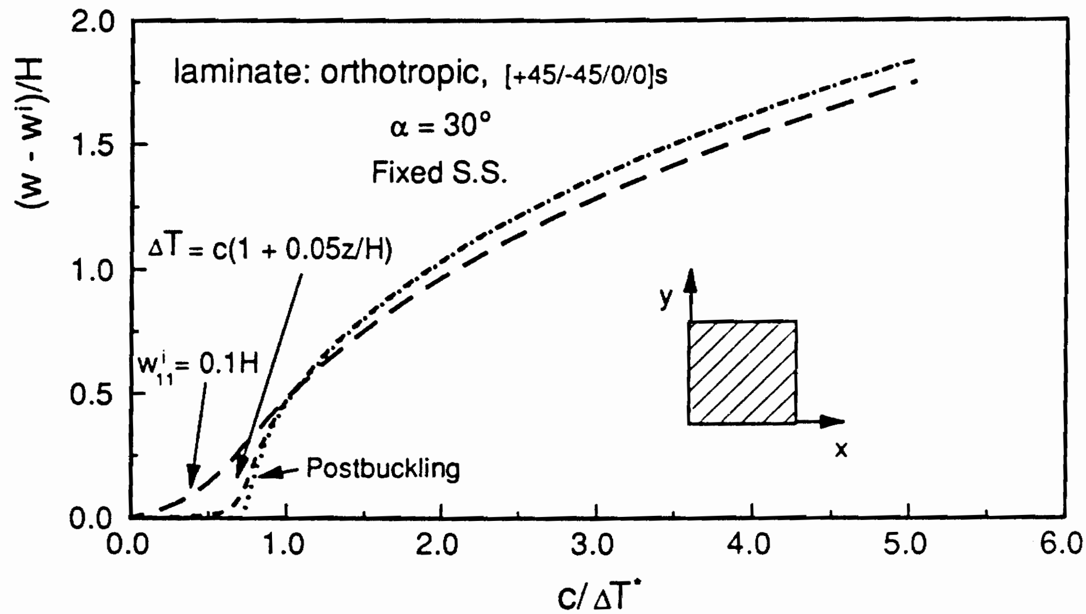

Fig. 40. Imperfection analyses: $(\pm 45/0_2)_S$ plate with $\alpha = 30°$ and fixed simple supports.

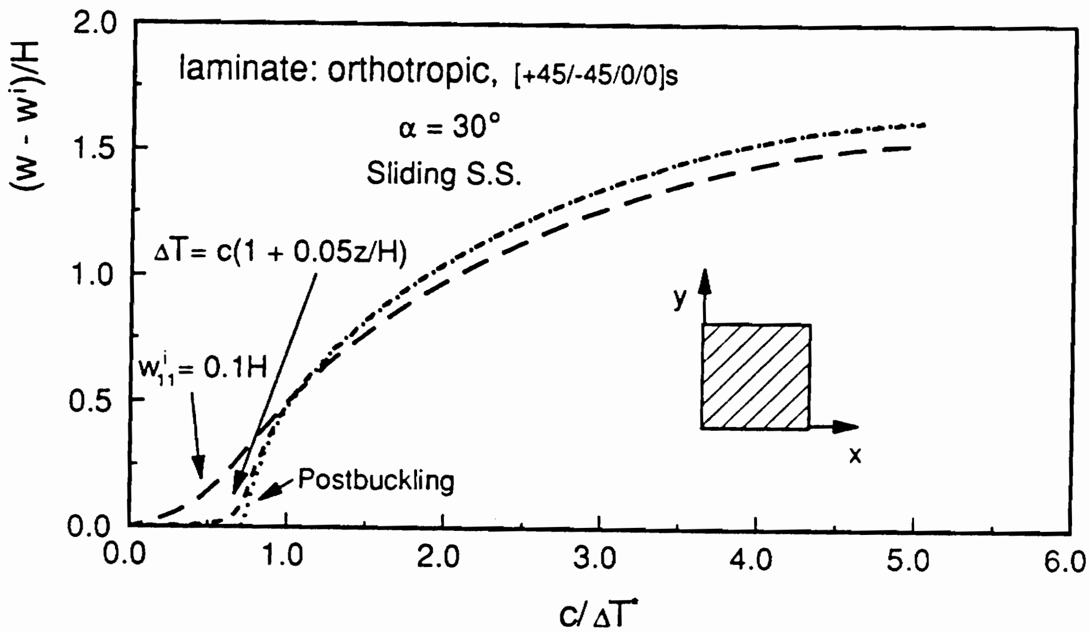

Fig. 41. Imperfection analyses: $(\pm 45/0_2)_S$ plate with $\alpha = 30°$ and sliding simple supports.

temperature-deflection relation for the case of fixed simple supports and $\alpha = 0°$ tends to flatten as $c/\Delta T^*$ exceeds 4, rotating the laminate material axes by $\alpha = 30°$ eliminates this flattening. This effect is even more pronounced for the case of sliding simple supports. For sliding simple supports and $\alpha = 0°$, the relationship indicates decreasing deflections with increasing temperature beyond $c/\Delta T^* = 3$. Rotating the laminate by $\alpha = 30°$ eliminated this tendency.

In all of the cases examined above, the responses in the presence of imperfections approach the postbuckling response for a given laminate. This indicates that the presence of these small imperfections do not greatly affect the response of heated laminates, so that the postbuckling response obtained for laminates under ideal conditions can be considered valid for laminates with minor imperfections.

This chapter concludes what can be considered an extensive study of the influence of boundary conditions, material axis skewing, and lamination properties on the buckling, postbuckling, and imperfection response of composite plates that result from increases in temperature. A large amount of information has been presented. This information will be summarized shortly, and recommendations for future study made. However, before closing the study, an important issue must be addressed. That is the issue of experimental confirmation of the findings. In all that has been presented, it has been assumed that, for example, fixed boundary conditions can be achieved. In reality, any fixturing that is to be used to support the plates in experiments would not have infinite stiffness, and it may have its own thermal expansion, or contraction, characteristics. Hence, the next chapter is a brief look at the influence of the lack of ideal conditions on the predicted response. Though no experimental results are presented here, it is quite important to at least evaluate how important the lack of ideal conditions are in contributing to the response of the composite plate. This information can then be used to put the results of the previous chapters into context, and it can be used as the starting point when considering the design of experiments. Two important deviations from the ideal will be addressed here. Those issues are: The influence of boundary compliance, and; The influence of thermal deformations at the boundary due, presumably, to the thermal deformations of the fixture or frame supporting the composite plate.

7.0 Experimental Considerations

To study the lack of ideal conditions, for simplicity only the $(\pm 45/0/90)_s$ and $(\pm 45/0_2)_s$ laminates with $\alpha = 0°$ will be considered. Also, it is assumed that the fixturing or support for the composite plate is made entirely of isotropic materials. In addition, only the buckling temperatures will be studied. The issue of interest will be to determine how the lack of ideal conditions contribute to deviations of the buckling temperature from those associated with ideal conditions. Recall that for these two laminates under the condition $\alpha = 0°$, the prebuckling solution was trivial. With experience, it is possible to anticipate that these cases would indeed lead to trivial prebuckling stress resultant calculations and it would be possible to correctly anticipate that the stress resultants are simply the negative of the thermal stress resultants N_x^T, N_y^T, and N_{xy}^T. In that context, then, the approach to determining the prebuckling stress resultants resembles a strength of materials approach. That is the approach that will be used here to evaluate the influence of the lack of ideal conditions on the buckling temperature. This is opposed to the variational approach, where, for example, contributions to the total potential energy due to compliance of the boundary would be included and a series solution assumed.

7.1 Influence of Fixture Thermal Expansion

If the frame or fixture supporting the plate is not ideal, the boundary conditions given in eqn. 4.14- 4.15 are no longer valid and new boundary conditions must be formulated. This is accomplished as follows: If the frame can expand, then when the temperature is increased, the supports for the edges of the plate, which are assumed to be part of the frame, will separate from one another by

$$\begin{aligned} \Delta_x &= a\alpha_f\Delta T \\ \Delta_y &= b\alpha_f\Delta T, \end{aligned} \tag{7.1}$$

where α_f denotes the coefficient of thermal expansion of the frame, and a and b are the length and width of both the interior of the frame and of the plate, since it is assumed that the frame fits the plate snugly. A schematic of the frame deformation is given in Fig. 42. The conditions at the edges of the plate can then be given by

$$\begin{aligned} &\text{at} \quad x = 0,\ a \\ &\qquad \text{(i)} \ \ u = \mp\frac{a}{2}\,\alpha_f\Delta T \\ &\qquad \text{(ii)} \ \ v = 0 \text{ or } N_{xy} = 0 \\ &\text{at} \quad y = 0,\ b \\ &\qquad \text{(i)} \ \ u = 0 \text{ or } N_{xy} = 0 \\ &\qquad \text{(ii)} \ \ v = \mp\frac{b}{2}\,\alpha_f\Delta T, \end{aligned} \tag{7.2}$$

where the minus is associated with the edge at x or y = 0, and the plus is associated with the opposite edge in each case. Whereas the prebuckling displacements throughout the plate for either the $(\pm 45/0/90)_s$ or the $(\pm 45/0_2)_s$ laminate with $\alpha = 0°$ were zero in the case of an ideal frame, the displacements at the edges of the plate are now the same as those of the frame, given in eqn. 7.1 and eqn. 7.2. Thus, in the presence of frame thermal expansion, the prebuckling strains in the plate are given by

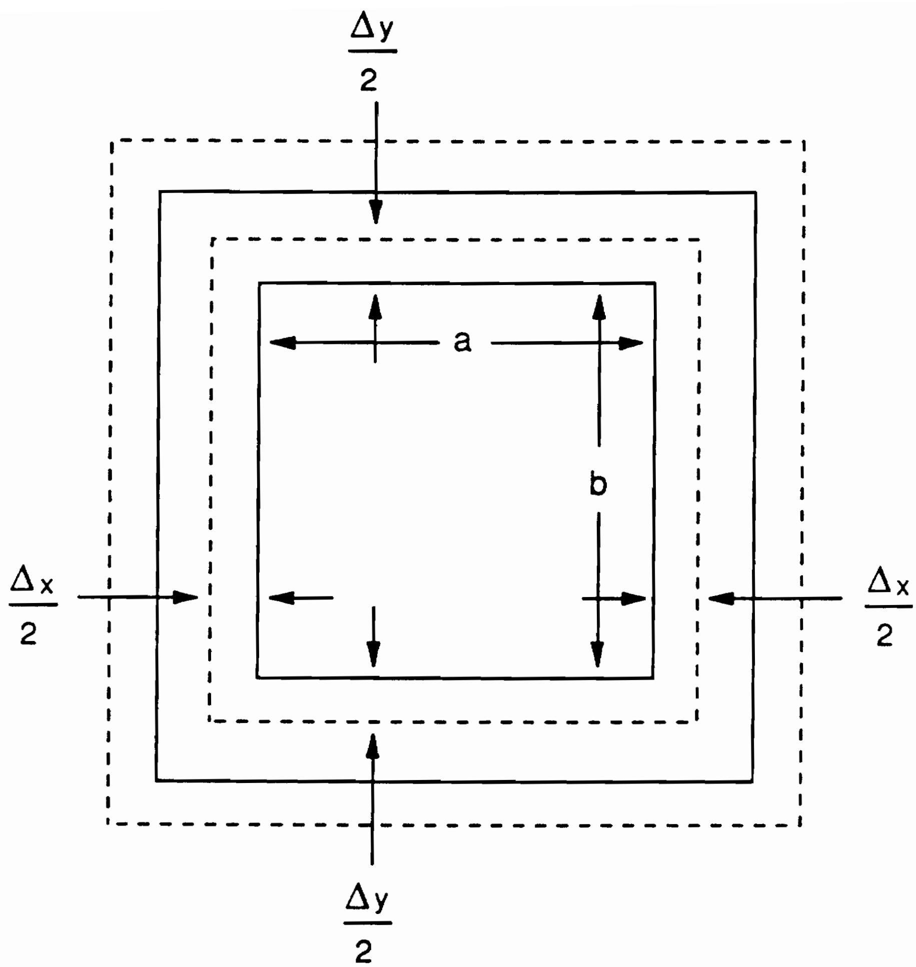

Fig. 42. Schematic of frame deformation.

$$
\begin{aligned}
\varepsilon_x^o &= \frac{\Delta_x}{a} = \alpha_f \Delta T \\
\varepsilon_y^o &= \frac{\Delta_y}{b} = \alpha_f \Delta T \\
\gamma_{xy}^o &= 0.
\end{aligned}
\tag{7.3}
$$

Using these expressions for strain and the fact that for the $(\pm 45/0/90)_s$ and $(\pm 45/0_2)_s$ laminates with $\alpha = 0°$, $A_{16} = A_{26} = \overline{N}_{xy}^T = 0$, the prebuckling stress resultants can be written as

$$
\begin{aligned}
N_x &= \left(A_{11}\alpha_f + A_{12}\alpha_f - \overline{N}_x^T\right)\Delta T \\
N_y &= \left(A_{12}\alpha_f + A_{22}\alpha_f - \overline{N}_y^T\right)\Delta T \\
N_{xy} &= 0.
\end{aligned}
\tag{7.4}
$$

Substituting the expressions in eqn. 7.4 into the first variation of the second variation of the total potential energy, eqn. 4.13, results in an equation for the thermal buckling of the $(\pm 45/0/90)_s$ and $(\pm 45/0_2)_s$ laminates with $\alpha = 0°$ which includes the the effect of a thermally expanding frame. The thermal buckling solution then proceeds as before. Note, though they are not needed, it can be determined that the prebuckling displacements are linear functions of x and y.

In Fig. 43 the buckling temperatures of square $(\pm 45/0/90)_s$ and $(\pm 45/0_2)_s$ laminates, normalized by ΔT^*, the buckling temperature for either laminate with an ideal frame, are plotted versus α_f. These results correspond to a 6 in. by 6 in. plate. This figure indicates that the thermal buckling temperature is highly sensitive to a thermally expanding frame. For α_f as low as 0.5 ppm/°F the buckling temperature for both laminates more than doubles. For α_f greater than this, increasing α_f affects the buckling temperature of the $(\pm 45/0/90)_s$ laminate much more than the buckling temperature of the $(\pm 45/0_2)_s$ laminate. Referring to eqn. 7.4, it can be seen that for a quasi-isotropic laminate, since $A_{11} = A_{22}$ and $\overline{N}_x^T = \overline{N}_y^T$, at some value of α_f both N_x and N_y will simultaneously become equal to zero. This value of α_f occurs at roughly 1.0 ppm/°F. When α_f is greater than this value, with increasing temperature the frame expands more rapidly than the $(\pm 45/0/90)_s$ laminate, so that the laminate can only be buckled by

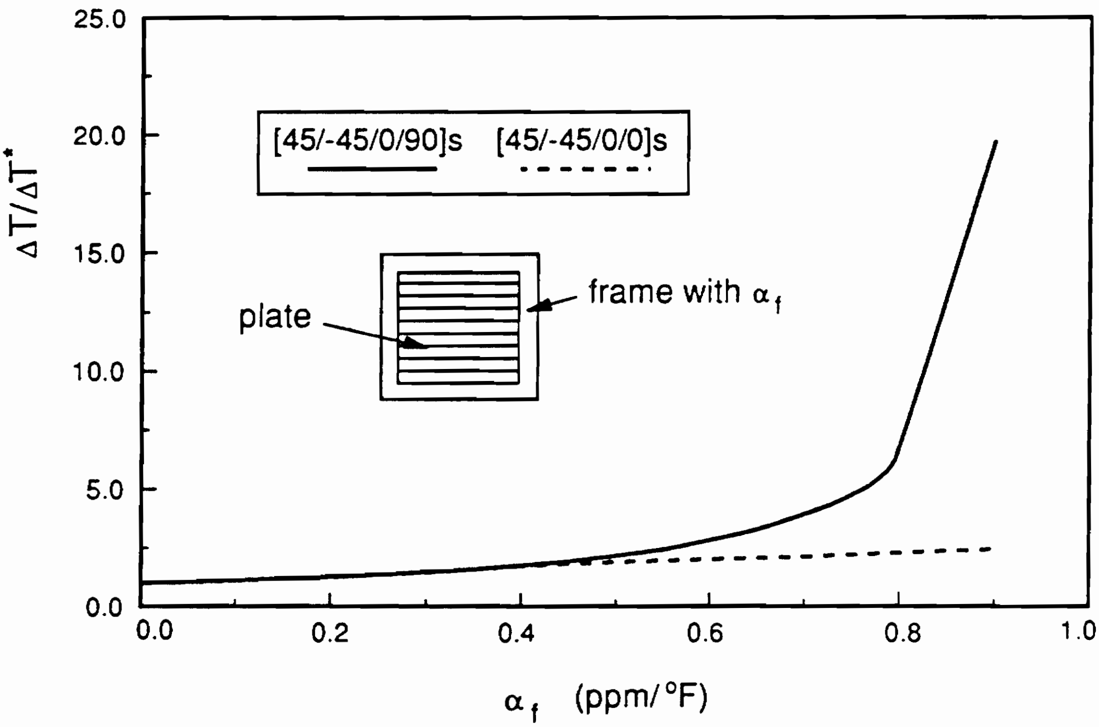

Fig. 43. Influence of frame thermal expansion on buckling temperatures.

by lowering the temperature! Note that this would be the case for a steel or aluminum frame, as the coefficients of thermal expansion for both of these materials are much greater than 1.0 ppm/°F. Fixture design must clearly take this important effect into account.

7.2 Influence of Frame Compliance

Assuming α_f has a value such that the expansion of the plate could actually exert compression force resultants on the frame, if the frame has finite stiffness then an equivalent spring constant, K_f, can be determined for the frame such that

$$\begin{aligned} bN_x &= -K_f\frac{\Delta_x}{2} \\ aN_y &= -K_f\frac{\Delta_y}{2}, \end{aligned} \tag{7.5}$$

where Δ_x and Δ_y are as shown in Fig. 42. Note that the minus sign is necessary because a $+N_x$ causes the frame to contract. In the above, the quantites bN_x and aN_x are forces, and hence K_f is a classic stiffness with units of force/length. Including the thermal expansion of the frame, when temperature is applied, the edges of the frame separate by

$$\begin{aligned} \Delta_x &= a\alpha_f\Delta T - \frac{2bN_x}{K_f} \\ \Delta_y &= b\alpha_f\Delta T - \frac{2aN_y}{K_f}. \end{aligned} \tag{7.6}$$

The conditions at the edges of the plate are then be given by

$$
\begin{aligned}
&\text{at} \quad x = 0,\, a \\
&\qquad \text{(i)} \quad u = \mp\left(\frac{a}{2}\alpha_f \Delta T - \frac{2bN_x}{K_f}\right) \\
&\qquad \text{(ii)} \quad v = 0 \text{ or } N_{xy} = 0 \\
&\text{at} \quad y = 0,\, b \\
&\qquad \text{(i)} \quad u = 0 \text{ or } N_{xy} = 0 \\
&\qquad \text{(ii)} \quad v = \mp\left(\frac{b}{2}\alpha_f \Delta T - \frac{2aN_y}{K_f}\right),
\end{aligned}
\tag{7.7}
$$

where, as before, the minus sign is associated with the edge at x or y = 0 and the plus sign with the opposite edges. As a result, the strains in the plate can be written as

$$
\begin{aligned}
\varepsilon_x^o &= \frac{\Delta_x}{a} = \alpha_f \Delta T - \frac{2bN_x}{aK_f} \\
\varepsilon_y^o &= \frac{\Delta_y}{b} = \alpha_f \Delta T - \frac{2aN_y}{bK_f} \\
\gamma_{xy}^o &= 0.
\end{aligned}
\tag{7.8}
$$

Once again, using the fact that $A_{16} = A_{26} = \overline{N}^T_{xy} = 0$ for both $(\pm 45/0/90)_s$ and $(\pm 45/0_2)_s$ laminates with $\alpha = 0°$, and considering only square laminates, a = b, the prebuckling stress resultants can be expressed as

$$
\begin{aligned}
N_x &= A_{11}\left(\alpha_f \Delta T - \frac{2N_x}{K_f}\right) + A_{12}\left(\alpha_f \Delta T - \frac{2N_y}{K_f}\right) - \overline{N}^T_x \Delta T \\
N_y &= A_{12}\left(\alpha_f \Delta T - \frac{2N_x}{K_f}\right) + A_{22}\left(\alpha_f \Delta T - \frac{2N_y}{K_f}\right) - \overline{N}^T_y \Delta T \\
N_{xy} &= 0.
\end{aligned}
\tag{7.9}
$$

Rearranging the first two expressions in eqn. 7.9 yields

$$
\begin{aligned}
\left(1 + \frac{2A_{11}}{K_f}\right)N_x + \left(\frac{2A_{12}}{K_f}\right)N_y &= \left\{(A_{11} + A_{12})\alpha_f - \overline{N}^T_x\right\}\Delta T \\
\left(\frac{2A_{12}}{K_f}\right)N_x + \left(1 + \frac{2A_{12}}{K_f}\right)N_y &= \left\{(A_{11} + A_{12})\alpha_f - \overline{N}^T_y\right\}\Delta T.
\end{aligned}
\tag{7.10}
$$

Using eqn. 7.10 the prebuckling stress resultants can be written

$$
\begin{aligned}
N_x &= \left\{ \frac{\left[\left((A_{11}+A_{12})\alpha_f - \bar{N}_x^T\right)\left(1+\frac{2A_{22}}{K_f}\right) - \left((A_{12}+A_{22})\alpha_f - \bar{N}_y^T\right)\left(\frac{2A_{12}}{K_f}\right)\right]}{\left(1+\frac{2A_{11}}{K_f}\right)\left(1+\frac{2A_{22}}{K_f}\right) - \left(\frac{2A_{12}}{K_f}\right)^2} \right\}\Delta T \\
N_y &= \left\{ \frac{\left[\left((A_{12}+A_{22})\alpha_f - \bar{N}_y^T\right)\left(1+\frac{2A_{11}}{K_f}\right) - \left((A_{11}+A_{12})\alpha_f - \bar{N}_x^T\right)\left(\frac{2A_{12}}{K_f}\right)\right]}{\left(1+\frac{2A_{11}}{K_f}\right)\left(1+\frac{2A_{22}}{K_f}\right) - \left(\frac{2A_{12}}{K_f}\right)^2} \right\}\Delta T \\
N_{xy} &= 0.
\end{aligned}
\tag{7.11}
$$

Substituting these expressions for the prebuckling stress resultants into the buckling equation, eqn. 4.13, results in an equation for thermal buckling which includes the effects of a frame with finite stiffness and a non-zero coefficient of thermal expansion. In Fig. 44 the buckling temperatures of square $(\pm 45/0/90)_s$ and $(\pm 45/0_2)_s$ laminates, normalized by ΔT^*, are plotted as a function of the equivalent spring constant of the frame, K_f. These results were obtained for 6 in. by 6 in. plates with α_f assumed to be zero. As can be seen, the buckling temperature is sensitive to a lack of infinite stiffness in the frame. For frames with $K_f \geq 1 \times 10^7$ lb/in., there is very little change in the buckling temperature for either laminate. However, the buckling temperature increases rapidly for both laminates as K_f decreases below this value. When designing fixtures, the value of K_f must be determined based on how fixture components are fastened together, i. e., bolt diameters, weld sizes, etc., as well as the fixture material.

From the results presented, it appears that the thermal expansion of the frame could be the more serious of the issues. Increased stiffness can be achieved with increased thickness or redesign of supports. However, thermal expansion of a material is independent of its thickness. Thicker frames expand the same as thinner frames. It would seem that material for fixturing would focus only on materials with very low thermal expansion coefficients. To

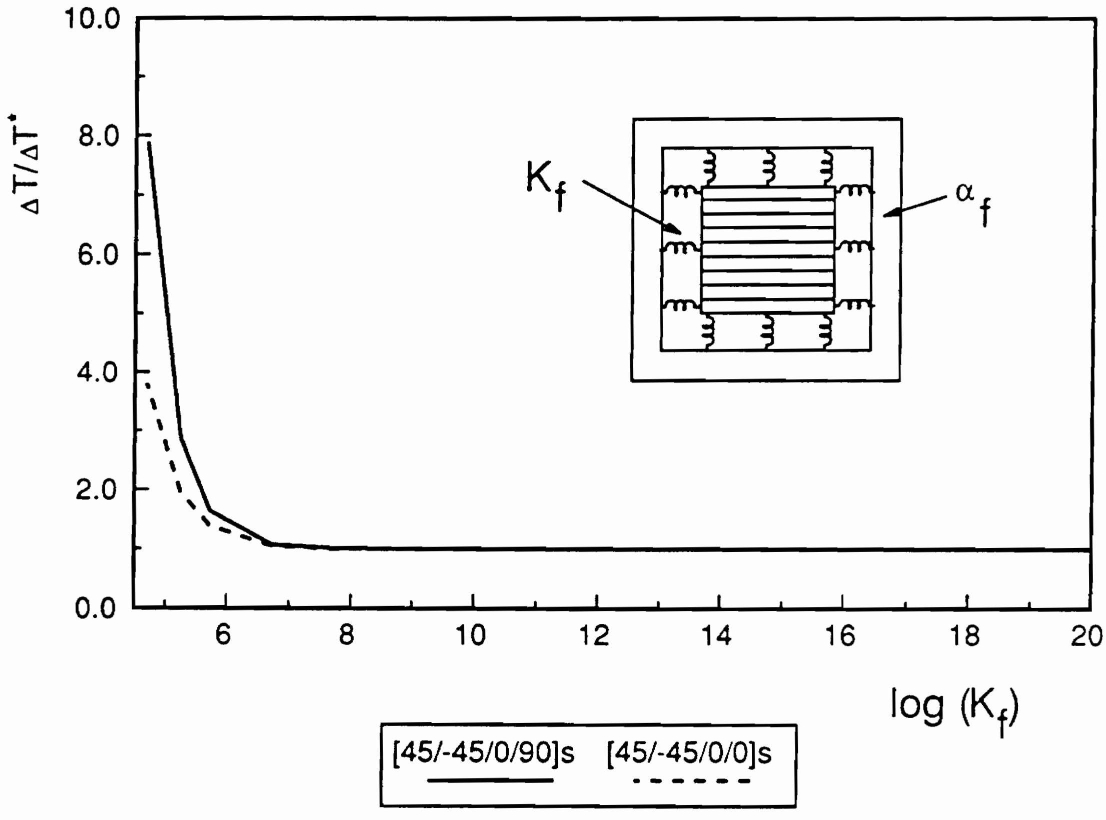

Fig. 44. Influence of frame stiffness on buckling temperatures.

do otherwise would have a profound influence on correlation between experimental findings and predictions.

8.0 Summary, Conclusions and Recommendations

In this thesis the prebuckling, buckling, postbuckling, and imperfection response of symmetrically laminated composite plates in the presence of increasing temperature are studied under a variety of physical conditions. This is accomplished using the Rayleigh-Ritz method in conjunction with variational methods. This analysis has been applied to a graphite-reinforced composite with $(\pm 45/0/90)_s$ and $(\pm 45/0_2)_s$ lamination sequences. Numerical results have been obtained for these laminates and also for the cases of the material axes of these laminates being rotated inplane by an angle α.

The first case to be studied here is the simplest, a spatially uniform change in temperature. Sensitivity studies have been conducted for this case to determine the sensitivity of the buckling temperature to variations in material properties. The buckling temperature is found to be sensitive to variations in α_1, α_2, E_1, and E_2, and to be insensitive to variations in G_{12} and ν_{12}. Two boundary conditions, fixed and sliding simple supports, have been considered. For the case of fixed simple supports, the prebuckling solution is the trivial solution. This is also true for the case of sliding simple supports if the laminate in question is such that $N^T_{xy} = 0$. For this situation, the buckling solutions for fixed and sliding simple supports are identical. When $N^T_{xy} \neq 0$, for a laminate under sliding simple support conditions, the prebuckling stress resultants are found to vary throughout the laminate. However, even though the prebuckling solution does vary throughout the laminate, it makes only a small difference in the buckling solution as compared to the buckling solution for the same laminate with fixed simple supports, a condition that produces a prebuckling solution that is constant throughout the laminate. Hence the buckling solution for the case of sliding simple supports is relatively insensitive to the number of terms taken in the prebuckling solution.

Square laminates under either boundary condition experience a decrease in buckling temperature when the material axes are skewed, $\alpha \neq 0$. Nevertheless, the buckling temperatures of these laminates are quite high as compared to the buckling temperatures of steel or aluminum plates of the same dimensions. The buckling temperature of square laminates is strongly dependent on the term $D = D_{11} + 2(D_{12} + 2D_{66}) + D_{22}$, thus the $(\pm 45/0/90)_s$ and the $(\pm 45/0_2)_s$ square laminates have very similar buckling solutions because the term D is the same for both laminates at all values of α. For these laminates with rectangular planform, $a/b = 2$, the buckling temperatures are lower than for square laminates and increase monotonically as the skew angle ranges from $\alpha = 30°$ to $\alpha = -30°$. The buckled shapes in all cases consist primarily of just one half-wave in each direction, however, the buckled shape is slightly asymmetric with respect to the plates' square or rectangular geometry. This asymmetry is due to the D_{16} and D_{26} bending stiffness terms, and in some cases, to the thermal stress resultant N_{xy}^T as well.

The buckling of laminates in the presence of a linearly varying temperature gradient, $\Delta T = c + dx$, is also studied. For this case the prebuckling solution is never trivial, and is in fact quite complicated. The buckling solution, however, is relatively insensitive to the number of terms taken in the prebuckling solution. The solutions for laminates with fixed simple supports and with sliding simple supports are never the same. However, the buckling temperatures, c, of rectangular plates are lower than the buckling temperatures of square plates, and the buckling temperatures of square pates with $\alpha = 30°$ are lower than the buckling temperatures of square plates with $\alpha = 0°$. An interesting feature of this situation is that for rectangular plates or for plates with $\alpha = 30°$, when d is fairly large and positive, meaning that the right end of the plate is much warmer than the left end, the left end must actually be cooled in order for the plate to buckle, i. e., c<0. Furthermore, the asymmetry of the buckled shape, seen for a uniform change in temperature, is exaggerated by the presence of a thermal gradient.

Thermal postbuckling is investigated for square plates under a uniform change in temperature. All of the laminates studied show considerable resistance to thermal postbuckling, deflecting by less than two plate thicknesses at changes in temperature as much as five times the buckling temperature. In all cases, laminates with fixed simple supports exhibit greater deflections than laminates with sliding simple supports. Laminates with skewed material axes, $\alpha = 30°$, also deflect more than on-axis, $\alpha = 0°$, laminates. The postbuckling response can be complex. In most cases, the postbuckling response consists mainly of the deflections associated with the Rayleigh-Ritz coefficient w_{11}, however, for the $(\pm 45/0_2)_s$ laminate with $\alpha = 0°$ with temperatures greater than 1.5 times the buckling temperature, the deflections associated with w_{13}, and, to a lesser extent, w_{31}, begin to influence the postbuckling response more and more with increasing temperature. For the $(\pm 45/0_2)_s$ laminate with $\alpha = 0°$ and sliding simple supports, this influence becomes so great that the deflections at the center of the plate actually begin to decrease as the temperature increases beyond three times the buckling temperature. The influence of orthotropy on postbuckling response depends strongly on the skew angle, α. For $\alpha = 0°$ there is a significant difference between the postbuckling response of the $(\pm 45/0_2)_s$ laminate and the $(\pm 45/0/90)_s$ laminate. For $\alpha = 30°$, there is a minimal difference in the responses.

The influence of imperfections is also studied for square laminates. Two specific forms of imperfection have been studied: a thermal gradient through the thickness of the laminate; and a lack of initial flatness. In all cases, the presence of a 5% temperature gradient through-the-thickness of the laminate results in a response which, with increasing temperature, swiftly approaches the postbuckling response. With a lack of initial flatness, the response increases much more at the outset, but also approaches the postbuckling response. It is interesting to note that even when the plate has as initial deformation of the form associated with w_{11}, the influence of the w_{13} and the w_{31} terms in the solution still causes the deflection at the center of the plate to decrease as the temperature increases beyond three times the buckling temperature, the imperfection response following the postbuckling response.

Lastly, the influence of a lack of ideal fixturing conditions on the buckling temperatures of square $(\pm 45/0/90)_s$ and $(\pm 45/0_2)_s$ laminates with $\alpha = 0°$ is considered. The two issues of interest are the fixturing compliance and thermal expansion which would occur in any real set-up. Both of these factors raise the buckling temperatures obtained for ideal conditions. Of the two, the presence of fixture thermal expansion has the greatest impact on buckling temperature. Indeed, for fixtures with coefficients of thermal expansion greater than 1.0ppm/°F, the quasi-isotropic laminate cannot be buckled except by lowering the temperature, while so long as the equivalent spring constant of the fixture is greater than 1×10^7 lb/in. there is very little change in the buckling temperature for either laminate. In planning an experimental fixture, sufficient stiffness could be achieved in the design of the supports, by providing enough thickness, for example. However, the thermal expansion of the fixture can only be controlled through material choice. To avoid a profound impact on correlation between analytical and experimental results, candidate materials would have to have extremely low coefficients of thermal expansion. This severely limits the choices available. A fixture could be constructed of composite materials designed to have near zero thermal expansion in the appropriate direction, but the difficulty of designing such a fixture, and the possibly prohibitive cost of manufacturing it, make this option unattractive. The remaining materials to choose from with low enough thermal expansion coefficients generally fall into the categories of glasses or glass ceramics. Due to the brittleness usually associated with such materials, the next most important consideration in material choice would then have to be strength and machinability. Even so, the laminates to be tested would have to be designed to have fairly low buckling temperatures under ideal conditions so that the presence of compliance and thermal expansion in the experimental fixture would not necessitate the use of unreasonable high temperatures to obtain buckling.

should be conducted to confirm analytical results. No such data appears to be available at this time. However, the design and implementation of thermal buckling experiments is non-trivial. Also of importance would be the inclusion of time- and temperature-dependent material properties in the formulations. Understanding these effects will be particularly important if polymer-based composites are to be used in elevated temperature environments for sustained periods of time. Other recommendations for future research include extending the analysis to unsymmetric laminates, studying the effects of other boundary conditions and the effects of including transverse shear deformations in the analysis. Finally, the philosophy of the computational scheme, namely, the Rayleigh-Ritz approach, could be re-evaluated. Though the buckling calculations do not seem to be very sensitive to the prebuckling problem, it is important to understand this aspect of the problem. A finite-element approach might lead to a more efficient examination of the influence of temperature gradients and a variety of boundary conditions on the prebuckling response. Details of the buckling response might be more efficiently studied with a finite-element formulation of that aspect of the problem. The postbuckling response, and the response in the presence of imperfections, are nonlinear problems and finite-element schemes can be just as computationally intense as the Rayleigh-Ritz approach. Again, the effects of a variety of boundary conditions and temperature gradients might be more efficiently studied using a finite-element approach. The effect of imperfect boundaries could perhaps be incorporated into response prediction with this alternate approach.

9.0 References

1. Whitney, J. M., and Ashton, J. E., 1971, "Effect of Environment on the Elastic Response of Layered Composite Plates," *AIAA Journal*, vol. 9, pp. 1708-1713.

2. Whitney, J. M., 1987, *Structural Analysis of Laminated Anisotropic Plates,* Technomic Publishing Company.

3. Flaggs, D. L., and Vinson, J. R., 1978, "Hygrothermal Effects on the Buckling of Laminated Composite Plates," *Fibre Science and Technology,* vol. 11, pp. 353-365.

4. Stavsky, Y., 1963, "Thermoelasticity of Heterogeneous Aeolotropic Plates," *ASCE J. Eng. Mech. Div.,* vol. 89, pp. 89-105.

5. Stavsky, Y., 1975, "Thermoelastic Stability of Laminated Orthotropic Circular Plates," *Acta Mechanica,* vol. 22, pp.31-51.

6. Biswas, P., 1976, "Thermal Buckling of Laminated Composite Plates," *J. Appl. Mech.,* vol. 43, pp.361-363.

7. Chen, L. W., and Chen, L. Y., 1987, "Thermal Buckling of Laminated Composite Plates," *J. Therm. Stresses,* vol. 10, pp.345-356.

8. Thangaratnam, K. R., Palaninathan, and Ramachandran, J., 1989, "Thermal Buckling of Composite Laminated Plates," *Computers and Structures,* vol. 35, pp.1117-1124.

9. Huang, N. N., and Tauchert, T. R., 1987, "Thermal Buckling of Symmetric Angle-Ply Laminates," *4th Int. Conf. on Composite Structures,* Paisley, U. K., Elsevier Applied Science Publishers, pp.1.424-1.435.

10. Huang, N. N., and Tauchert, T. R., 1986, "Thermal Buckling and Postbuckling Behavior of Antisymmetric Angle-PLy Laminates," *Proc. Int. Symp. Composite Materials and Structures,* Beijing, China, T. T. Loo and C. T. Sun, eds., pp.

11. Tauchert, T. R., 1987, "Thermal Buckling of Thick Antisymmetric Angle-Ply Laminates," *J. Therm. Stresses,* vol. 10, pp. 113-124.

12. Biswas, P., 1981, "Nonlinear Analysis of Heated Orthotropic Plates," *Indian J. Pure Appl. Math.*, vol. 12, pp. 1380-1389.

13. Chen, L. W., and Chen, L. Y., 1989, "Thermal Postbuckling of Laminated Composite Plates by the Finite Element Method," *Computers and Structures*, vol. 12, pp. 257-270.

14. Huang, N. N., and Tauchert, T. R., 1989, "Postbuckling Response of Antisymmetric Angle-ply Laminates to Uniform Temperature Loading," *Acta Mechanica*, vol. 72, pp. 173-183.

15. Huang, N. N., and Tauchert, T. R., 1988, "Large Deformation of Antisymmetric Angle-Ply Laminates Resulting from Nonuniform Temperature Loadings," *J. Therm. Stresses*, vol. 11, pp. 287-297.

16. Wu, C. H., and Tauchert, T. R, 1980, "Thermoelastic Analysis of Laminated Plates. 1: Symmetric Specially Orthotropic Laminates," *J. Therm. Stresses*, vol 3, pp. 247-259.

17. Wu, C. H., and Tauchert, T. R, 1980, "Thermoelastic Analysis of Laminated Plates. 1: Antisymmetric Cross-PLy and Angle-PLy Laminates," *J. Therm. Stresses*, vol 3, pp. 365-378.

18. Brush, D. O., and Almroth, B. O., 1975, *Buckling of Bars, Plates, and Shells*, McGraw-Hill Book Company.

19. Meirovich, L., 1986, *Elements of Vibration Analysis*, McGraw-Hill Book Company.

20. International Mathematical Subroutine Library, level. 2, 2500 Parkwest Tower One, 2500 Citywest Blvd., Houstan, TX.

21. Chia, C. Y., 1980, *Nonlinear Analysis of Plates*, McGraw-Hill Book Company.

Vita

Carol Meyers was born in Pittsburgh, Pa. on December 16, 1965. She graduated second in her class from Rutherford B. Hayes High School in 1984. She received a National Merit Scholarship and an Alumni Distinguished Scholarship to attend Michigan State University where she graduated with honors in 1988 with a dual B. S. degree in Engineering Mechanics and Mathematics. She is currently doing graduate work at Virginia Tech and living in Blacksburg with her husband and her two dogs. Her other interests include volunteering at the Humane Society, martial arts, history, and reading and writing science fiction/fantasy.